Well-defined Al-containing Lewis Acids for Organic Transformations

NANYANG TECHNOLOGICAL UNIVERSITY

Well-defined Al-containing Lewis Acids for Organic Transformations

LIU ZHIZHOU

SCHOOL OF PHYSICAL AND MATHEMATICAL SCIENCES

2016

LIU ZHIZHOU

2016

Well-defined Al-containing Lewis Acids for Organic Transformations

LIU ZHIZHOU

School of Physical and Mathematical Sciences

A thesis submitted to the Nanyang Technological University

in fulfilment of the requirement for the degree of

Doctor of Philosophy

2016

ACKNOWLEDGENTS

First and foremost, I would like to thank my supervisor Nanyang Assistant Professor Dr. Vidovic Dragoslav for not hesitating even for a moment to give me the chance to be a part of his research group in the summer of 2012. Yet, still, it was one of the most important turning points in my life's path. I started to face my life cheerfully and determinedly. His endless knowledge, insights, instructions and enthusiasm are truly inspirational.

I also thank all my coworkers from Dr. Vidovic Dragoslav's research group for their valuable suggestions and help in the lab for the last four years. It is really a precious and wonderful experience working with them. They are: Dr. M. Senthilkumar, Dr. Zhu Di, Dr. Madelyn Tay, Dr. Alexey Smarun, Dr. B. Murugesapandian, Dr. Chitra Gurnani, Nemanja Djordjevic, Gordana Ilic and Monika Bjelcic.

I would like to thank the CBC technical support staff: Dr. Li Yongxin, Dr. Ganguly Rakesh, Ms Goh Ee Ling, Ong Yiren Derek, Ms Zhu Wenwei and Ms Pui Pang Yi for their assistance with common laboratory instruments. I would also like to thank the School of Physical and Mathematical Sciences of Nanyang Technological University for the financial support.

Also I would like to thank all my friends I met in NTU and Singapore, who brought me joy and support in the last four years. It's a great memory to live in this beautiful tropical isle.

And most of all, I would like to thank my family for their love and encouragement. They always supported my decision and allowed me to determine my life's path freely.

TABLE OF CONTENTS

TABLE OF SCHEMES

TABLE OF FIGURES

TABLE OF TABLES

ABSTRACT

This thesis focuses on designing and catalytic applications of aluminum based Lewis acids. It contains four parts:

Chapter 1 gives a brief introduction of the development of Lewis acid chemistry and its increasing influence on modern synthetic organic chemistry. Aluminum compounds are widely used as efficient and powerful Lewis acid catalysts. Hence, we proposed our strategy to prepare various Al-based Lewis acids and investigate their potential applications.

Chapter 2 describes the design, synthesis and characterization of a series of aluminum bistriflate complexes supported by β-diketiminate ligands. Several approaches to cationic aluminum complexes were also illustrated in this chapter.

Chapter 3 focuses on the catalytic application of these aluminum bistriflate complexes on Diels-Alder transformations. Less reactive dienes such as 2,3-dimethylbutadiene, 1,3-cyclohexadiene and isoprene and a series of dienophiles were examined. A competition between Diels-Alder reaction and Michael polymerization was also described when cyclic dienophiles were used.

Chapter 4 describes the synthesis of several aluminum compounds stabilized by an NCN pincer ligand. Several experiments indicated that the cationic aluminum complex **50** was the active species for Diels-Alder catalytic reactions.

PUBLICATIONS

1. A Well-Defined Aluminum-Based Lewis Acid as an Effective Catalyst for Diels–Alder Transformations. **Zhizhou Liu,** Jazreen Hui Qi Lee, Dr. Rakesh Ganguly, Dr. Dragoslav Vidović, *Chem. Eur. J.*, **2015,** *32*, 11344–11348.
2. Diels Alder cycloaddition vs Michael addition polymerization: a subtle steric modification of a Lewis acid catalyst leads to a vastly different chemistry of cyclic dienophiles, **Zhizhou Liu**, Rakesh Ganguly, Mihaiela C. Stuparu*, Dragoslav Vidović*, *Chem. Eur. J.,* submitted.
3. Pursuing the active species in an aluminum-based Lewis acid system for catalytic Diels Alder cycloadditions, **Zhizhou Liu**, Rakesh Ganguly, Dragoslav Vidović*, *Dalton Trans.*, submitted.

ABBREVIATIONS

Xyl	2,6-dimethylphenyl
Mes	1,3,5-trimethylphenyl
Dip	2,6-diisopropylphenyl
Ph	phenyl
OTf	trifluoromethanesulfonate
dbpy	2,6-di-tertbutylpyridine
Equiv	equivalent
HRMS	high−resolution mass spectrometry
^{i}Pr	isopropyl
IR	infrared Spectroscopy
Me	methyl
Et	ethyl
η	eta
β	beta
^{t}Bu	tert-butyl
π	pi
σ	sigma

Chapter 1
Introduction

1.1 Lewis acid catalysts applied in organic synthesis

The concept of Lewis acid was given by Gilbert N. Lewis in 1923, where an acid is described as a molecule or ion capable of coordinating with a lone pair of electrons and a base as a molecule or ion having a lone pair of electrons to share.[1] It can be then concluded that all Lewis acids are electron deficient while Lewis bases are electron rich. It is a much more general concept than that given by Brønsted, where acid is simply described as a proton donor and a base as a proton acceptor.[2] According to these two definitions, all the Brønsted acids can be considered as Lewis acids. Nevertheless, the Lewis acid definition has expanded the application of acids to a much wider range. Besides the classic acids, many metallic and nonmetallic species that lack electron density can be also considered as acids. For example, boron trifluoride, which has no protons to donate, can accept the lone pair from ammonia as it possesses an empty p orbital i.e. the central B is electron deficient. In this case, boron trifluoride acts as a Lewis acid and ammonia acts as a Lewis base to form an adduct (Scheme 1.1).

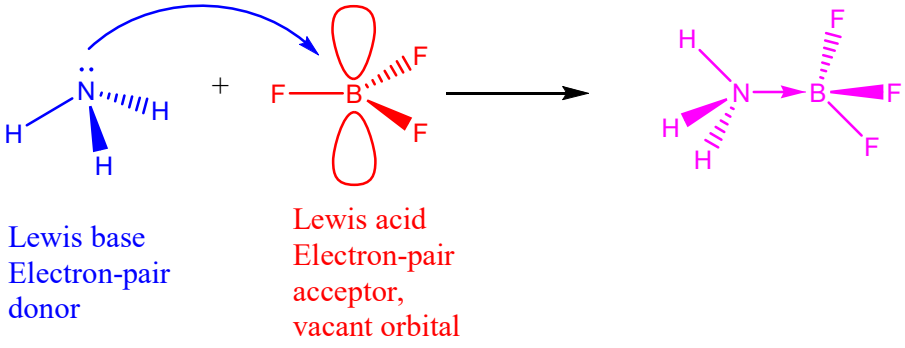

Scheme 1.1 Lewis acid and Lewis base.

In the following decades, the chemistry of Lewis acids has attracted more and more attention and played an extremely important role in modern synthetic organic chemistry. Many Lewis acids have been found to be quite suitable for the catalysis of a variety of

useful and powerful organic transformations, which include, but are not limited to alkylation,[3] Friedel-Crafts reactions,[4-8] Ene reactions,[9,10] Aldol reactions[11] and cycloaddition reactions.[12] The most common mode of Lewis acid catalytic activity is their ability to lower the LUMOs of electrophilic substrates by binding to a heteroatom (e.g. O, N, etc.).[13,14,15] Traditionally, the Diels-Alder reaction,[16] Mukaiyama aldol synthesis[17,18] and Friedel–Crafts reaction[19] are usually catalyzed by common Lewis acids such as $BF_3 \cdot Et_2O$, $AlCl_3$ and $TiCl_4$. When dissolved in solution, these Lewis acids usually exist as dimers, trimers or oligomers, and can activate various kinds of functional groups efficiently. However, as a disadvantage, they usually provide relatively low regio-, stereo-, and chemoselectivities. One of the strategies to improve on these selectivities, is to modify these Lewis acids with a supporting ligand. Research showed that binding organic ligands to these Lewis acids led not only to the formation of monomeric structures but it also to improved selectivities. For example, as a common used Lewis acid, $TiCl_4$ is a respectable catalyst for the usual Diels-Alder cycloadditions. However, when two of the chloride atoms were replaced by (R,R)-3-Aza-3-benzyl-1,5-dihydroxy-1,5-diphenylpentane ligand (L), the resulting L-$TICl_2$ complex was proved to be an excellent chiral Lewis acid catalyst for the synthesis of a series of asymmetric tetrahydroquinoline derivatives via inverse electron demand (IED) Diels-Alder reactions between electron-poor diene benzylidene aniline and several electron-rich dienophiles.[20] This Ti-based Lewis acid produced moderate yields and at times high enantioselectivities (up to 92%) for these IED Diels-Alder reactions as shown in Table 1.1.

Table 1.1 IED Diels-Alder Reactions with Various Dienophiles

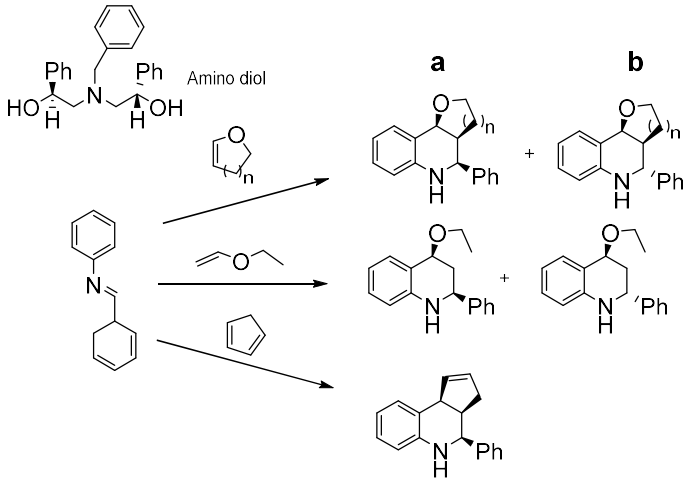

#	dienophile	T ºC	Conversion %	**a**/**b**	ee % **a**	**b**
1	dihydropyran (n=2)	0	60	0.25	92	10
2	dihydrofuran (n=1)	0	50	2.33	82	90
3	dihydrofuran (n=1)	-40	60	2.33	56	18
4	ethylvinyl ether	35	65	0.67	90	50
5	cyclopentadiene	35	58		21	

Over the years, various Lewis acids supported by different ligands have been prepared and studied, among which, many have been applied in chemical industry. In these cases, Lewis acid catalysts showed both high activities and good selectivity. There is no doubt that, the discovery that Lewis acid can be used as catalysts for so many organic reactions is one of the most significant events in chemistry in the past century.

1.1.1 Lewis acids used for C-C bond formation

Since discovered by Borodin [21] and Wurtz [22-24] in 1872, Aldol addition has been widely applied in the formation of carbon-carbon bonds. Due to this great significance to organic synthetic chemistry, a large amount of work has been undertaken to investigate this kind of reactions in the past years. These reactions can easily occur in the presence of a strong base such as LDA (lithium diisopropylamide) or NaOH. However, when the unsymmetrical carbonyl compounds were used for the addition, the formation of crossed products was observed. In contrast, when Lewis acids are used as catalysts, this problem can be solved.[25] Recently, Aldol reactions have been widely applied in the synthesis of a wide variety of compounds that contain stereoselective carbon-carbon bonds. One method is to use asymmetric modified electrophiles or enolates [26] as substrates, the other method is to use chiral Lewis acids as catalysts for these Adol reactions. In the latter case, Lewis acids usually coordinate i.e. activate aldehydes followed by the addition of various substrates such as silyl enol ether.[27]

For example, Fu[28] and coworker reported a planar chiral Lewis acid based on boron, which can catalyze Aldol reactions between a wide range of different dienophiles and aldehydes, resulting in high yields and stereoselectivities. The proposed mechanism for the catalytic reaction is shown in Scheme 1.2. The designed chiral Lewis acid can activate and organize the aldehydes via a π-interaction, following with the highly stereoselective addition to dienphiles.

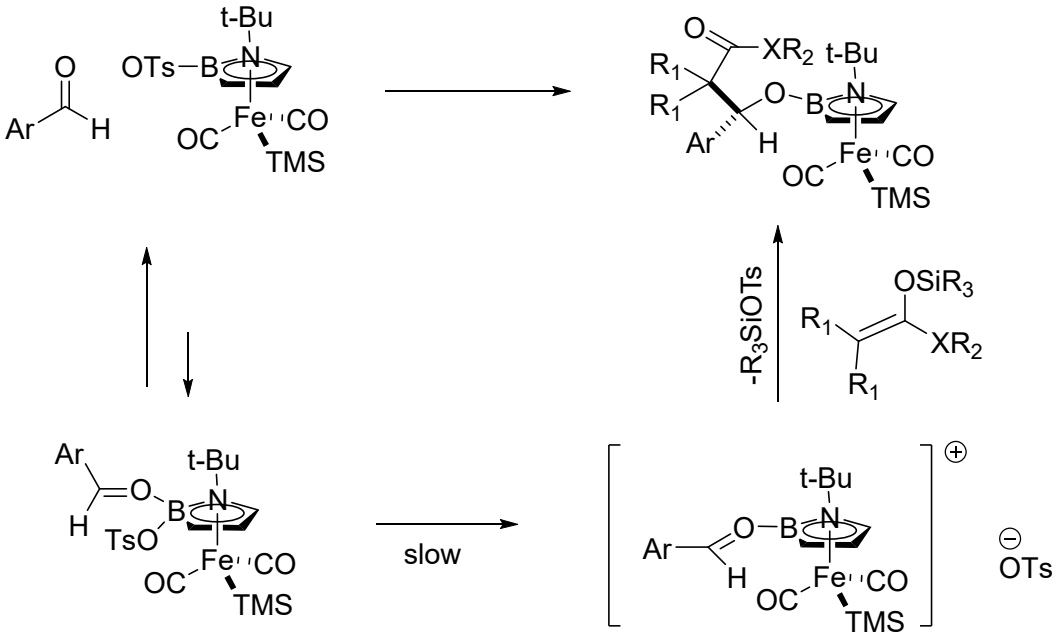

Scheme 1.2 Possible mechanism for Aldol reactions in the presence of Lewis acid

Nowadays, the Ene reactions is one of the most valuable tools for the organic synthesis.[29-33] However, the carbonyl-Ene reaction usually requires high temperature or highly activated reagents as it is a group transfer reaction. Also the enophile and the ene in this reaction can be modified by various functional groups, allowing for a valuable access to useful carbon-carbon bonds formation. As a result, various catalysts have been investigated to catalyze the Ene reactions in the past decades. Among those, Lewis acids have revealed their potential for these reactions as they showed both high activity and selectivity. For example, one of the methods to prepare chiral alcohols is the Ene reaction between aldehyde and alkene catalyzed by chiral Lewis acids. In 1988, Yamamoto [34] and coworker used a chiral aluminum Lewis acid based on BINOL as catalyst and successfully synthesized a series of chiral alcohols with high yields and enantioselectivity up to 88% as shown in Scheme 1.3.

.

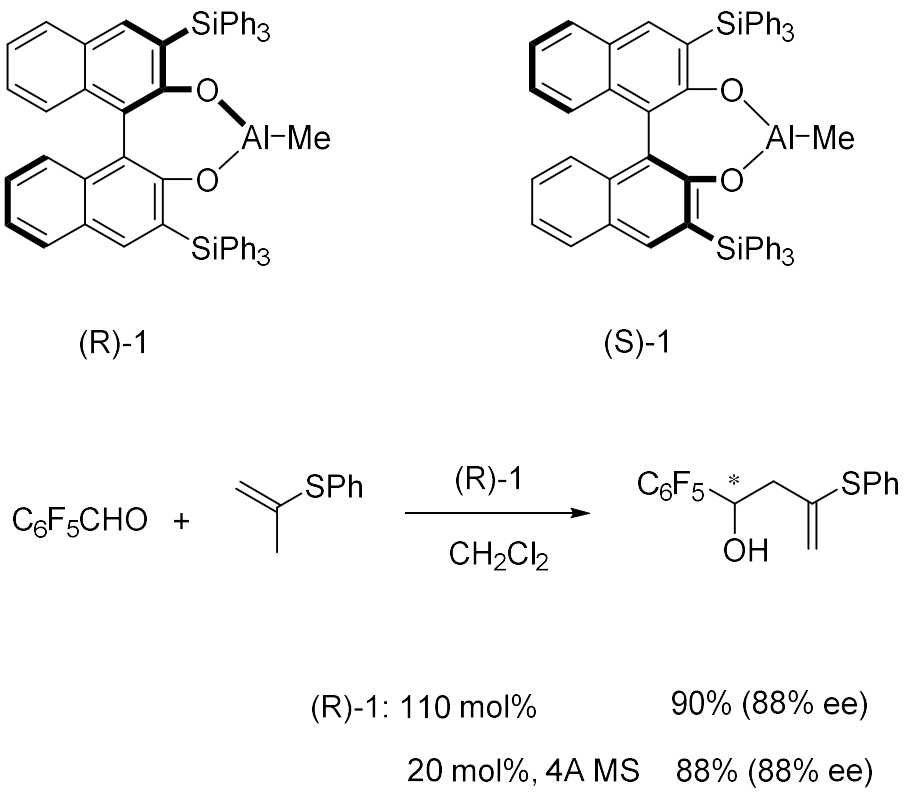

Scheme 1.3 Ene reaction catalyzed by chiral aluminum complexes.

Subsequently, Mikami and other researchers reported that titanium complexes based on BINOL can also catalyze the asymmetric carbonyl-ene reactions [35-37]. After that, a lot of other metal canions have also been explored as efficient catalysts for these reactions.[38-40] Evans and coworkers reported a series of chiral scandium-pybox compounds and used them as attractive Lewis acid catalysts for the ene reaction of 1, 1- disubstituted olefins and N-phenyl glyoxamide at the beginning of this century.[41] As shown in the Table 1.2, in the presence of 4Å molecular sieves, 5 mol% of the scadium-pybox compounds can catalyze the reaction efficiently, affording both high yields and excellent enantioselectivities (up to 99%).

Table 1.2 Ene reaction with trisubstituted olefins

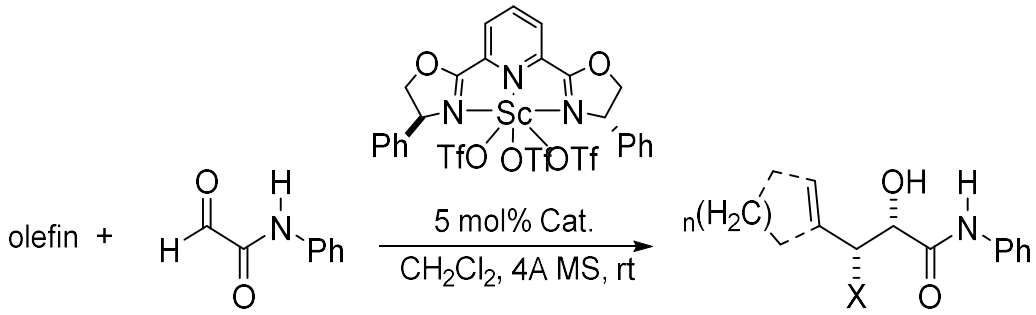

olefin		product	ee %	yield %	dr
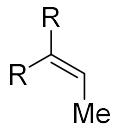	R = Me	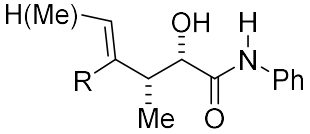	94	78	13: 1
	Et		99	76	24: 1
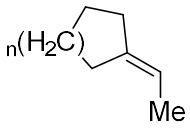	n = 1	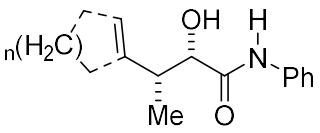	98	82	9.3: 1
	2		98	78	9.3: 1
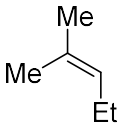		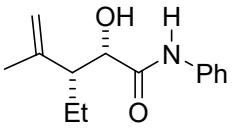	96	58	9: 1

It was first reported 1942 by Wassermann[42] that Diels-Alder reactions can be catalyzed by Brønsted acids. However, not much attention was paid to this area for a long time. In contrast, the Lewis acid catalyzed Diels-Alder reactions have been well-developed and widely used in organic synthesis and industry, although the first Lewis acid catalyzed reactions were discovered almost two decades after the ones catalyzed by Brønsted acids.[43] Yate and Eaton [44] pointed out that the simple Lewis acids such as $AlCl_3$ and $BF_3.OEt_2$ allow Diels-Alder reaction to run in quite mild conditions. This discovery promoted the development of the Diels-Alder reactions, making this type of C-C bond formation a powerful tool to form six-membered ring.[45] In the catalytic process, a Lewis acid first

activates the substrates by coordinating to the oxygen atom of the carbonyl group of dienophiles, lowering the energy of LUMO. However, because Lewis acids such as $AlCl_3$ and $BF_3 \cdot OEt_3$ are usually corrosive and non-recyclable, it is important to modify these particular Lewis acids with different ligands. Furthermore, the introduction of chiral ligands makes it possible to catalyze asymmetric Diels-Alder reactions.[46,47] Kelly [48] prepared a chiral boron Lewis acid through the reaction of a disubstituted 1, l'-binaphthol and juglone in 1986. This complex can react with a variety of dienes stoichiometrically to give Diels-Alder products with high enantioselectivities up to 98% (Scheme 1.4).

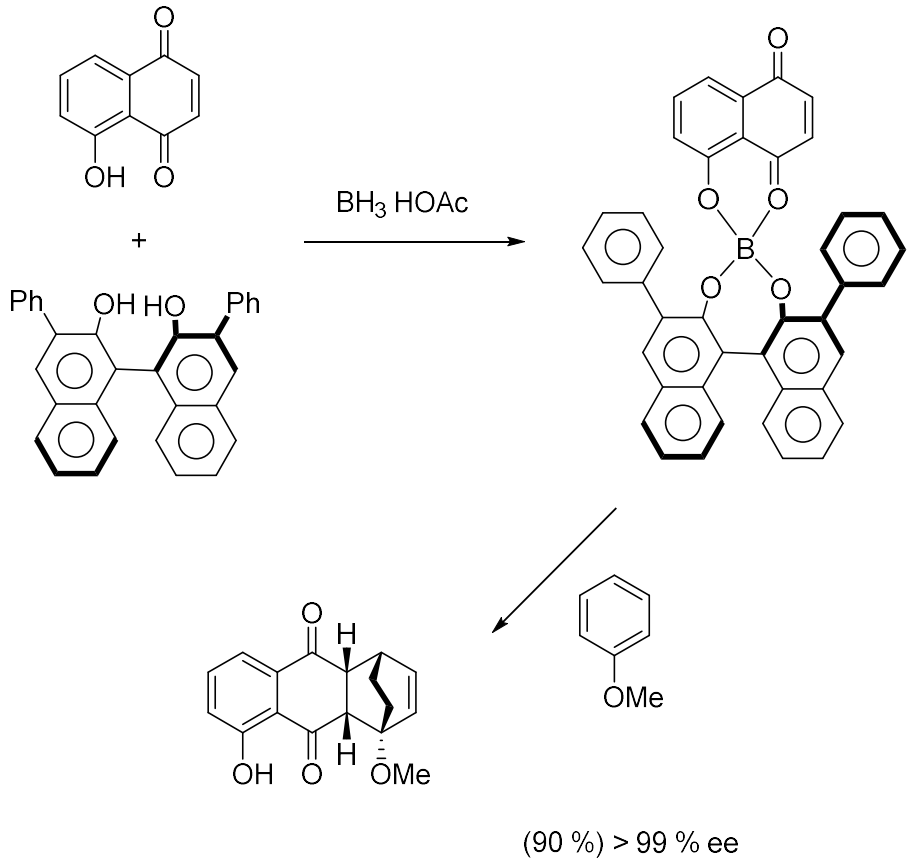

Scheme 1.4 Asymmetric Diels-Alder reaction catalyzed by boron Lewis acid.

More recently, E. P. Kündig [49] and coworker reported a series of chiral indenyl ruthenium complexes which can be used as efficient Lewis acid catalysts for asymmetric Diles-Alder reactions between methacrolein with cyclopentadiene. They showed unprecedented high

exo selectivity (>99%) as well as high enantioselectivity up to 97% as shown in Table 1.3. Also, these ruthenium Lewis acid catalysts are room-temperature stable and can be recovered.

Table 1.3 Reaction of methacrolein with cyclopentadiene.

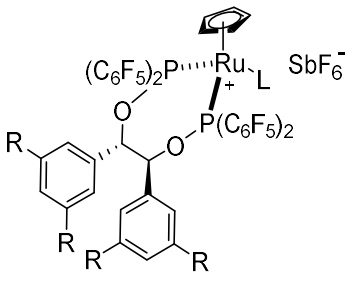

a R = H, L = Me_2CO
b R = Me, L = Me_2CO

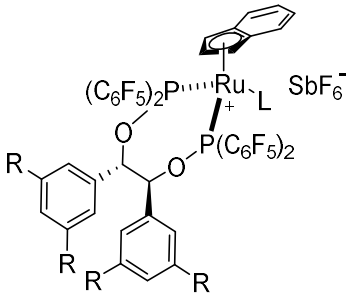

c R = H, L = Me_2CO
d R = Me, L = Me_2CO

Entry	Catalyst	Time (h)	Yield (%)	exo: endo	ee (%)
1	[CpFe((R,R)-biphop-F)][SbF_6]	1	85	98: 2	97 (R)
2	(S,S)-**a**	22	91	97: 3	92 (S)
3	(S,S)-**b**	22	87	97: 3	97 (S)
4	(S,S)-**c**	2.5	85	99.7: 0.3	88 (S)
5	(S,S)-**d**	4	80	99.8: 0.2	95 (S)

1.1.2 Lewis acids used in oxidation and reduction reactions

Lewis acids are also widely used in catalytic enantioselective oxidation and reduction reactions. Mikami[50] reported a series of chiral diamine–Zn–diol Lewis acid catalytic systems which are prepared by mixing chiral diamines, $ZnEt_2$ and achiral diols in situ. When polymethylhydrosiloxane (PMHS) was used as the source of hydride and in the presence of 3 Å molecular sieves, ortho-multisubstituted benzophenones can be reduced to the corresponding optically active alcohols via hydrosilylation using 10 mol% of the

diamine–Zn–diol compounds. As shown in Scheme 1.5, both high yield and excellent enantioselectivity (97% and 96%, respectively) can be obtained for this reaction under mild reaction conditions.

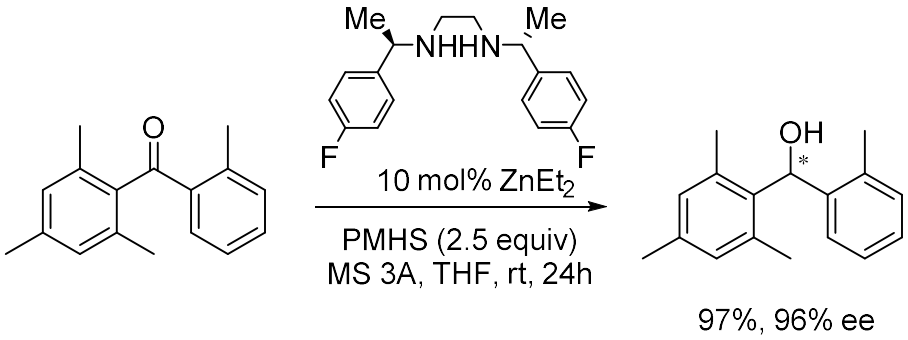

Scheme 1.5 Reduction catalyzed by zinc Lewis acid

Cozzi[51] and coworker also reported the application of zinc Lewis acid catalysts for the enantioselective reductions. When catecholborane was used as the source of hydride, a series of aromatic methyl ketones can be reduced to corresponding chiral alcohols by adding 4 mol% of chiral iminooxazoline (IMOX) ligand and $Zn(OTf)_2$ in situ. These catalytic reductions are performed in dichloromethane at -15ºC with high enantioselevtivities up to 93% ee and moderate yield as shown in Scheme 1.6.

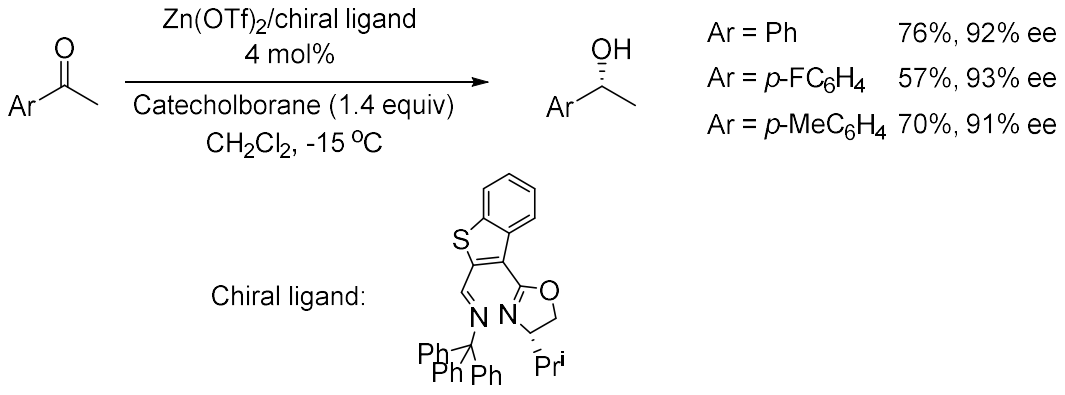

Scheme 1.6 Reductions catalyzed by chiral zinc Lewis acid.

1.1.3 Lewis acids used for polymerizations

Another important application of Lewis acids is the catalysis of a wide range of polymerization reactions.[52-55] For example, in the presence of Lewis acids such as rare-earth metal triflates, bis(silylketene acetal)s and dialdehydes can be polymerized via Mukaiyama aldol reaction, affording poly(hydroxy ester)s as products with high molecular weights and unique chain structure as shown in Table 1.4.[56]

Table 1.4 Lewis-Acid-Catayzed Aldol Polymerization.

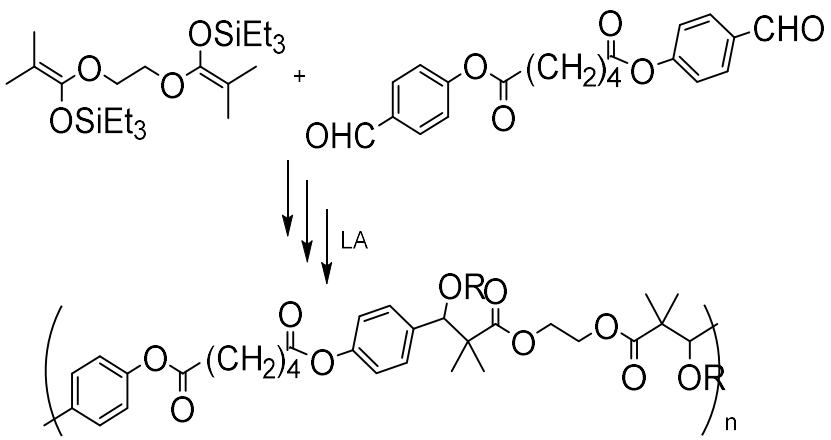

LA (mol %)	Yield (%)	Mn
$Sc(OTf)_3$ (10)	50	55 700
$Yb(OTf)_3$ (20)	15	11 300
$TiCl_4$ (200)	29	2 700

Recently, Cui's group[57] reported a series of multinuclear aluminum complexes that can initiate the ring-opening polymerization of ε-caprolactone and L-Lactide efficiently. Moreover, with addition of excess isopropyl alcohol, these complexes can also catalyze the

copolymerization of the two monomers with narrow molecular weight distributions and the copolymerization process shows “immortal” characters (Scheme 1.7).

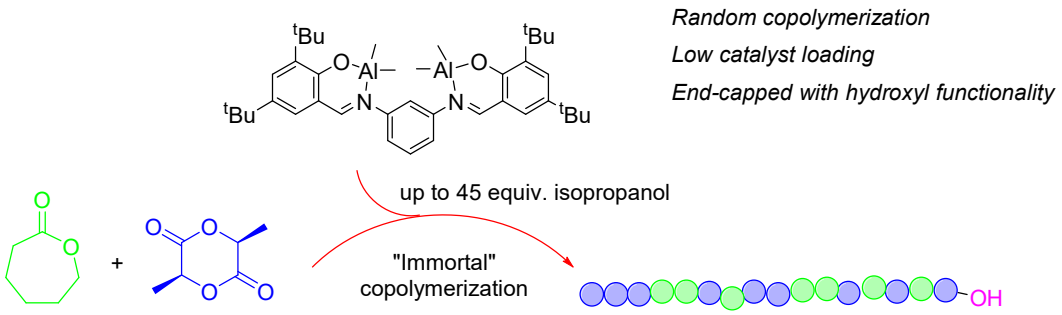

Scheme 1.7 Immortal copolymerization of ε-caprolactone and L-Lactide.

1.2 Aluminum based Lewis acids

It is not surprising that with the development of Lewis acid chemistry, a wide variety of Lewis acids based on various metals have been well investigated and documented. Arguably, the most important Lewis acids are compounds incorporating group 13 elements. This is because they are capable of accepting an additional electron lone pair in their three-coordinate, neutral state. Among these, aluminum-based Lewis acids are plausibly the most appealing because of their inexpensiveness and availability. As aluminum is the most abundant metallic element in the Earth’s crust (about 8.3% by weight).[58]

So far, aluminum Lewis acids have been found increasing important applications in both academia and industry. In 1986 Shibasaki[59] and coworkers reported the synthesis of a heterobimetallic complex through the reaction of (R)-BINOL and lithium aluminum hydride. This chiral aluminum complex can used as an efficient catalyst for asymmetric Michael addition reactions of a range of malonic esters and cyclic enones with good reactivity and enantioselectivity up to 99% as indicated in Scheme 1.8.

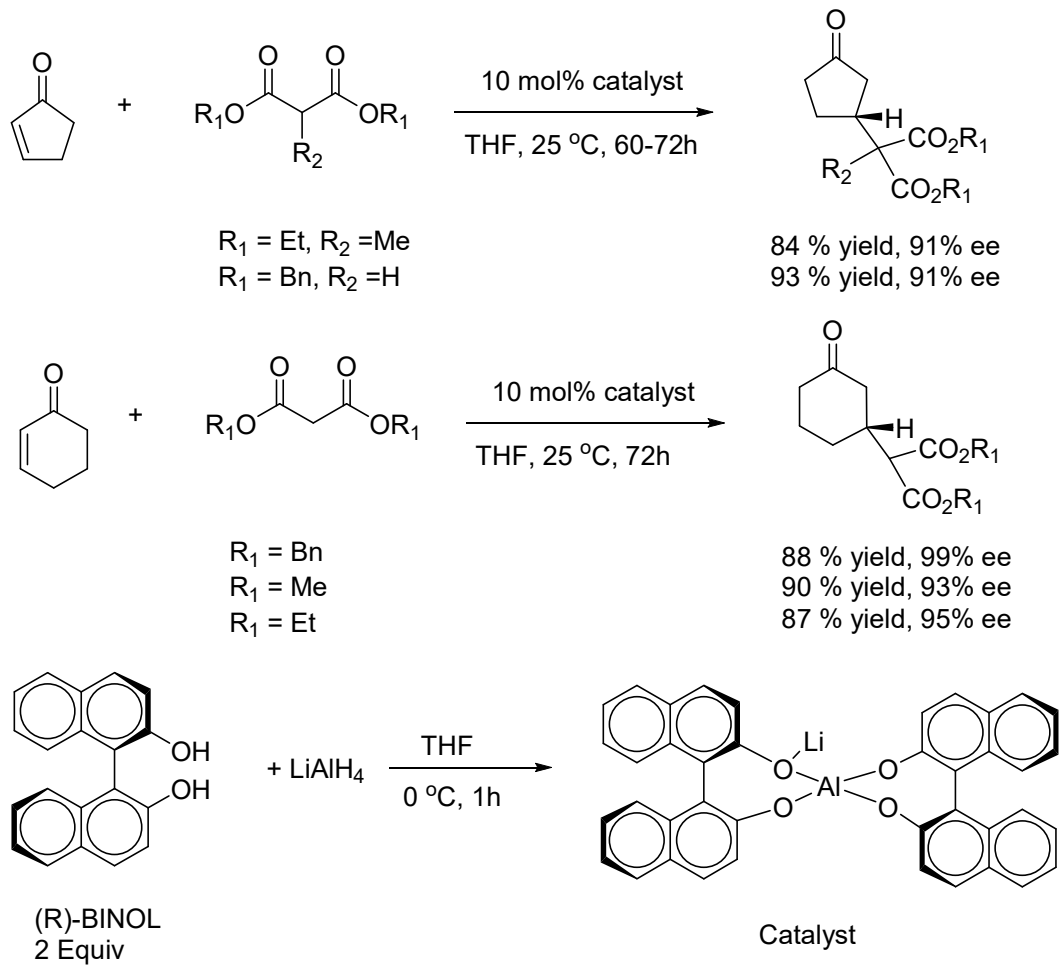

Scheme 1.8 Michael additions catalyzed by chiral aluminum complex.

Wang[60] and co-workers reported the preparation of several polysubstituted indanes through an unprecedented formal [2 + 3]-cycloaddition promoted by $AlCl_3$. When 1,2-DCE was used as solvent, in the presence of two equivs of $AlCl_3$, a large amount of 1,1-cyclopropanes can react with N-benzylic sulfonamides to form highly functionalized and stereoslective indane compounds with high yields. $AlCl_3$ also can be used as an efficient Lewis acid catalyst to promote the Silane Reduction of Glycopyranoside to prepare SGLT-2 inhibitor Empagliflozin.[61]

However, non-recyclable and corrosive properties of aluminum trichloride limit its wide-spread use. This could be avoided by the replacement of halogens with triflates (OTf;

Tf = O_2SCF_3) substituents, affording both higher stability and Lewis acidity. $Al(OTf)_3$ is evidently the most common triflate containing aluminum species that has been investigated in a variety of organic transformations. For example, Williams[62] reported that $Al(OTf)_3$ can promote the conversion of 3,4,6-Tri-O-acetyl-D-galactal to chiral bridgedbenzopyrans or 1-O-aryl-2-deoxy derivatives depending on different reaction conditions as shown in Scheme 1.9. These reactions are processed in a tandem fashion with high yields and stereoselectivity. It revealed a new and efficient approach to the synthesis of chiral chromenes, chromans and benzopyrans.

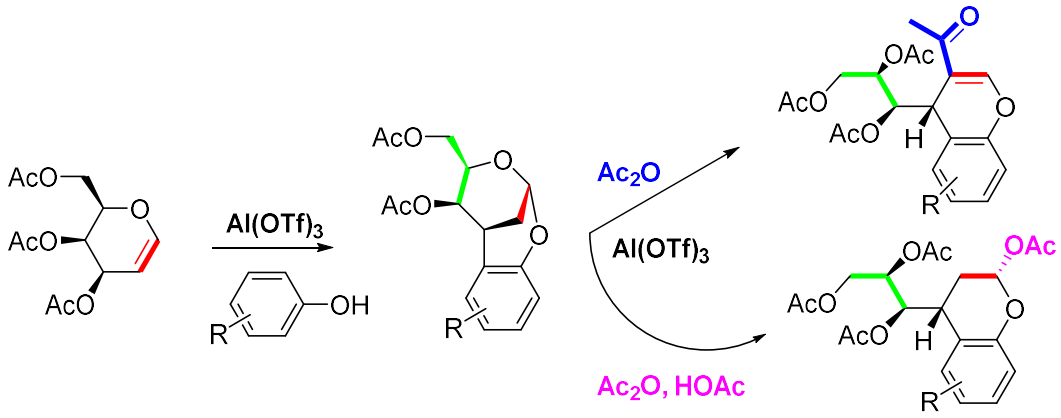

Scheme 1.9 Tandem reactions catalyzed by aluminum triflate.

As a cheap and non-toxic Lewis acid, $Al(OTf)_3$ was also found to be an efficient catalyst to construct a variety of tetrahydropyrido [1,2-a]indol-6-one skeletons via an intramolecular reaction following by protonation and Mannich-type nucleophilic addition of indoles.[63]

1.3 HBA activity

As already indicated, a large portion of Lewis acid catalytic systems, including the Al-based ones, were usually prepared and used in situ. This could be a big problem because in certain reaction conditions these Lewis acids are capable of generating hidden Brønsted

acids (HBAs) which also can catalyze the target organic transformations.[64-70] For instance, Pizzo[71] and co-workers reported that $AlCl_3 \cdot 2THF$ can be used as a reactive Lewis acid catalytic system for Diels-Alder transformations. But in this work all experimental procedures were performed at a benchtop without any attempts to eliminate the influence of air/moisture. As $AlCl_3$ is quite air- and moisture-sensitive[72], it can be concluded that hydrolysis of $AlCl_3$ cannot be avoided in this particular setting, resulting in the formation of a Brønsted acid. Therefore, the observed catalytic activity might have been performed by an HBA (presumably HCl).

In 2011 Hintermann[73] and co-workers reported a useful strategy to generate HBA and suggested several important control experiments to minimize the possibility of HBA activity. Oestreich[74] also reported an efficient Lewis acid catalyst for Diels-Alder reaction. Although the ferrocene-stabilized silicon cation used for the catalysis was deactivated in the presence of common hindered base dbpy (2,6-di-tertbutylpyridine) (Scheme 1.10), the Lewis acid activity was demonstrated by a serious of comparative experiments.

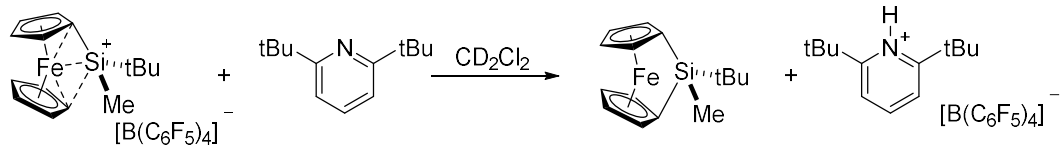

Scheme 1.10 Proposed proton release mechanism.

Hence, it is very meaningful to characterize the designed Lewis acids in order to identify the active species in corresponding Lewis acid catalysis.

1.4 β-Diketiminato Ligands

It is quite important to select a proper supporting ligand for Lewis acid catalyst because it can impact both the reactivity and selectivity of the resulting complex via its electronic and steric properties. In the past decades, various ligands has been investigated and documented to support aluminum-based Lewis acids, providing them with better stability, activity and selectivity. Perhaps the most outstanding representatives are the β-difunctional, monoanionic, chelating ligands as shown in Scheme 1.11.

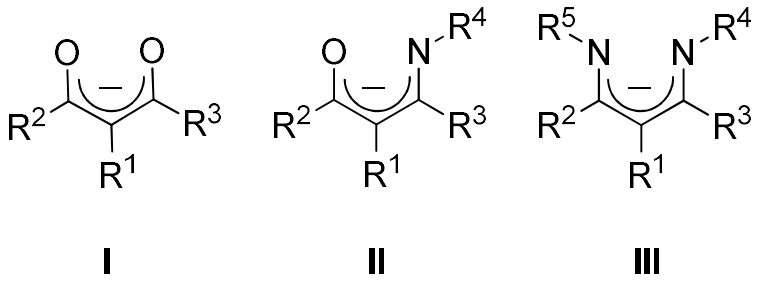

Scheme 1.11 β-difunctional, monoanionic, chelating ligands.

In the past five decades, large amount of experimental evidence have been generated on the research of β-diketonato I and β-enaminoketonato II ligands, which are widely used as chelating ligands in coordination chemistry.[75] However, β-diketiminato III ligands, which are also referred as "nacnac" ligands, have demonstrated their wide appeal in the new century. This is due to the possibility of various substituents on nitrogen, which might be hydrogen, alkyl, silyl or aryl groups.

The studies on β-diketiminato III ligands stared in the mid-1960s, focusing on the synthesis and structures of homoleptic M(II) β-diketiminates where M = Ni, Co, Cu.[76a-i] In the mid-1990s people recognized that β-diketiminato III ligands can act as useful cyclopentadienyl-like spectator ligands because they can form strong metal-ligand bonds

and possess exceptional and tunable steric demands.[77a,b] Since then, β-diketiminato III gained significantly increasing attentions and, hence, developed rapidly as an important ligand choice.[78] This class of ligands can coordinate to metals in a variety of bonding modes, as shown in Scheme 1.12.

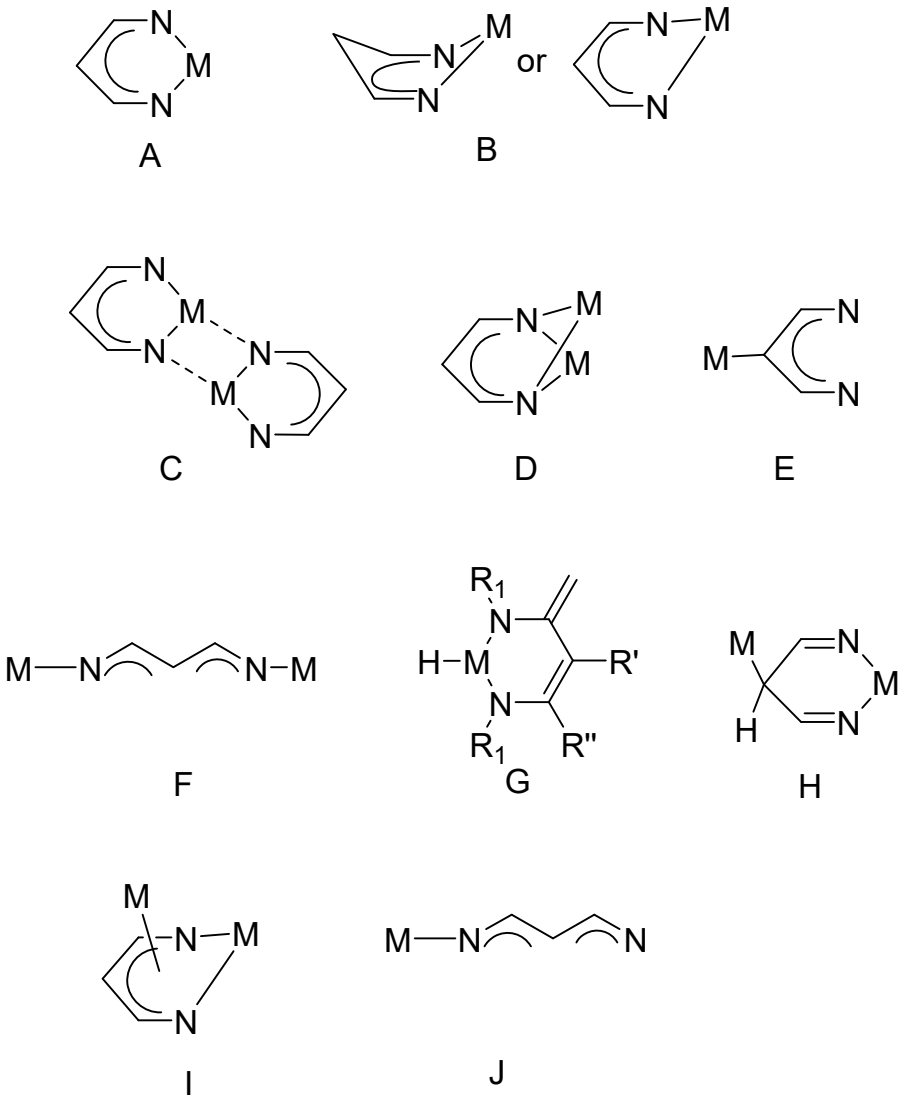

Scheme 1.12 Bonding modes of β-diketiminato III ligands to metals

The most common bonding mode is structure A, where both the two nitrogen atoms of the ligand coordinate to the metal in a N,N-chelating fashion and the resulting MNCCCN six-membered metallacyclic ring is planar. When the metal possesses empty d orbitals with appropriate symmetry, it can bond to the β-diketiminato III ligand in mode B, where the

MNCCCN ring lies in a boat fashion. In a binuclear complex, the β-diketiminato III ligand may adopt the type C binding mode, with one of the nitrogen is additionally bonded to the M centre of another molecule. In this instance, the metallacyclic rings could be in many conformations. In mode D both nitrogen atoms of the β-diketiminato III binuclear complex are four-coordinate. An example of a complex in which M is bound at the γ-C of the ligand backbone (type E) would be $[GeC(C(Me)N(C_6H_3{}^iPr_2\text{-}2,6))_2Cl_3]$.[79] Type F is different from C as both of the nitrogen atoms are three-coordinate and function as terminal ligands. Type G is a tautomer of type A or type B. Beside these, other bonding modes are also listed.

The β-diketiminato III ligands are widely used to support group 13 compounds. For example, a large amount of neutral boron and aluminum complexes supported by nacnac lingands have been reported as shown in Scheme 1.13. These ligands are also used to stabilize monocationic boron complexes. However, there are quite few examples were reported using nacnac ligands to stabilize dicationic boron complexes and cationic aluminum complexes.[80-82]

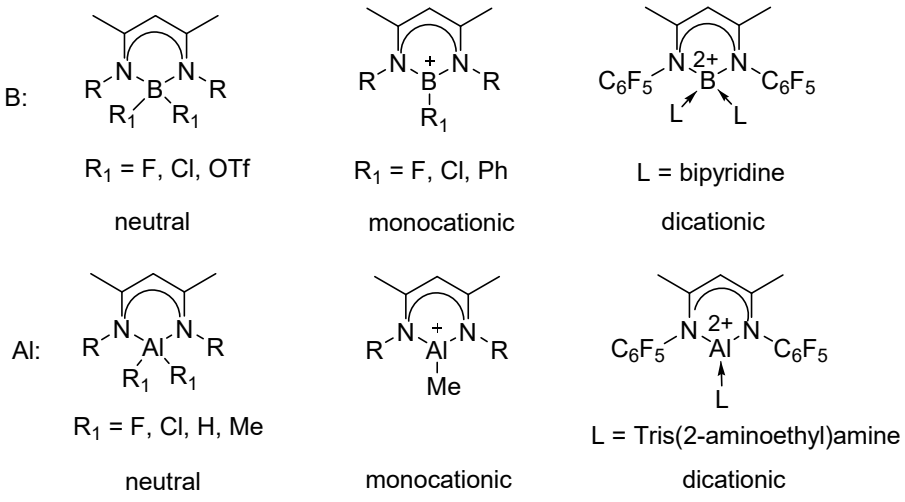

Scheme 1.13 Group 13 compounds supported by β-diketiminato III ligands

The β-diketiminato III ligands can be prepared using several synthetic routes, most of which involving the condensation reaction of a primary amine with either a β-diketone or 1,1,3,3-tetraethoxypropane. In 1968 McGeachin[83] reported the first synthetic route using a β-diketone to form β-diketiminato ligand as shown in Scheme 1.14.

.

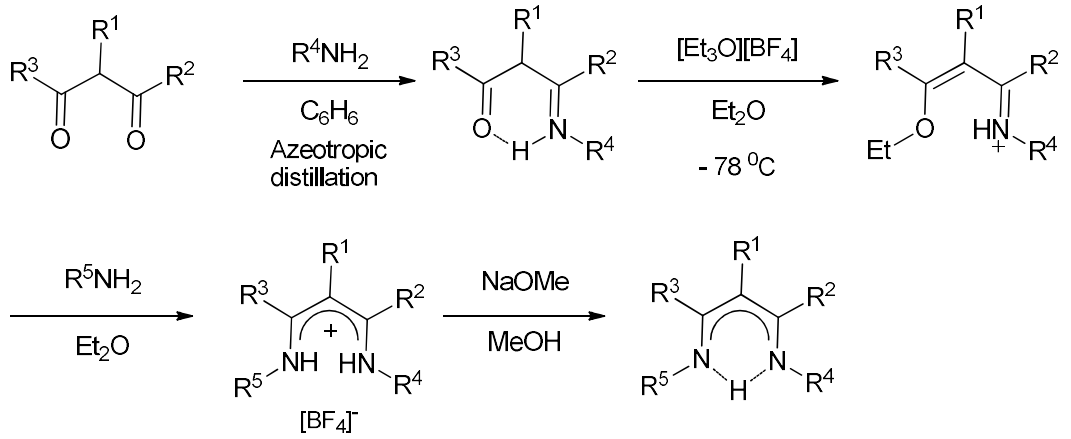

Scheme 1.14 Synthetic route to β-diketiminato ligands.

An alternative procedure involved converting a 1,3-diketone into a ketoketal and then into the β-diketimine through the condensation with analine as shown below.[84]

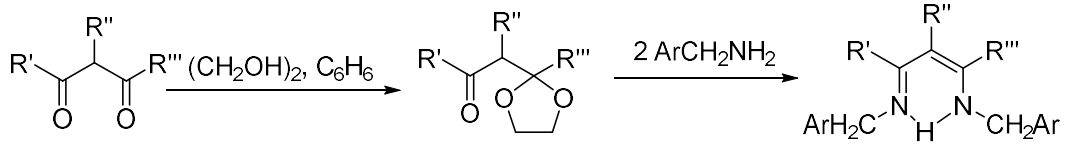

Scheme 1.15 Synthetic route to β-diketiminato ligands.

These ligands can also prepared from a β- diacetal such as 1,1,3,3-tetraalkoxypropane. In hot aqueous ethanol 1,1,3,3-tetraethoxypropane was treated with an aromatic amine hydrochloride for 1h, after which β-diketimine hydrochloride can be crystalized at ambient temperature. Then, the desired β-diketimine can be obtained by adding aqueous sodium hydroxide.[76b]

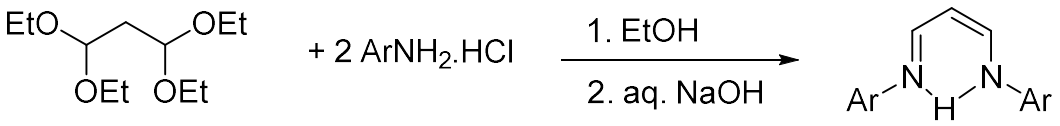

Scheme 1.16 Synthetic route to β-diketiminato ligands.

In 1997 Dip-substituted β-diketimine was first reported as a supporting ligand for Ni(II)- and Pd(II) catalysts used in ethylene polymerization.[85] Since then, it started to play an important part in many fields as a useful and common supporting ligand. Various metal complexes based on this kind of ligands have been investigated and widely used as catalysts for wide range of organic reactions.

1.5 Research objective

Based on all above mentioned observations, it is not surprising that aluminum Lewis acids have extensively been used for the catalysis of organic transformations including Diels–Alder cycloadditions. However, a recent book by Yamamoto and Ishihara[83] indicated that Al-catalyzed Diels-Alder reactions involving less reactive dienes and dienophiles were not well documented. Moreover, most of these Al-based catalytic systems were not well structurally characterized, lacking of identification of the active species. Hence, we synthesized several aluminum complexes based on different ligands and used them for the catalysis of a handful of Diels-Alder reactions involving less reactive dienes and dienophiles. Additional experiments were also performed to gain evidence against HBA activity.

Reference

1 Lewis, G.N. Valence and the Structure of Atoms and Molecules **1923**, 142.

2 Brønsted, J. N. *Recl. Trav. Chim. Pays-Bas* **1923**, *42*, 718.

3 Ooi, T.; Uraguchi, D.; Kagashima, N.; Maruoka, K. *Tetrahedron Lett.* **1997,** *38*, 5679.

4 Belen'kii, L. I.; Yakubov, A. P.; Gol'dfarb, Y. L. *Zh. Org. Khim*. **1970**, *6*, 2518.

5 Erre, C. H.; Roussel, C. *Bull. Soc. Chim. Fr.* **1984**, 449.

6 Singh, P. K.; Rajeswari, K.; Ulu, K. R. *Indian J. Chem.*, Sect. B **1985**, 24B, 651.

7 Uto, K.; Sakamoto, T.; Matsumoto, K.; Kikugawa, Y. *Heterocycles* **1996**, *43*, 633.

8 Boulanger, W. A.; Flavin, M. T.; Kucherenko, A.; Sheynkman, A. K. Patent US 5489697, 1996.

9 Snider, B. B.; Rodini, D. J.; Kirk, T. C.; Cordova, R. *J. Am. Chem. Soc.* **1982,** *104*, 555.

10 Snider, B. B.; Phillips, G. B. *J. Org. Chem.* **1983,** *48*, 464.

11 Mahrwald, R. *Chem. Rev.* **1999,** *99*, 1095.

12 *Cycloaddition Reactions in Organic Synthesis* (Eds.: Kobayashi, S.; Jorgensen, K.-A.), Wiley-VCH, Weinheim, 2001.

13 Moberg, C. *Lewis Acid–Lewis Base Catalysis.* In *Cooperative Catalysis,* Wiley-VCH Verlag GmbH & Co. KGaA: 2015; pp 35.

14 Shambayati, S.; Schreiber, S.L. In *Comprehensive Organic Synthesis*, B.M. Trost, I. Fleming, L.A. Paquette (Eds.), Vol. 1, Chapter 1.10, p. 283, Pergamon Press, New York (1991).

15 Santelli, M.; Pons, J.-M. *Lewis Acids and Selectivity in Organic Synthesis*, CRC Press, Boca Raton, 1995.

16 Oppolzer, W. In *Comprehensive Organic Synthesis*, Trost, B.M.; Fleming, I. (Eds.), Vol. 5, Chapter 4.1, Pergamon: Oxford, 1991; pp 315.

17 Mukaiyama, T.; Banno,K.; Narasaka, K. *J. Am. Chem. Soc*. **1974**, *96*, 7503.

18 Mukaiyama, T. Angew. Chem. Int. Ed. Engl. **1977,** 16, 817.

19 Olah, G. A.; Krishnamuri, R.; Prakash, G. K. S. In *Comprehensive Organic Synthesis* (B. M. Trost, I.Fleming, eds), Vol. 3, Ch. 1.8. Pergamon Press, Oxford (1991).

20 Sundararajan, G.; Prabagaran, N.; Varghese, B. *Org. Lett.* **2001,** *3*, 1973.

21 Borodin observed the dimerization of acetaldehyde to 3-hydroxybutanal under acidic conditions.

22 Wurtz, C. A. *Bull. Soc. Chim. Fr.***1872**, *17*: 436.

23 Wurtz, C. A. *J. Prakt. Chem.* **1872**, *5*, 457.

24 Wurtz, C. A. Comptes rendus de l'Académie des sciences (in French) **1872**, 74, 1361.

25 Eliel, E. L.; Wilen, S. H. *Stereochemistry of Organic Compounds*; Wiley: New York, 1994; 835.

26 Siegel, C.; Thorton, E. R. *J. Am. Chem. Soc.* **1989**, *111*, 5722.

27 Naruse, Y.; Ukai, J.; Ikeda, N.; Yamamoto, H. *Chem. Lett*. **1985**, 1451.

28 Liu, S.-Y.; Hills, I. D.; Fu, G. C. *J. Am. Chem. Soc.* **2005,** *127*, 15352.

29 Corkey, B. K.; Toste, F. D. *J. Am. Chem. Soc.* **2005,** *127*, 17168.

31 Lu, X. *Org. Lett.* **2004**, *6*, 2813.

32 Lee, G.; Shiau, C.; Chen, C.; Chen; J. *J. Org. Chem.* **1995**, *60*, 3565.

33 Resek, J. E. *J. Org. Chem*. **2008**, *73*, 9792.

34 Maruoka, K.; Hoshino, Y.; Shirasaka, T.; Yamamoto, H. *Tetrahedron Lett.* **1988,** *29*, 3967.

35 Mikami, K.; Terada, M.; Nakai, T. *J. Am. Chem. Soc.* **1989**, *111*, 1940.

36 Mikami, K.; Terada, M.; Nakai, T. *J. Am. Chem. Soc.* **1990**, *112*, 3949 .

37 Pandiaraju, S.; Chen, G.; Lough, A.; Yudin, A. K. *J. Am. Chem. Soc.* **2001**, *123*, 3850.

38 Hao, J.; Hatano, M.; Mikami, K. *Org. Lett.* **2000**, *2*, 4059 .

39 Ruck, R. T.; Jacobsen, E. N. *J. Am. Chem. Soc*. **2002**, *124*, 2882.

40 Evans, D. A.; Tregay, S. W.; Burgey, C. S.; Paras, N. A.; Vojkovsky, T. *J. Am. Chem. Soc*. **2000**, *122*, 7936.

41 Evans, D. A.; Wu, J. *J. Am. Chem. Soc*. **2005**, *127*, 8006.

42 Wassermann, A. *J. Chem. Soc.* **1942**, 618.

43 *Lewis Acids in Organic Synthesis*; Yamamoto, H., Ed.; Wiley-VCH: Weinhelm, 2000; Vols. 1 and 2.

44 Yate, P.; Eaton, P. *J. Am. Chem. Soc.* **1960**, *82*, 4436.

45 Kagan, H. B.; Riant, O. *Chem. Rev.* **1992,** *92*, 1007.

46 Narasaka, K. Synthesis 1991,l.

47 Hawkins, J. M.; Loren, S. *J. Am. Chem. Soc.* **1991**,*112*, 7794.

48 Kelly, T. R.; Whiting, A.; Chandrakumar, N. S. *J. Am. Chem. Soc.* **1986,** *108*, 3510.

49 Kündig, E. P.; Saudan, C. M.; Alezra, V.; Viton, F.; Bernardinelli, G. *Angew. Chem. Int. Ed.* **2001,** *40*, 44814.

50 Ushio, H.; Mikami, K. *Tetrahedron Lett.* **2005,** *46*, 2903.

51 Locatelli, M.; Cozzi, P. G. *Angew. Chem. Int. Ed.* **2003,** *42*, 4928.

52 Isobe, Y.; Fujioka, D.; Habaue, S.; Okamoto, Y. *J. Am. Chem. Soc*. **2001**, *123*, 7180.

53 Isobe, Y.; Nakano, T.; Okamoto, Y. *J. Polym. Sci., Part A: Polym. Chem.* **2001**, *39*, 1463.

54 Baraki, H.; Habaue, S.; Okamoto, Y. *Macromolecules* **2001**, *34*, 4724.

55 Möller, M.; Nederberg, F.; Lim, L. S.; Kånge, R.; Hawker, C. J.; Hedrick, J. L.; Gu, Y.; Shah, R.; Abbott, N. L. *J. Polym. Sci., Part A: Polym. Chem.* **2001**, *39*, 3529.

56 Komura, K.; Itsuno, S.; Ito, K. *Chem. Commun*. **1999**, 35.

57 Li, L.; Liu, B.; Liu, D.; Wu, C.; Li, S.; Liu, B.; Cui, D. *Organometallics* **2014,** *33*, 6474.

58 Greenwood, N. N.; Earnshaw, A. (1997). “Chemistry of the Elements” (2nd ed)”, Oxford: Butterworth–Heinemann, pp 217.

59 Arai, T.; Sasai, H.; Aoe, K.-i.; Okamura, K.; Date, T.; Shibasaki, M. *Angew. Chem.* **1996,** *108*, 103.

60 Zhu, M.; Liu, J.; Yu, J.; Chen, L.; Zhang, C.; Wang, L. *Org. Lett.* **2014,** *16*, 1856.

61 Wang, X.-j.; Zhang, L.; Byrne, D.; Nummy, L.; Weber, D.; Krishnamurthy, D.; Yee, N.; Senanayake, C. H. *Org. Lett.* **2014,** *16*, 4090.

62 Simelane, S. B.; Kinfe, H. H.; Muller, A.; Williams, D. B. G. *Org. Lett.* **2014,** *16*, 4543.

63 Wang, J.-J.; Zhou, A.-X.; Wang, G.-W.; Yang, S.-D. *Adv. Synth. Catal.* **2014,** *356*, 3356.

64 Fürstner, A.; Szillat, H.; Gabor, B.; Mynott, R. *J. Am. Chem. Soc*. **1998,** *120*, 8305.

65 Liu, P. N.; Zhou, Z. Y.; Lau, C. P. *Chem. Eur. J.* **2007,** *13*, 8610.

66 Dumeunier, R.; Markó, I. E. *Tetrahedron Lett.* **2004,** *45*, 825.

67 Rosenfeld, D. C.; Shekhar, S.; Takemiya, A.; Utsunomiya, M.; Hartwig, J. F. *Org. Lett.* **2006,** *8*, 4179.

68 Tschan, M. J. L.; Thomas, C. M.; Strub, H.; Carpentier, J.-F. *Adv. Synth. Catal.* **2009,** *351*, 2496.

69 Mathia, F.; Szolcsanyi, P. *Org. Biomol. Chem.* **2012,** *10*, 2830.

70 Hague, C.; Patmore, N. J.; Frost, C. G.; Mahon, M. F.; Weller, A. S. *Chem. Commun.* **2001,** 2286.

71 Fringuelli, F.; Girotti, R.; Pizzo, F.; Vaccaro, L. *Org. Lett.* **2006,** *8*, 2487.

72 Cowley, A. H.; Cushner, M. C.; Davis, R. E.; Riley, P. E. *Inorg. Chem.* **1981,** *20*, 1179.

73 Dang, T. T.; Boeck, F.; Hintermann, L. *J. Org. Chem.* **2011,** *76*, 9353.

74 Schmidt, R. K.; Müther, K.; Mück-Lichtenfeld, C.; Grimme, S.; Oestreich, M. *J. Am. Chem. Soc.***2012,** *134*, 4421.

75 Holm, R. H.; Everett, G. W.; Chakravorty, A. Prog. *Inorg. Chem.***1966**, *7*, 83.

76 (a) Dorman, L. C. *Tetrahedron Lett*. **1966**, *4*, 459; (b) Barry, W. J.; Finar, I.; Mooney, E. F. *Spectrochim. Acta.* **1965**, *21*, 1095; (c) Bonnett, R.; Bradley, D. C.; Fisher, K. J. *Chem. Commun*. **1968**, 886; (d) Bonnett, R.; Bradley, D. C.; Fisher, K. J.; Rendall, I. F. *J. Chem. Soc*. *(A)* **1971**, 1622; (e) Parks, J. E.; Holm, R. H. *Inorg. Chem.* **1968**, *7*, 1408; (f) Richards, C. P.; Webb, G. A. *J. Inorg. Nucl. Chem*. **1969**, *31*, 3459; (g) Tsybina, N. M.; Vinokurov, V. G.; Protopopova, T. V.; Skoldinov, A. P. *J. Gen. Chem., USSR* **1966**, *36*, 1383; (h) Cotton, F.

A.; DeBoer, B. G.; Pipal, J. R. *Inorg. Chem*. **1970**, *9*, 783; (i) Elder, M.; Penfold, B. R. *J. Chem. Soc. (A)* **1969**, 2556; (k) Honeybourne, C. L.; Webb, G. A. *Mol. Phys*. **1969**, *17*, 17.

77 (a) Hitchcock, P. B.; Lappert, M. F.; Liu, D.-S. J. Chem. Soc., *Chem. Commun*. **1994**, 1699; (b) Hitchcock, P. B.; Lappert, M. F.; Liu, D.-S. J. Chem. Soc., *Chem. Commun*. **1994**, 2637.

78 Bourget-Merle, L.; Lappert, M. F.; Severn, J. R. *Chem. Rev.* **2002,** *102*, 3031.

79 Räke, B.; Zülch, F.; Ding, Y.; Prust, J.; Roesky, H. W.; Noltemeyer, M.; Schmidt, H. G. *Z. Anorg. Allg. Chem.* **2001,** *627*, 836.

80 Vidovic, D.; Findlater, M.; Cowley, A H. *J. Am. Chem. Soc.* **2007,** *129*, 11296.

81 Radzewich, C E.; Guzei, I A.; Jordan, R F. *J. Am. Chem. Soc.* **1999,** *121*, 8673.

82 Vidovic, D.; Findlater, M.; Gregor, R.; Cowley, A H. *J. Organomet. Chem.* **2007,** *692*, 5683.

83 McGeachin, S. G. *Can. J. Chem*. **1968**, *46*, 1903.

84 Dorman, L. C. *Tetrahedron Lett.* **1966**, *4*, 459.

85 Feldman, J.; McLain, S. J.; Parthasarathy, A.; Marshall, W. J.; Calabrese, C. J.; Arthur, S. D. *Organometallics* **1997**, *16*, 1514.

86 Acid Catalysis in Modern Organic Synthesis, Vol. 1 and 2 (Eds.: H. Yamamoto, K. Ishihara), Wiley-VCH, Weinheim, 20.

Chapter 2

Synthesis and characterization of β-diketiminate-supported aluminum compounds

The importance of Lewis acids in various catalytic and stoichiometric organic transformations has been extensively reported.[1a,b,c] Arguably, the most widely used Lewis acids are simple group 13 trihalides such as $BF_3 \cdot OEt_2$ and $AlCl_3$. However, their applications are limited because these compounds are usually non-recyclable and corrosive. In recent years, a quantity of reports have surfaced describing the use of triflate substrates in place of halogens in order not only to increase stability but also to enhadnce the activity of the target Lewis acids. Examples include LiOTf, $B(OTf)_3$ and $Sc(OTf)_3$. However, the majority of reaction conditions have been optimized simply by employing different triflate-containing metal compounds. Only a handful of reports investigated catalytic properties of metal triflate together with organic ligands of which the majority had been prepared and used in situ. As it is the case with many other elements, $Al(OTf)_3$ is the most common triflate containing aluminum species that has been investigated in a variety of organic transformations. Few compounds containing "Al-OTf" fragment(s) have been reported but predominantly for structural information. In fact, structural information on aluminum compounds containing triflate substituents is generally limited and only one of these compounds has been explored as a catalyst but with limited success. Thus we set to explore the influence of triflate substituents on Lewis acidic properties of several β-diketiminate-supported aluminum compounds and their potential application as Lewis acid catalysts.

2.1 Synthesis of β-diketiminato ligands

A series of symmetric and asymmetric monoanionic β-diketiminato ligands with different substituents at nitrogen atoms were screened in this chapter as summarized in Scheme 2.1.

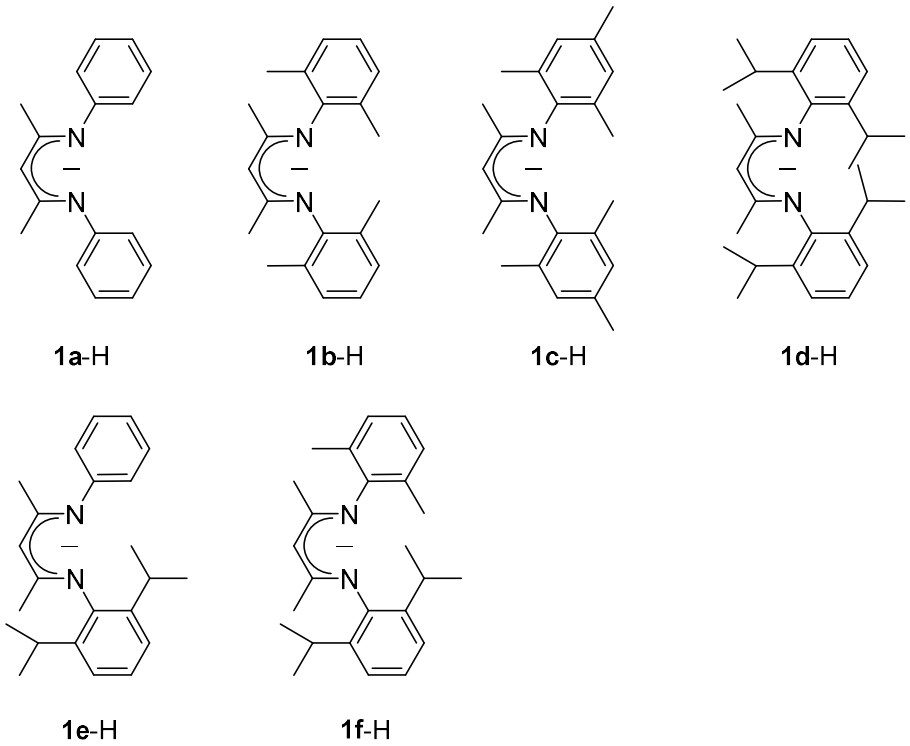

Scheme 2.1 β-Diketiminato Ligands used.

The corresponding LH ligands were synthesized though condensation of 2,4-pentanedione and a series of anilines. As shown in Scheme 2.2, the symmetric LH ligands **1a** -**1d** can be synthesized by simple reflux of the two reagents in toluene together with 1 equiv of *para*-toluenesulfonic acid monohydrate. The water generated can be removed by the use of a Dean–Stark apparatus. After workup, all these four ligands can be isolated as colorless crystals with high yield (> 85%).

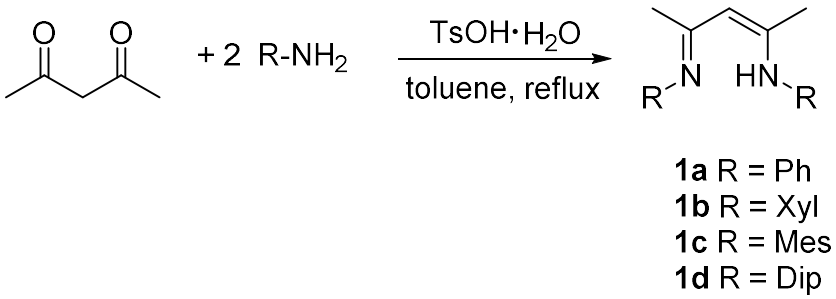

Scheme 2.2 synthesis of LH ligands **1a** – **1d**

Two asymmetric LH ligands **1e** and **1f** were prepared by a two-step method as shown in Scheme 2.3.[2] In the first step, 2-(2,6-Diisopropylphenylimido)-2-pentene-4-one was synthesized from 2,4-pentanedione and 2,6-diisopropylaniline by dehydration in toluene catalyzed by concentrated H_2SO_4. Then, the resulting β-ketoamine was subsequently treated with corresponding anilines in the presence of 1 equiv of para-toluenesulfonic acid monohydrate with water removed by a Dean-Stark apparatus. After work up the desired β-diketimines were recrystallized from cold ethanol in good yield (~ 80%).

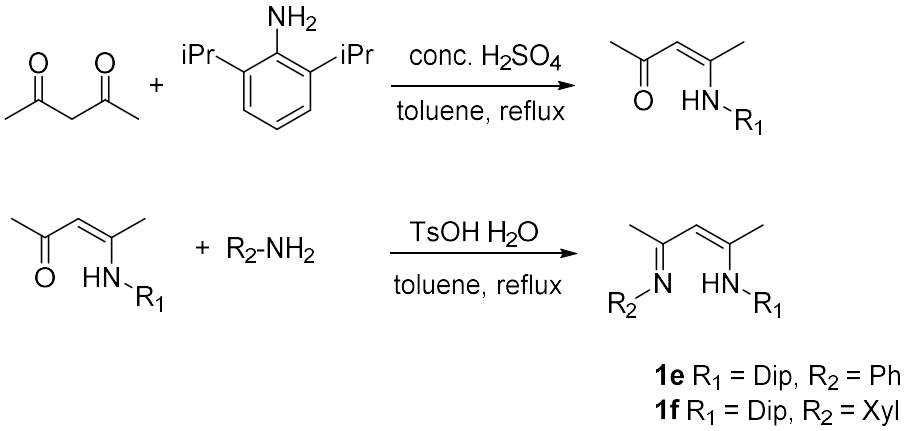

Scheme 2.3 Synthesis of asymmetric LH ligands **1e** and **1f**

In order to study the catalytic properties of aluminum bitriflates incorporating nacnac L^- ligands, it was necessary to prepare aluminum dichloro complexes as precursors to the aluminum bistriflate complexes. For this purpose several strategies were carried out to optimize the synthesis of the aforementioned complexes and the most important results are summarized in the following section.

2.2 Synthesis of $LAlCl_2$ precursors.

In order to find a convenient and a high-yield method to prepare the aluminum dichloro complexes ($LAlCl_2$), a variety of salt elimination approaches such as potassium and lithium salt eliminations were examined. As shown in Scheme 2.4, the LH ligands were first treated with potassium bis(trimethylsilyl)amide (KHMDS) in toluene at room temperature.[3,4] After stirring the reaction mixture overnight a volatile oil $HN(SiMe_3)_2$ was formed as a by-product. After removing $HN(SiMe_3)_2$ under reduced pressure, 1.05 equiv of $AlCl_3$ was added at low temperature. Unfortunately, NMR spectroscopic analysis showed that besides the desired aluminum dichloro compounds several unidentified impurities were also present in the crude reaction mixture. Several attempts have been made to purify the desired product but all of them were unsuccessful.

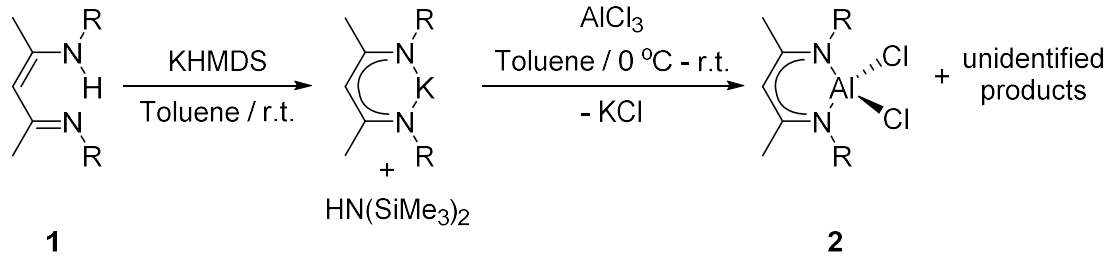

Scheme 2.4 Attempted synthesis of complexes **2** via Potassium Salt Elimination.

Since the potassium salt elimination method appeared not to be an ideal approach for the synthesis of aluminum dichloro complexes, we decided to switch to lithium salt elimination. As shown in Scheme 2.5, LiHMDS was used as a base to deprotonate the LH ligand instead of KHMDS. As before, the elimination was carried out in toluene at room temperature. After stirring overnight the side product $HN(SiMe_3)_2$ was removed from the reaction mixture by vacuum and the resulted lithium salt was re-dissolved in toluene before 1.05 equiv of $AlCl_3$ was added to the reaction mixture. To our delight, after lithium chloride was

filtered away and toluene was removed under reduced pressure, pure product can be obtained by washing with hexane in good yield.

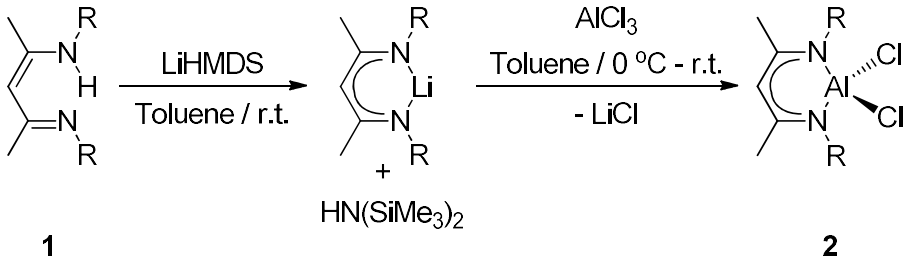

Scheme 2.5 Synthesis of compound **2** via Lithium Salt Elimination, LiHMDS as a base.

Inspired by this achievement, we decided to investigate a more convenient strategy to synthesize aluminum dichloride complexes as the abovementioned method was time consuming due to reaction times and the need to remove the by-product ($HN(SiMe_3)_2$). Therefore, the use of a more reactive base *n*-butyl lithium (^{n}BuLi) that does not produce a potentially reactive by-product was our choice. As shown in Scheme 2.6, the lithium salt elimination can be completed in 1 hour when the ligands were treated with ^{n}BuLi in toluene at 0 °C. $AlCl_3$ was subsequently added without any extra treatment of the reaction mixture. Six aluminum dichloride complexes **2a-2f** were synthesized using this method in high yields (> 80%).

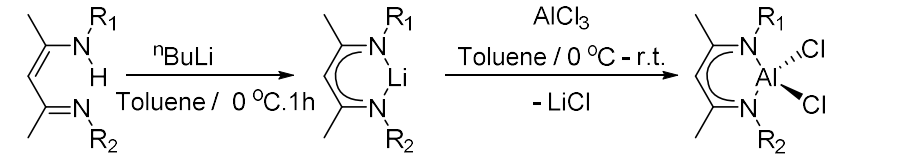

1a $R_1 = R_2 =$ Ph
1b $R_1 = R_2 =$ Xyl
1c $R_1 = R_2 =$ Mes
1d $R_1 = R_2 =$ Dip
1e $R_1 =$ Dip, $R_2 =$ Ph
1f $R_1 =$ Dip, $R_2 =$ xyl

2a $R_1 = R_2 =$ Ph
2b $R_1 = R_2 =$ Xyl
2c $R_1 = R_2 =$ Mes
2d $R_1 = R_2 =$ Dip
2e $R_1 =$ Dip, $R_2 =$ Ph
2f $R_1 =$ Dip, $R_2 =$ xyl

Scheme 2.6 Synthesis of compound **2** via Lithium Salt Elimination, ^{n}BuLi as a base.

^{1}H NMR spectroscopic identifications of **2a**-**2f** revealed a dramatic γ-H chemical shift from ~4.8 ppm to 5.4 ppm compared to their LH ligands, indicating the formation of new compounds. ^{27}Al NMR spectroscopic identifications of **2a**-**2f** revealed the presence of a δ_{Al} signal around 103 ppm for all six precursors (Table 2.2), while the other multinuclear NMR data were consistent with the reported values.[5,6] Moreover, crystals of compounds **2c** and **2f** suitable for X-ray analysis were grown from a toluene/hexane solvent mixture. Molecular structures of these compounds are shown in Figure 2.1 and Figure 2.2, with the crystallographic data summarized in Table 2.1.

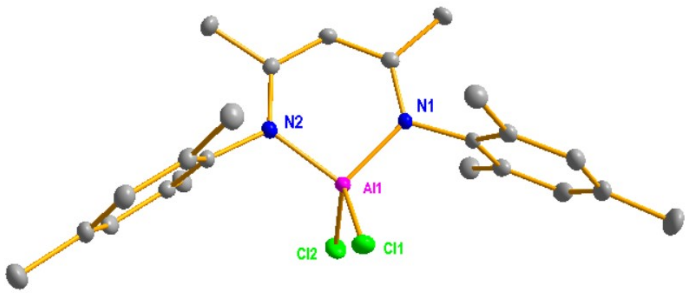

Figure 2.1 Molecular structure for **2c**.

Thermal ellipsoids have been drawn at 50% probability level. All hydrogen atoms have been omitted for clarity. Selected bond lengths (Å) and angles (°): Al1-N1 1.8582(12), Al1–N2 1.8633(12), Al1-Cl1 2.1299(6), Al1-Cl2 2.1295(6), N1-Al1-N2 98.94(5), Cl1-Al1-Cl2 106.54(2).

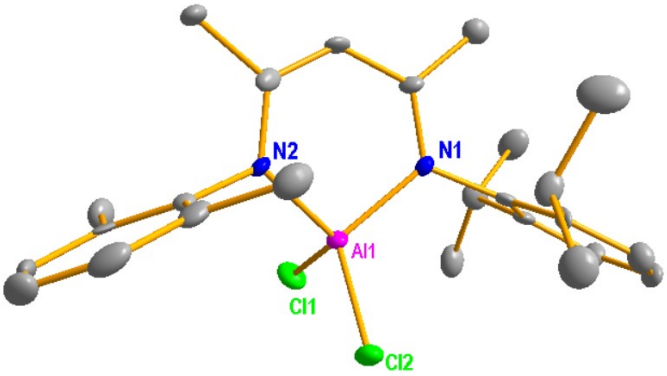

Figure 2.2 Molecular structure for **2f**.

Thermal ellipsoids have been drawn at 50% probability level. All hydrogen atoms have been omitted for clarity. Selected bond lengths (Å) and angles (°): Al1-N1 1.860(7), Al1–N2 1.846(9), Al1-Cl1 2.124(7), Al1-Cl2 2.116(9), N1-Al1-N2 99.31(8), Cl1-Al1-Cl2 109.10(3).

The central aluminum atoms of both the two complexes are four-coordinate, adopting distorted tetrahedral geometries. The Al-Cl bond lengths for **2c** (2.1299(6) and 2.1295(6) Å) and **2f** (2.124(7) and 2.116(9) Å) are similar with that reported by Kemp (2.1253(10) and 2.1146(10) Å for ^{Dip}DAB-$AlCl_2$ (^{Dip}DAB = Dip-substituted diazabutadiene))[7] and Jordan (2.124(2) and 2.113(2) Å for $\{Me_2NC(N^iPr)_2\}AlCl_2$)[8], but shorter than that reported by Dagorne (2.174(1) Å for (bis-phenol imidazolinium)Al(CH_3)(Cl))[9] and Roesky (2.1531(11) Å for [(3,5-^{t}Bu$_2$-N-CH=C($SiMe_3$)-pz)AlCl(3,5-^{t}Bu$_2$pz)]).[10]

Table 2.1 Summary of the crystallographic data for compounds **2c**, 2**f**

	2c	**2f**
Formula	$C_{23}H_{29}AlCl_2N_2$	$C_{25}H_{33}AlCl_2N_2$
Formula weight	431.36	459.41
Crystal system	triclinic	monoclinic
Space group	P -1	P 1 21/n 1
a /Å	7.9153(7)	11.8734(18)
b /Å	8.6925(7)	15.792(2)
c /Å	18.0519(14)	15.792(2)
β/°	93.343(2)	108.616(4)
V / Å^3	1139.58(16)	2550.3(6)
Z	2	4
Dc/ g cm^{-3}	1.257	1.197
F(000)	456	976
Crystal size/ mm	0.200 x 0.380 x 0.400	0.010 x 0.020 x 0.240
θ range/°	2.80 to 30.94	2.69 to 25.07
No. of reflns collected	28389	30483
No. of indep reflns	7218	4514
*R*1 [*I* >2σ (*I*)]	0.0420	0.0597
wR2 (all data)	0.1157	0.1526
Peak and hole/e Å^{-3}	0.495 and -0.420	0.380 and -0.402

All the six aluminum dichloro complexes were well characterized by ^{1}H, ^{13}C and ^{27}Al NMR spectroscopic analysis and used as precursors for the preparation of target aluminum bistriflate complexes.

2.3 Synthesis of LAl(OTf)$_2$

The target aluminum bistriflate complexes were synthesized using the triflate-for-chloride exchange procedure between pre-prepared aluminum dichloro complexes and silver triflate (AgOTf), which seemed to be the most appropriate reagent for this kind of exchange.[11] As shown in Scheme 2.7, complexes **2a**-**2f** can react with two equiv of silver triflate, in the absence of light, in a non-coordination solvent such as 1,2-difluorobenzene, affording aluminum bistriflate complexes **3a**-**3f**. The substrates exchange was clearly supported by

^{27}Al NMR spectroscopy as an upfield δ_{Al} signal around 60 ppm displaced the original δ_{Al} signal of $LAlCl_2$ precursors around 103 ppm as shown in Table 2.2. These complexes were also identified by the presence of a δ_F signal around -77.3 ppm, which is different from the δ_F value observed for a free triflate anion at ~ -79 ppm.[12]

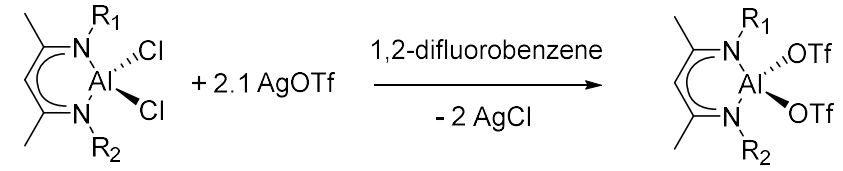

2a $R_1 = R_2$ = Ph
2b $R_1 = R_2$ = Xyl
2c $R_1 = R_2$ = Mes
2d $R_1 = R_2$ = Dip
2e R_1 = Dip, R_2 = Ph
2f R_1 = Dip, R_2 = xyl

3a $R_1 = R_2$ = Ph
3b $R_1 = R_2$ = Xyl
3c $R_1 = R_2$ = Mes
3d $R_1 = R_2$ = Dip
3e R_1 = Dip, R_2 = Ph
3f R_1 = Dip, R_2 = xyl

Scheme 2.7 Synthesis of aluminum bistriflate complexes

Table 2.2 ^{27}Al NMR (ppm) for complexes **2** and **3**

2a	102	**3a**	64
2b	101	**3b**	64
2c	101	**3c**	63
2d	102	**3d**	56
2e	102	**3e**	66
2f	102	**3f**	64

Complex **3a** was quite difficult to isolate and purify possibly due to more-than-expected air/moisture sensitivity, even though we managed to obtain few crystals that were used for single crystal X-ray and NMR spectroscopic analyses. The other complexes **3b- 3f** were all prepared in good yield and characterized by multinuclear NMR spectroscopic analysis. Crystals for these complexes were grown from a concentrated 1,2-difluorobenzene solution which was layered with *n*-hexane. The molecular structures of compounds **3a-3f** are shown in Figure 2.3-2.8, together with the selected bond lengths and angles, while the

crystallographic data are summarized in Table 2.4. Crystallographic characterizations of **3a** through **3f** showed that these bistriflate compounds, reminiscent of the dichloro precursors, were four-coordinate. This might be a bit unusual considering (i) possible multidentate nature of triflate substrates[11] and (ii) the ability of similar Al-based complexes to expand the coordination number to six.[13] The Al-N bond lengths and the N1-Al1-N2 bond angles for **3c**, **3d** and **3f** have shortened (~ 0.03 Å, Table 2.3) and widened (~ 3°), respectively, with reference to complexes **2c**, **2d**[14] and **2f**, potentially hinting at a decrease in electron density at the aluminum centers after the ligand exchange. In addition, the Al-N bond lengths for complexes **3a** – **3d** decreased gradually by ~ 0.02 Å, which might be due to the increasing electron donating group on N-aryl ring.

Table 2.3 Al-N bond lengths (Å) for complexes **2** and **3**

2a	-	**3a**	1.826(4) 1.828(4)
2b	-	**3b**	1.8306(16) 1.8322(16)
2c	1.8582(12) 1.8633(12)	**3c**	1.8350(19) 1.8377(19)
2d	1.8663(9) 1.8843(9)	**3d**	1.841(3) 1.853(3)
2e	-	**3e**	1.830(6) 1.843(6)
2f	1.846(9) 1.860(7)	**3f**	1.8363(10) 1.8399(10)

Furthermore, the values for the Al-O (i.e. Al-OTf) bond in **3a** (1.767(3) and 1.755(4) Å), **3b** (1.7570(14) and 1.7611(14) Å), **3c** (1.7605(17) and 1.7652(19)Å), **3d** (1.765(3) and 1.769(3)Å), **3e** (1 1.756(5) and 1.768(5) Å), and **3f** (1.7686(9) and 1.7630(9) Å) provide additional evidence for the electron deficiency at the central aluminum atoms as these Al-O bond lengths are the shortest with respect to the other crystallographically elucidated triflate-containing aluminum compounds with Al-OTf bond lengths ranging from 1.807(10) to 2.074(4) Å.[15a,b,c,d]

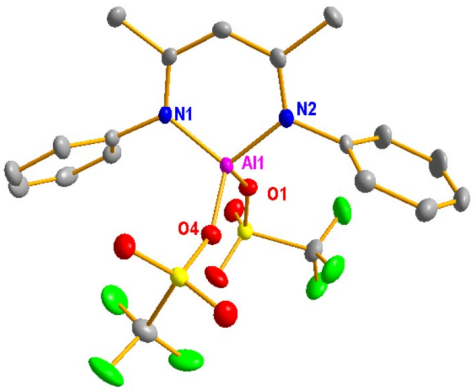

Figure 2.3 Molecular structure for **3a**.

Thermal ellipsoids have been drawn at 50% probability level. All hydrogen atoms have been omitted for clarity. Selected bond lengths (Å) and angles (°): Al1-N1 1.826(4), Al1-N2 1.828(4), Al1-O1 1.767(3), Al1-O4 1.755(4); N1-Al1-N2 101.82(17), O1-Al1-O4 101.77(17).

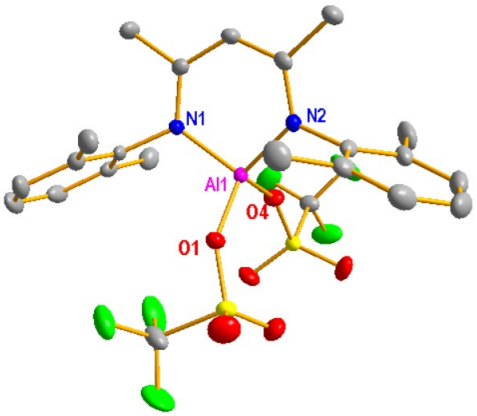

Figure 2.4 Molecular structure for **3b**.

Thermal ellipsoids have been drawn at 50% probability level. All hydrogen atoms have been omitted for clarity. Selected bond lengths (Å) and angles (°): Al1-N1 1.8306(16), Al1-N2 1.8322(16), Al1-O1 1.7570(14), Al1-O4 1.7611(14); N1-Al1-N2 101.53(7), O1-Al1-O4 109.28(7).

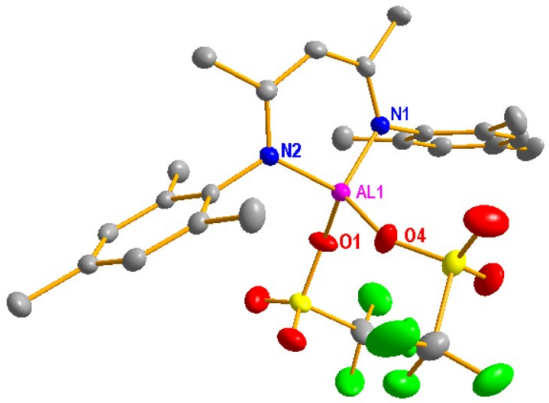

Figure 2.5 Molecular structure for **3c**.

Thermal ellipsoids have been drawn at 50% probability level. All hydrogen atoms have been omitted for clarity. Selected bond lengths (Å) and angles (°): Al1-N1 1.8350(19), Al1-N2 1.8377(19), Al1-O1 1.7605(17), Al1-O4 1.7652(19); N1-Al1-N2 102.14(8), O1-Al1-O4 105.38(10).

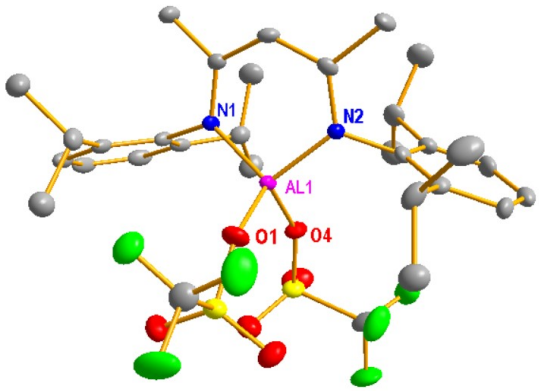

Figure 2.6 Molecular structure for **3d**.

Thermal ellipsoids have been drawn at 50% probability level. All hydrogen atoms have been omitted for clarity. Selected bond lengths (Å) and angles (°): Al1-N1 1.853(3), Al1-N2 1.841(3), Al1-O1 1.765(3), Al1-O4 1.769(3); N1-Al1-N2 101.3(1), O1-Al1-O4 106.1(1).

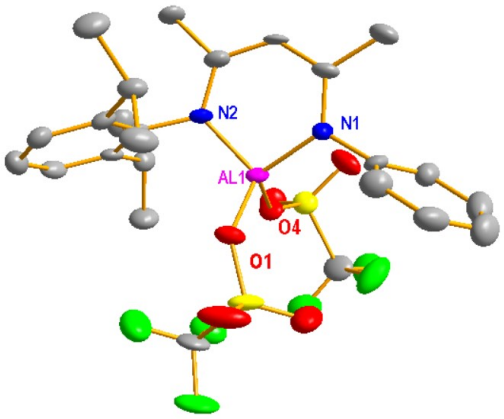

Figure 2.7 Molecular structure for **3e**.

Thermal ellipsoids have been drawn at 50% probability level. All hydrogen atoms have been omitted for clarity. Selected bond lengths (Å) and angles (°): Al1-N1 1.830(6), Al1-N2 1.843(6), Al1-O1 1 1.756(5), Al1-O4 1.768(5); N1-Al1-N2 100.7(3), O1-Al1-O4 103.2(2).

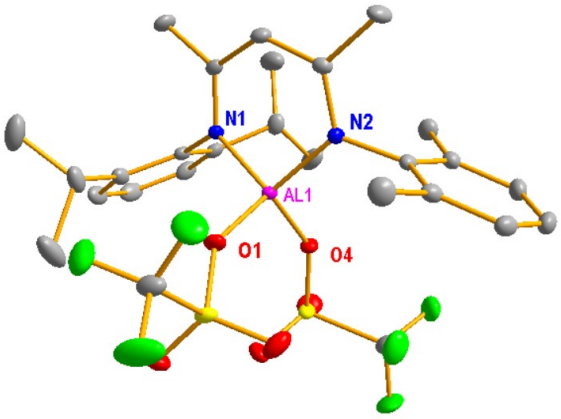

Figure 2.8 Molecular structure for **3f**.

Thermal ellipsoids have been drawn at 50% probability level. All hydrogen atoms have been omitted for clarity. Selected bond lengths (Å) and angles (°): Al1-N1 1.8399(10), Al1-N2 1.8363(10), Al1-O1 1.7686(9), Al1-O4 1.7630(9); N1-Al1-N2 101.64(5), O1-Al1-O4 109.71(4).

Table 2.4 Summary of the crystallographic data for compounds **3a**- **3f**

	3a	**3b**	**3c**
Formula	$C_{19}H_{17}AlF_6N_2O_6S_2$	$C_{23}H_{25}AlF_6N_2O_6S_2$	$C_{25}H_{29}AlF_6N_2O_6S_2$
Formula weight	574.45	630.55	658.60
Crystal system	Triclinic	Triclinic	Monoclinic
Space group	P -1	P-1	C 1 2/c 1
a /Å	9.885(2)	9.4142(3)	35.666(6)
b /Å	11.505(3)	11.1193(3)	11.6490(17)
c /Å	12.865(3)	15.5284(5)	14.667(3)
β/°	92.182(7)°	72.923(2)	92.590(10)
V / Å^3	1181.3(5)	1405.07(7)	6087.5(17)
Z	2	2	8
Dc/ g cm^{-3}	1.615	1.490	1.437
F(000)	584	648	2720
Crystal size/ mm	0.300 x 0.400 x 0.420	0.40 x 0.40 x 0.18	0.240 x 0.300 x 0.400
θ range/°	1.78 to 29.00°	1.39 to 28.39	2.78 to 27.09
No. of reflns collected	18967	27133	52291
No. of indep reflns	6253	6830	6678
*R*1 [*I* >2σ (*I*)]	0.0663	0.0397	0.0425
wR2 (all data)	0.2381	0.1199	0.1271
Peak and hole/e Å^{-3}	0.578 and -0.968	0.415 and -0.410	0.461 and -0.434

	3d	**3e**	**3f**
Formula	$C_{124}H_{164}Al_4F_{24}N_8O_{24}S_8$	$C_{25}H_{29}AlF_6N_2O_6S_2$	$C_{27}H_{33}AlF_6N_2O_6S_2$
Formula weight	2971.02	658.60	686.65
Crystal system	monoclinic	triclinic	Triclinic
Space group	P 1 21/c 1	P -1	P -1
a /Å	36.0533(16)	10.5596(10)	9.3172(3)
b /Å	19.9087(8)	15.4198(17)	12.1746(4)
c /Å	19.2748(7)	19.116(2)	15.5472(4)
β/°	90.427(2)	96.852(5)	74.1182(13)
V / Å^3	13834.6(10)	3087.0(6)	1588.64(9)
Z	4	4	2
Dc/ g cm^{-3}	1.426	1.417	1.435
F(000)	6208	1360	712
Crystal size/ mm	0.180 x 0.220 x 0.360	0.040 x 0.200 x 0.400	0.280 x 0.320 x 0.380
θ range/°	1.52 to 26.45	1.66 to 26.07	1.36 to 31.13
No. of reflns collected	167728	41273	58582
No. of indep reflns	28340	12014	10196
*R*1 [*I* >2σ (*I*)]	0.0589	0.0951	0.0351
wR2 (all data)	0.1643	0.2659	0.1143
Peak and hole/e Å^{-3}	1.219 and -0.718	0.375 and -0.570	0.641 and -0.538

2.4 Synthesis of the cationic aluminum complexes

In general, one of the efficient approaches to increase the Lewis acidities of compounds is to make them cationic. After the synthesis of the aluminum bistriflate complexes **3a-3f**, we made several attempts to synthesize the cationic aluminum complexes as summarized in Scheme 2.8.

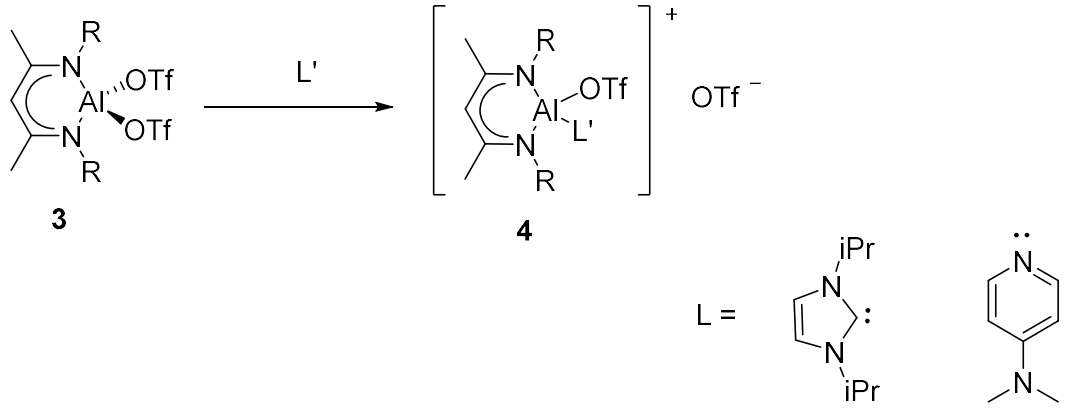

Scheme 2.8 Formation of cationic compounds

Triflate group is considered to be one of the best leaving groups. Initially, a neutral nucleophilic reagent was added to the bistriflate complexes in order to promote the dissociation of the triflate substrates. First, we treated the aluminum bistriflate complex **3d** with 2 equiv of N-heterocyclic carbene, but this attempt was unsuccessful as multinuclear NMR spectroscopic analysis revealed the formation of unidentified and inseparable impurities.

Then, we tried another nucleophile 4-dimethylaminopyridine (DMAP) to perform ligand exchange at the aluminum center. When 2 equiv of DMAP was added into the CD_2Cl_2 solution of complexes **3c**, ^{1}H NMR clearly revealed that aluminum coordinate to DMAP as

shown in Figure 2.9. The δ_H signal of free DMAP H_1 at 8.20 ppm was replaced by an upfield signal at 7.77 ppm, which indicated the coordination of DMAP at the Al center has occurred.

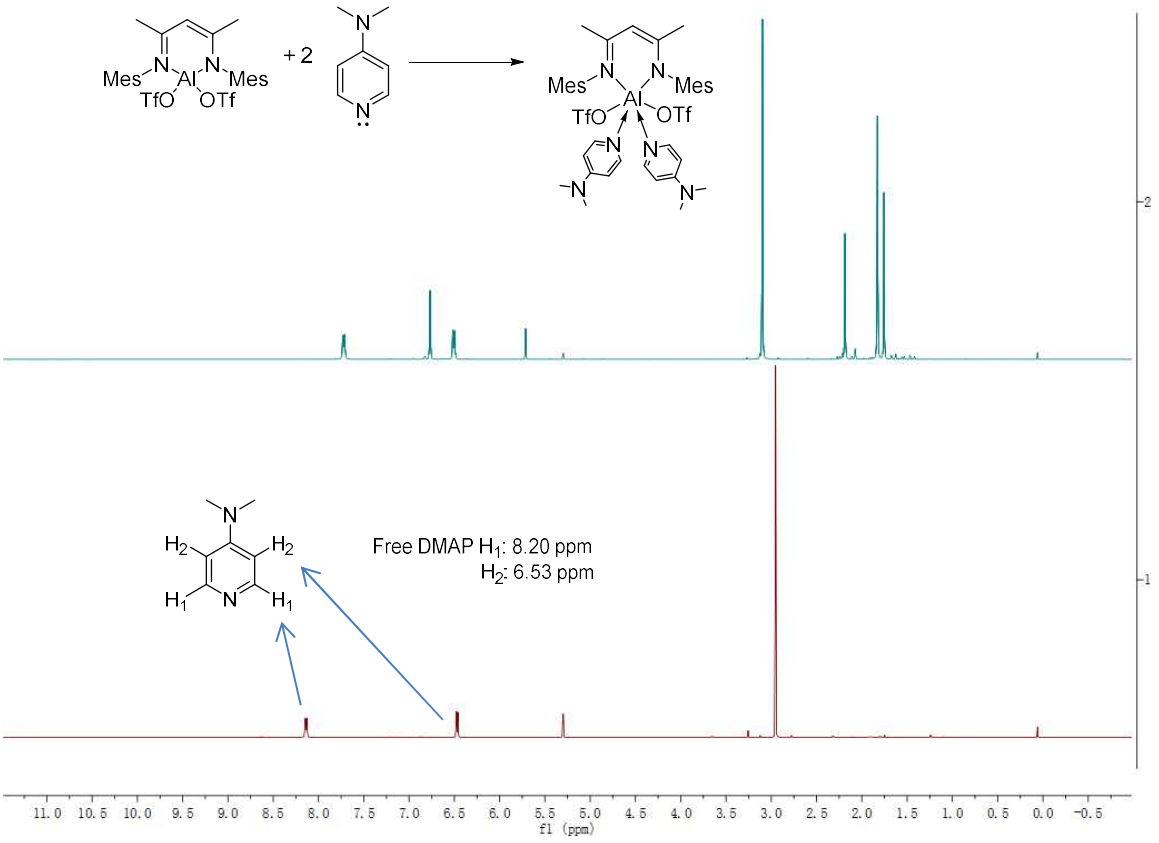

Figure 2.9 Reaction between **3c** and DMAP

Even though no valuable structural information was obtained due to the hydrolysis in the recrystallization step, this coordination can also be confirmed by the upfield shift of δ_F signal from ~ -77.3 ppm to ~ -78.4 ppm (Table 2.5). This δ_F signal is similar with that of the free triflate anion which is usually at around -79 ppm, suggesting that the new formed aluminum had a positive charge, with triflate groups replaced by DMAP. However, no crystal was obtained and we cannot confirm the structure.

Table 2.5 ^{19}F NMR (ppm) for **3** and **3**+ DMAP

3b	-77.29	**3b** + 2 DMAP	-78.42
3c	-77.28	**3c** + 2 DMAP	-78.43
3d	-77.28	**3d** + 2 DMAP	-78.50

Additionally, when dissolved in a coordinating solvent such as CD_3CN, the values for δ_{Al} of **3b** dramatically shifter upfield in comparison to the CD_2Cl_2-dissolved system suggesting acetonitrile coordination to aluminum centers in **3**. In fact, the value for δ_F of **3** in CD_3CN around -79.04 ppm (vs -77.28 ppm in CD_2Cl_2) indicated that the triflate substituents were no longer bound to the aluminum center, affording cationic compounds as shown in Scheme 2.9.

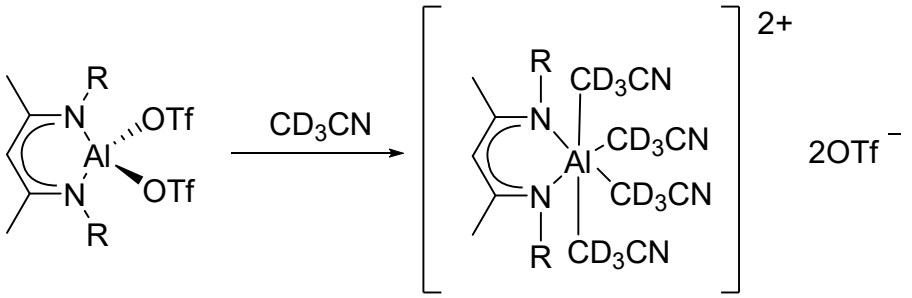

Scheme 2.9 Proposed reaction of **3d** with CD_3CN

.

As all the methods above failed to provide the desired cationic aluminum compounds, we decided to investigate whether these neutral aluminum bistriflates (**3**) would be able to catalyze Diels-Alder reactions. We investigated the [4 + 2]-cycloaddition of 2,3-dimethylbudadiene (**4**), which is 250 times less reactive than cyclopentadiene,[16] and chalcone (**5**). Unfortunately, no targeted cycloaddition product was obtained when 5 mol% $^{Dip}LAl(OTf)_2$ was used as catalyst. Nevertheless when the aluminum bistriflate complexes were mixed with the dienophile, an obvious color change was observed. ^1H NMR spectroscopy also clearly revealed the coordination between chalcone and the aluminum

centre (Figure 2.10). With this information in hand, we decided to activate the aluminum bistriflate complex further by adding 1 equiv of sodium tetrakis[3,5-bischlorophenyl] borate ($NaBAr^{Cl}_4$). To our delight, the new formed catalytic system showed quite good activity and excellent endo/exo selectivity for the Diels-Alder transformation. It is, however, worth noting that this cycloaddition cannot be catalyzed by using $NaBAr^{Cl}_4$ only.

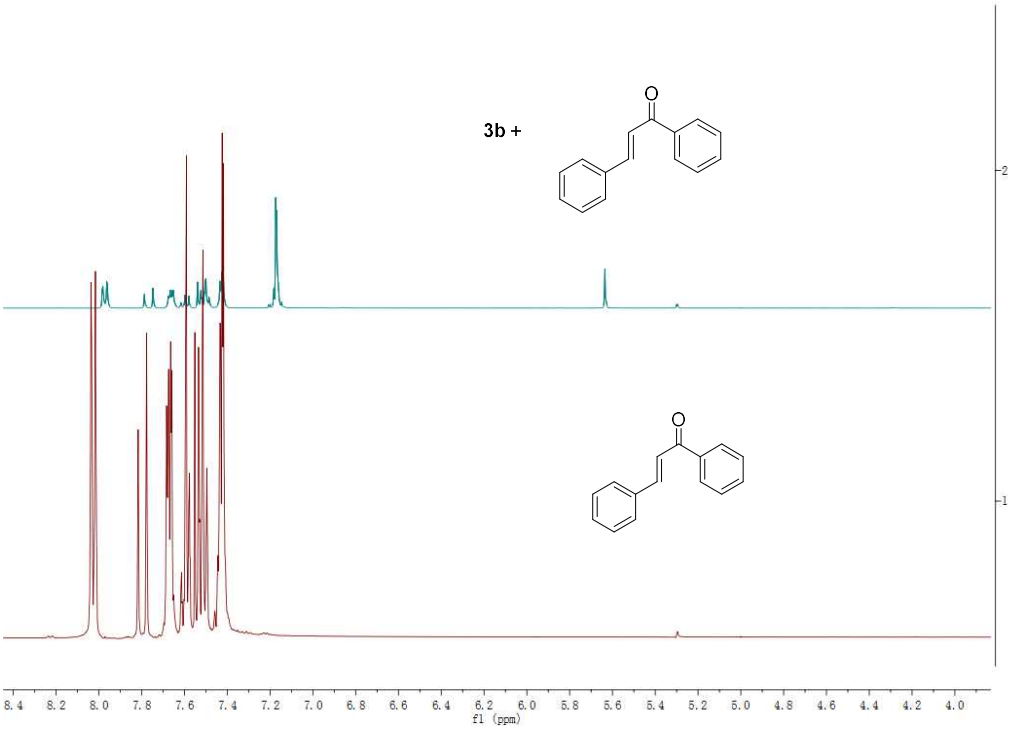

Figure 2.10 Coordination between **3b** and chalcone

Even though we obtained this initially exciting result, it was of paramount importance to gather more spectroscopic information about (i.e. identify) the active species before we started to expend its catalytic properties. Multinuclear NMR spectroscopic analysis clearly suggested interaction between the bistriflate complex and $NaBAr^{Cl}_4$. For example, the ^{19}F signal shifted downfield from δ = -77.2 ppm to -76.5 ppm, which suggested that the triflate ligands of new formed compound possessed a higher "degree of coordination".[12] Furthermore, the ^{27}Al NMR signal originally assigned to the initial bistriflate compounds disappeared presumably due to signal broadening. Also, no free or protonated

β-diketiminate ligand signals were found in ^{1}H NMR spectroscopy which suggested that no decomposition or hydrolysis occurred in this process. On the other hand, lack of any precipitate formation (NaOTf) implied that the formation of an uncharged aluminum compound was most likely outcome for this reaction. Fortunately, after several trials, we successfully obtained a few crystals suitable for single crystal X-ray diffraction analysis. The crystal structure (Figure 2.11) shows that both triflate ligands were still bound to the aluminum center, while they were also coordinate to an sodium ion using different oxygen atoms, forming a $[LAl(OTf)_2Na]^+$ unit **6**. The crystallographic data are summarized in Table 2.6

One of the OTf ligands and one of the aryl substituents were further coordinated to a second Na ion belonging to a different cationic unit, and vice versa, effectively creating a dimeric $[LAl(OTf)_2Na]_2^{2+}$ fragment. Each sodium cation was further weakly coordinated by two Cl atoms found on two distinct $[BAr^{Cl}_4]^-$ anions, resulting in the formation of a 2-dimensional coordination polymer. To the best of our knowledge, this is the first example of a coordination polymer that involves a tetraaryl borate anion. Nevertheless, we do not expect that this particular solid-state structure is retained in solution, as the Na ion is weakly coordinated to the anion and the aryl substituent.

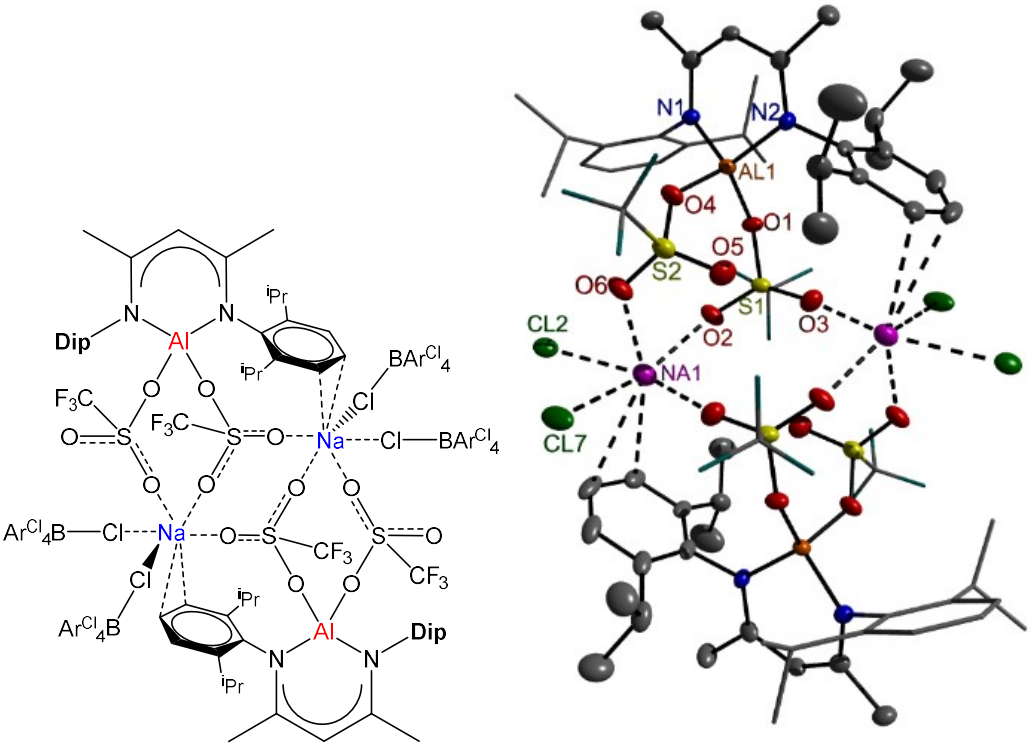

Figure 2.11 Structure for $([LAl(OTf)_2Na][BAr^{Cl}{}_4])_n$.

The ellipsoids (apart from the CF_3 and non-bonding Dip groups) have been drawn at 50% probability level. All hydrogen atoms and $[BAr^{Cl}{}_4]$- (apart from coordinating Cl atoms) anions have been removed for clarity. Selected bond lengths (Å) and angles (°): Al1-N1 1.814(3), Al1-N2 1.849(3), Al1-O1 1.772(3), Al1-O4 1.770(3), S1-O1 1.497(2), S1-O2 1.417(3), S1-O3 1.419(3), S2-O4 1.485(3), S2-O5 1.425(3), S2-O6 1.427(3), Na1-O2 2.368(3), Na1-O6 2.334(3), Na1-O3# 2.251(3), Na1-Cl2 2.867(3), Na1-Cl7 3.033(2), N1-Al1-N2 105.2(2), O1-Al1-O4 106.3(1).

Compared with its precursor **3d**, no drastic structural change has occurred in **6** because the role of Na might be just to keep two OTf ligands together. For example, the average value of Al-N bond lengths (~1.832 Å) and Al-O bond lengths (~1.771 Å) are virtually identical to the same parameters obtained for **3d**.

With this information in hand we decided to investigate the influence of the alkali metal and the anion on the overall structural and reactivity properties of the Lewis acidic system. For this purpose we mixed $^{Dip}LAl(OTf)_2$ with either $KBAr^{Cl}_4$ or $LiB(C_6F_5)_4 \cdot Et_2O$. First of all, as it was the case using $NaBAr^{Cl}_4$ there was no visible elimination of MOTf (M = Li or K) suggesting that no aluminum-based cationic species has formed. Then, it was not surprising that there was absolutely no change in the reaction rates regarding the cycloaddition between **4** and **5**. This provided additional evidence that the central Al is responsible for the observed catalytic activity. On one occasion we were fortunate enough to obtain few crystals from the reaction between $^{xyl}LAl(OTf)_2$ and $LiB(C_6F_5)_4 \cdot Et_2O$ suitable for single crystal X-ray diffraction. Molecular structure of the new compound **7** is shown in Figure 2.12 with the crystallographic data summarized in Table 2.6. Again, both triflate ligands were still coordinated to the Al center while the lithium cation is bridging between two triflates forming familiar $[^{Xyl}LAl(OTf)_2Li]+$ unit **7**. However, in this case due to the presence of OEt_2 molecules the solid state structure is not polymeric. Considering these information it can be concluded that the role of the alkali metal is presumably to "tie-up" the two triflate ligands in order to alleviate steric congestion at the Al center leading to a higher catalytic activity in comparison to $^{xyl}LAl(OTf)_2$.

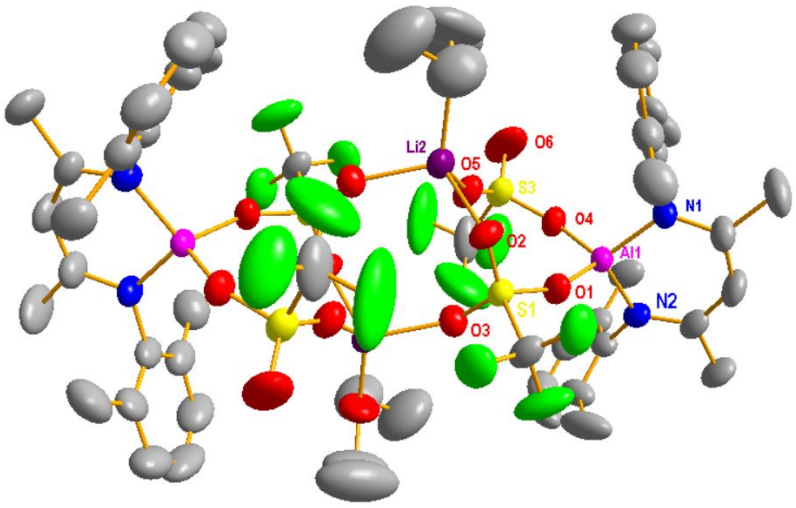

Figure 2.12 Structure for ([LAl(OTf)$_2$Li][B(C$_6$F$_5$)$_4$])

All hydrogen atoms and [B(C$_6$F$_5$)$_4$]- anions have been removed for clarity. Selected bond lengths (Å) and angles (°): Al1-N1 1.817(3), Al1-N2 1.822(3), Al1-O1 1.770(3), Al1-O4 1.755(3), Li2-O2 2.031(7), Li2-O5 2.018(8); N1-Al1-N2 102.08(15), O1-Al1-O4 104.03(13).

Table 2.6 Summary of the crystallographic data for compounds **6, 7**

	6	**7**
Formula	$C_{110}H_{106}Al_2B_2Cl_{16}F_{12}N_4Na_2O_{12}S_4$	$C_{102}H_{70}Al_2B_2F_{52}Li_2N_4O_{14}S_4$
Formula weight	2720.98	2781.32
Crystal system	Monoclinic	Triclinic
Space group	P2/n	P -1
a /Å	17.2647(11)	12.5725(6)
b /Å	20.3414(15)	15.7968(7)
c /Å	18.7463(13)	16.9105(7)
β/°	90.972(2)	98.387(2)
V / Å3	6582.5(8)	2894.1(2)
Z	2	1
Dc/ g cm-3	1.373	2.27843
F(000)	2784	1396

Crystal size/ mm	0.400 x 0.280 x 0.240	0.220 x 0.300 x 0.420
θ range/°	1.59 to 29.19	1.62 to 29.40
No. of reflns collected	17754	94461
No. of indep reflns	17754	15850
R1 [I >2σ (I)]	0.0637	0.0692
wR2 (all data)	0.1677	0.1702
Peak and hole/e $Å^{-3}$	0.961 and -0.738	0.572 and -0.479

2.5 Summary

In summary, we have prepared a series of β-diketiminate supported aluminum dichloro compounds. The corresponding aluminum bistriflate compounds were subsequently synthesized via triflate-for-chloride exchange using silver triflate. When these aluminum bistriflate compounds were combined with $NaBAr^{Cl}_4$, (or any other alkali borate salt) they formed quite active Lewis acid systems capable of catalyzing Diels-Alder transformation. Further information about the catalysis will be discussed in next chapter.

2.6 Experimental section

All operations were performed under argon or oxygen-free nitrogen pressure using standard Schlenk line and glovebox techniques. All glassware involving sensitive reaction was oven- and vacuum-dried and argon flow-degassed before use. All solvents were dried, distilled under nitrogen atmosphere, degassed under argon and stored with 4Å molecular sieves prior to use. The starting materials 2,4-pentanedione, $TsOH•H_2O$, amines, $AlCl_3$ and silver triflate were obtained from commercial source and used without further purification. ^{1}H, ^{13}C, ^{11}B, ^{19}F and ^{27}Al NMR spectra were measured on Bruker AV 300, 400, 500 MHz, JEOL ECA400 MHz, JEOL ECA400 SL, BBFO1 400MHz or BBFO2 400MHz

spectrometers at 298 K unless otherwise stated. NMR multiplicities are abbreviated as follows: s = singlet, d = doublet, t = triplet, m = multiplet, br = broad signal, sept = septet. Coupling constants J are given in Hz. Electrospray ionization (ESI) mass spectra were obtained at the Mass Spectrometry Laboratory at the Division of Chemistry and Biological Chemistry, Nanyang Technological University. Melting points were measured with OptiMelt Stanford Research System.X-ray data was collected on diffractometer Bruker X8 CCD and Bruker Kappa CCD, equipped with a liquid nitrogen-cooling stream. Nacnac ligands were preapared according to the literature, and the analytical and spectroscopic data are in accordance with those reported.[2, 17]

Preparation of $[CH(MeCNR)_2]H$ (1a - 1d).

2,4-pentanedione (10.0 g, 100 mmol) was mixed with substituent aniline (200 mmol) in 400 mL toluene containing $TsOH•H_2O$ (20 g). The reaction mixture was left to reflux overnight with water removed by a Dean-Stark apparatus. After which, the solution was cooled to ambient temperature and the solid was filtered off by Buchner funnel. The filtrate was neutralized by 1 equiv of Na_2CO_3 (10.6 g) following by extraction with 200 mL dichloromethane twice. The combined organic layers were dried with $MgSO_4$. Removal of volatiles via rotary evaporator afforded brown oil. The oil was re-dissolved in 30 mL ethanol and kept under -30°C overnight. Pure product was obtained as colorless crystals. β-diketiminate ligand **1a -1d** were prepared following this procedure.

Synthesis of 1a. Yield 81%. ^{1}H NMR (400 MHz, $CDCl_3$, 25 °C): δ 1.80 (s, 6H, C*H*$_3$ on backbone) 4.78 (s, 1H, γ-*H*), 6.89 (m, 6H, Ar*H*), 7.09 (m, 4H, Ar*H*), 13.17 (br s, 1H, N*H*).

Synthesis of 1b. Yield 85%. ^{1}H NMR (400 MHz, $CDCl_3$, 25 °C): δ 1.70(s, 6H, CH_3 on backbone), 2.16 (s, 12H, ArCH_3), 4.88 (s, 1H, γ-*H*), 6.93 (t, 2H, J_{H-H} = 7.36, p-Ar*H*), 7.03 (d, 4H, J_{H-H} = 7.36, m-Ar*H*), 12.10 (s, 1H, N*H*).

Synthesis of 1c. Yield 87%. ^{1}H NMR (400 MHz, $CDCl_3$, 25 °C): δ 1.68(s, 6H, CH_3 on backbone), 2.12 (s, 12H, m-ArCH_3), 2.26 (s, 6H, p-ArCH_3), 4.85 (s, 1H, γ-*H*), 6.85 (t, 4H, m-Ar*H*) , 12.11 (s, 1H, N*H*).

Synthesis of 1d. Yield 89%. ^{1}H NMR (400 MHz, $CDCl_3$, 25 °C): δ 1.11(d, 12H, J_{H-H} = 6.95, CH(CH_3)$_2$), 1.20(d, 12H, J_{H-H} = 6.95, CH(CH_3)$_2$), 1.71(s, 6H, CH_3 on backbone), 3.08 (sept, 4H, JH-H = 6.95, C*H*(CH_3)$_2$), 4.87 (s, 1H, γ-H), 7.10 (m, 6H, ArH), 12.10 (s, 1H, NH).

Synthesis of asymmetric β-diketiminate ligands (1e-1f).

2-(2,6-Diisopropylphenylimido)-2-pentene-4-one. 2,4-pentanedione (10.0 g, 100 mmol, 2 equivs) was mixed with 2,6-Diisopropylaniline (8.8 g, 50 mmol) in 400 mL toluene containing catalytic amount of conc. H_2SO_4. The reaction mixture was left to reflux overnight with water removed by a Dean-Stark apparatus. After cooled to ambient temperate, volatiles were removed under reduced pressure, affording a pale brown oil. The oil was then stirred with 30 mL petroleum ether at -20 °C, forming a white solid which was then washed by cold hexane and dried in vacuo. Yield: 11.3g, 87%.^{1}H NMR (400 MHz, $CDCl_3$, 25 °C): δ 1.14(d, 3H, J_{H-H} = 6.95, CH(CH_3)$_2$), 1.20(d, 3H, J_{H-H} = 6.95, CH(CH_3)$_2$), 2.11(s, 6H, CH_3 on backbone), 3.01 (sept, 2H, J_{H-H} = 6.95, C*H*(CH_3)$_2$), 5.20 (s, 1H, γ-H), 7.16-7.29 (t, 3H, ArH), 12.05 (s, 1H, NH).

2-(2,6-Diisopropylphenylimido)-2-pentene-4-one (5.18 g, 20 mmol), substituent aniline (20 mmol) and para-toluenesulfonic acid monohydrate (3.8 g, 20 mmol) was combined in a

500 mL round bottomed flask in 100 mL toluene. The solution was brought to reflux overnight with water removed by a Dean-Stark apparatus. After which the reaction mixture was cooled down to room temperature and reduced under vacuo to give yellow oil. The oil was treated with diethyl ether, water and Na_2CO_3. The water layer was separated and extracted with 200 mL ether. The organic layers were combined and dried over Na_2SO_4. The solvent was evaporated, yielding a yellow solid, which was recrystallized in cold ethanol. Asymmetric β-diketiminate ligands **1e**-**1f** were prepared following this procedure.

Synthesis of 1e. Yield 75%. ^{1}H NMR (400 MHz, $CDCl_3$, 25 °C): δ 1.14(d, 6H, J_{H-H} = 6.95, CH(CH_3)$_2$), 1.21(d, 6H, J_{H-H} = 6.95, CH(CH_3)$_2$), 2.08(s, 6H, CH_3 on backbone), 2.98 (sept, 2H, J_{H-H} = 6.95, CH(CH$_3$)$_2$), 4.89 (s, 1H, γ-H), 6.94-7.29 (m, 8H, ArH), 12.70 (s, 1H, NH).

Synthesis of 1f. Yield 80%. ^{1}H NMR (400 MHz, $CDCl_3$, 25 °C): δ 1.11(d, 6H, J_{H-H} = 7.04, CH(CH_3)$_2$), 1.21(d, 6H, JH-H = 7.04, CH(CH_3)$_2$), 1.70(s, 6H, CH_3 on backbone), 2.15(s, 6H, ArCH_3), 3.08 (sept, 2H, J_{H-H} = 7.04, CH(CH$_3$)$_2$), 4.88 (s, 1H, γ-H), 6.91-7.14 (m, 6H, ArH), 12.25 (s, 1H, NH).

Synthesis of 2a. ^{n}BuLi solution in cyclohexane (2M, 0.53 mL, 1.05 mmol) was added dropwise to 20 mL toluene solution of ligand **1a** (0.25 g, 1.0 mmol) at 0 ˚C. The reaction solution was allowed to warm to ambient temperature and left to stir for 1 hour, after which, the solution was added slowly to $AlCl_3$ (0.14g, 1.05 equiv). The reaction mixture was warmed to room temperature and left to stir for 5 hours. Then the solution was filtered to remove the precipitate (LiCl), after that, the solvent was evaporated under reduced pressure. The residue was washed by cold hexane, affording the designated product **2a** 0.30 g as white solid, yield 86%. ^{1}H NMR (400 MHz, $CDCl_3$, 25 °C): δ 1.91(s, 6H, CH_3 on backbone), 5.21 (s, 1H, γ-H), 7.20-7.42 (m, 10H, ArH). ^{13}C NMR (100 MHz, $CDCl_3$,

25 °C): δ 23.3 (s, 2C, *C*H_3, on backbone), 98.4 (s, 1C, γ-*C*), 126.8 (s, 2C, Ar*C*), 127.1 (s, 2C, Ar*C*), 129.4 (s, 2C, Ar*C*), 142.4 (s, 2C, Ar*C*), 171.0 (s, 2C, *C*N). ^{27}Al NMR (104 Hz, DCM, 25 °C): δ 99 (sharp, s).

Synthesis of 2b. Following the same procedure described for the synthesis of **2a**, treatment of **1b** (0.31 g, 1.00 mmol) with ^{n}BuLi (2.0 M in cyclohexane, 0.53 mL, 1.05 mmol) and then *in situ* adding $AlCl_3$ (0.14 g, 1.05 mmol) yielded complex **2b** (0.34 g, 84%).^{1}H NMR (400 MHz, $CDCl_3$, 25 °C): δ 1.81(s, 6H, C*H*$_3$ on backbone), 2.32(s, 12H, ArC*H*$_3$), 5.37 (s, 1H, γ-*H*), 7.11 (b, 6H, Ar*H*). ^{27}Al NMR (104 Hz, DCM, 25 ºC): δ 98 (sharp, s).

Synthesis of 2c. Following the same procedure described for the synthesis of **2a**, treatment of **1c** (0.33 g, 1.00 mmol) with ^{n}BuLi (2.0 M in cyclohexane, 0.53 mL, 1.05 mmol) and then *in situ* adding $AlCl_3$ (0.14 g, 1.05 mmol) yielded complex **2c** (0.35 g, 81%). ^{1}H NMR (400 MHz, $CDCl_3$, 25 °C): δ 1.80(s, 6H, C*H*$_3$ on backbone), 2.26(s, 18H, ArC*H*$_3$), 5.33 (s, 1H, γ-*H*), 6.92 (b, 4H, Ar*H*).^{13}C NMR (100 MHz, $CDCl_3$, 25 ºC): δ 18.4(s, 2C, Ar*C*H$_3$), 20.5 (s, 4C, Ar*C*H$_3$), 22.6 (s, 2C, *C*H$_3$, on backbone), 97.8 (s, 1C, γ-*C*), 129.3 (s, 2C, Ar*C*), 133.4 (s, 2C, Ar*C*), 136.1 (s, 2C, Ar*C*), 137.2 (s, 2C, Ar*C*), 171.8 (s, 2C, *C*N). ^{27}Al NMR (104 Hz, DCM, 25 ºC): δ 98 (sharp, s).

Synthesis of 2d. Following the same procedure described for the synthesis of **2a**, treatment of **1d** (0.42 g, 1.00 mmol) with ^{n}BuLi (2.0 M in cyclohexane, 0.53 mL, 1.05 mmol) and then *in situ* adding $AlCl_3$ (0.14 g, 1.05 mmol) yielded complex **2d** (0.44 g, 85%). ^{1}H NMR (400 MHz, $CDCl_3$, 25 °C): δ 1.16(d, 12H, $J_{H\text{-}H}$ = 6.88, CH(C*H*$_3$)$_2$), 1.19(d, 12H, $J_{H\text{-}H}$ = 6.88, CH(C*H*$_3$)$_2$), 1.89(s, 6H, CH_3 on backbone), 3.20 (sept, 4H, $J_{H\text{-}H}$ = 6.88, C*H*(CH$_3$)$_2$), 5.41 (s, 1H, γ-H), 7.21-7.32 (m, 6H, ArH). ^{27}Al NMR (104 Hz, DCM, 25 ºC): δ 99 (sharp, s).

Synthesis of 2e. Following the same procedure described for the synthesis of **2a**, treatment of **1e** (0.33 g, 1.00 mmol) with ^{n}BuLi (2.0 M in cyclohexane, 0.53 mL, 1.05 mmol) and then *in situ* adding $AlCl_3$ (0.14 g, 1.05 mmol) yielded complex **2e** (0.37 g, 86%). ^{1}H NMR (400 MHz, $CDCl_3$, 25 °C): δ 1.17(d, 6H, J_{H-H} = 6.84, CH(CH_3)$_2$), 1.27(d, 6H, J_{H-H} = 6.84, CH(CH_3)$_2$), 1.88(s, 3H, CH3 on backbone), 1.98(s, 3H, CH_3 on backbone), 3.09 (sept, 2H, J_{H-H} = 6.84, CH(CH$_3$)$_2$), 5.37 (s, 1H, γ-H), 7.16-7.42 (m, 8H, ArH). ^{13}C NMR (100 MHz, $CDCl_3$, 25 °C): δ 23.4(s, 2C, CH(*C*H$_3$)$_2$), 23.8 (s, 2C, CH(*C*H$_3$)$_2$), 24.8 (s, 1C, *C*H$_3$, on backbone), 24.9 (s, 1C, *C*H$_3$, on backbone), 28.3 (s, 2C, *C*H(CH$_3$)$_2$), 99.3 (s, 1C, γ-*C*), 124.5 (s, 1C, Ar*C*), 126.5 (s, 1C, Ar*C*), 127.0 (s, 1C, Ar*C*), 127.8 (s, 1C, Ar*C*), 129.5 (s, 1C, Ar*C*), 137.7 (s, 1C, Ar*C*), 142.8 (s, 1C, Ar*C*), 144.6 (s, 1C, Ar*C*), 170.4(s, 1C, *C*N), 172.4 (s, 1C, *C*N). ^{27}Al NMR (104 Hz, DCM, 25 °C): δ 102 (sharp, s).

Synthesis of 2f. Following the same procedure described for the synthesis of **2a**, treatment of **1f** (0.36 g, 1.00 mmol) with ^{n}BuLi (2.0 M in cyclohexane, 0.53 mL, 1.05 mmol) and then *in situ* adding $AlCl_3$ (0.14 g, 1.05 mmol) yielded complex **2b** (0.42 g, 91%). ^{1}H NMR (400 MHz, $CDCl_3$, 25 °C): δ 1.15(d, 6H, J_{H-H} = 6.84, CH(CH_3)$_2$), 1.17(d, 6H, J_{H-H} = 6.84, CH(CH_3)$_2$), 1.83(s, 3H, CH3 on backbone), 1.89(s, 3H, CH_3 on backbone), 2.31(s, 6H, ArCH_3), 3.18 (sept, 2H, J_{H-H} = 6.84, CH(CH$_3$)$_2$), 5.41 (s, 1H, γ-H), 7.11-7.31 (m, 6H, ArH). ^{13}C NMR (100 MHz, $CDCl_3$, 25 °C): δ 18.9(s, 2C, Ar*C*H$_3$), 23.1(s, 2C, CH(*C*H$_3$)$_2$), 23.9 (s, 2C, CH(*C*H$_3$)$_2$), 24.7 (s, 1C, *C*H$_3$, on backbone), 24.9 (s, 1C, *C*H$_3$, on backbone), 28.3 (s, 2C, *C*H(CH$_3$)$_2$), 99.3 (s, 1C, γ-*C*), 124.6 (s, 1C, Ar*C*), 127.0 (s, 1C, Ar*C*), 127.9 (s, 1C, Ar*C*), 129.0 (s, 1C, Ar*C*), 134.0 (s, 1C, Ar*C*), 137.4 (s, 1C, Ar*C*), 140.9 (s, 1C, Ar*C*), 144.7 (s, 1C, Ar*C*), 171.4(s, 1C, *C*N), 172.4 (s, 1C, *C*N). ^{27}Al NMR (104 Hz, DCM, 25 °C): δ 101 (sharp, s).

Synthesis of 3a. Compound **2a** (0.34 g, 1.00 mmol) and 2.1 equiv of AgOTf (0.54 g, 2.10 mmol) were mixed in 20 mL 1,2-difluorobenzene. The reaction mixture was left to stir overnight in the absence of light. After filtration, the clear solution obtained was concentrated to 5 mL and transferred to a smaller Schlenk flask, following by layering with 10 mL hexane. Colorless crystals were grown in 2 days. After dryness under vacuum, product 3a was obtained as white solid. Yield: 0.35g, 61%. ^{1}H NMR (400 MHz, $CDCl_3$, 25℃): δ 2.04 (s, 6H, C*H*$_3$ on backbone), 5.47 (s, 1H, γ-*H*), 7.22-7.49 (m, 10H, Ar*H*). ^{13}C NMR (100 MHz, $CDCl_3$, 25℃): δ 23.5 (s, 2C, *C*H$_3$, on backbone), 100.1 (s, 1C, γ-*C*), 111.4 (s, 2C, *C*F$_3$), 126.1 (s, 2C, Ar*C*), 128.3 (s, 2C, Ar*C*), 130.0 (s, 2C, Ar*C*), 140.0 (s, 2C, Ar*C*), 174.0 (s,2C, *C*N). ^{27}Al NMR (104 Hz, $CDCl_3$, 25℃): δ 64 (sharp, s). ^{19}F NMR (376 Hz, $CDCl_3$, 25℃): δ 77.29 (sharp, s).

Synthesis of 3b. Complex **3b** was prepared by treatment of **2b** (0.70 g, 1.74 mmol) and AgOTf (0.90 g, 3.50 mmol) following the same procedure described for **3a**. Yield: 0.72 g, 66%. ^{1}H NMR (400 MHz, $CDCl_3$, 25 °C): δ 1.94 (6H, s, C*H*$_3$ on backbone), 2.26 (12H, s, ortho-C*H*$_3$), 5.60 (1H, s, γ-C*H*), 7.18-7.19 (6H, m, Ar*H*). ^{13}C NMR (100 MHz, $CDCl_3$, 25 °C): δ 18.1 (s, *C*H$_3$ on backbone), 23.0 (s, *C*H$_3$ on R), 99.8 (s, γ-*C*), 128.2 (s, Ar*C*), 129.4 (s, Ar*C*), 133.6 (s, Ar*C*), 137.7 (s, Ar*C*), 175.0 (s, *C*N). ^{27}Al NMR (104 Hz, DCM, 25 °C): δ 61 (sharp, s). ^{19}F NMR (376 Hz, DCM, 25 °C): δ -77.29 (sharp, s). HRMS (ESI) calculated for $C_{23}H_{26}N_2O_6F_6AlS_2$ [M + H]: 631.0952; Found:631.0957.

Synthesis of 3c. Complex **3c** was prepared by treatment of **2c** (0.70 g, 1.62 mmol) and AgOTf (0.91 g, 3.50 mmol) following the same procedure described for **3a**. Yield: 0.62 g, 58%. ^{1}H NMR (400 MHz, $CDCl_3$, 25 °C): δ 1.91 (s, 6H, C*H*$_3$ on backbone), 2.20 (s, 12H, ortho-C*H*$_3$), 2.29 (s, 6H, p-C*H*$_3$), 5.57 (s, 1H, γ-*H*), 6.97 (s, 4H, Ar*H*). ^{13}C NMR (100 MHz, $CDCl_3$, 25 °C): δ 18.0 (s, p-*C*H$_3$), 20.9 (s, ortho-*C*H$_3$), 22.9 (s, *C*H$_3$ on backbone),

99.7 (s, γ-*C*), 130.0 (s, Ar*C*), 133.1 (s, Ar*C*), 135.2 (s, Ar*C*), 137.8 (s, Ar*C*), 175.1 (s, *C*N). ^{27}Al NMR (104 Hz, DCM, 25 °C): δ 61 (sharp, s). ^{19}F NMR (376 Hz, DCM, 25 °C): δ -77.28(sharp, s). HRMS (ESI) calculated for $C_{25}H_{30}N_2O_6F_6AlS_2$ [M + H]: 659.1265; Found: 659.1271.

Synthesis of 3d. Complex **3d** was prepared by treatment of **2d** (0.60 g, 1.16 mmol) and AgOTf (0.62 g, 2.41 mmol) following the same procedure described for **3a**. Yield: 0.54g, 63%. ^{1}H NMR (400 MHz, $CDCl_3$, 25 °C): δ 1.16(d, 12H, J_{H-H} = 6.88, CH(C*H*$_3$)$_2$), 1.23 (d, 12H, J_{H-H} = 6.88, CH(C*H*$_3$)$_2$), 2.00 (s, 6H, C*H*$_3$ on backbone), 3.03 (m, 4H, J_{H-H} = 6.88, C*H*(CH$_3$)$_2$), 5.77 (s, 1H, γ-*H*), 7.24-7.34 (m, 6H, Ar*H*). ^{13}C NMR (100 MHz, $CDCl_3$, 25 °C): δ 24.1 (s, *C*H$_3$ on backbone), 24.5 (s, CH(*C*H$_3$)$_2$), 24.6 (s, CH(*C*H$_3$)$_2$), 28.3 (s, *C*H(CH$_3$)$_2$), 100.7 (s, γ-*C*), 124.9 (s, Ar*C*), 128.5 (s, Ar*C*), 136.4 (s, Ar*C*), 144.2 (s, Ar*C*), 176.1 (s, *C*N). ^{27}Al NMR (104 Hz, DCM, 25 °C): δ 59 (sharp, s). ^{19}F NMR (376 Hz, DCM, 25 °C): δ -77.28 (sharp, s). HRMS (ESI) calculated for $C_{31}H_{42}N_2O_6F_6AlS_2$ [M + H]: 743.2204; Found: 743.2175.

Synthesis of 3e. Complex **3e** was prepared by treatment of **2e** (0.50 g, 1.16 mmol) and AgOTf (0.62 g, 2.41 mmol) following the same procedure described for **3a**. Yield: 0.47 g, 62%. ^{1}H NMR (400 MHz, $CDCl_3$, 25 °C): δ1.19(d, 6H, J_{H-H} = 6.84, CH(C*H*$_3$)$_2$), 1.22(d, 6H, J_{H-H} = 6.84, CH(C*H*$_3$)$_2$), 1.98(s, 3H, C*H*$_3$ on backbone), 2.11(s, 3H, C*H*$_3$ on backbone), 2.84 (sept, 2H, J_{H-H} = 6.84, C*H*(CH$_3$)$_2$), 5.63 (s, 1H, γ-H), 7.16-7.47 (m, 8H, ArH). ^{13}C NMR (100 MHz, $CDCl_3$, 25 °C): δ 23.5(s, 2C, CH(*C*H$_3$)$_2$), 23.6 (s, 2C, CH(*C*H$_3$)$_2$), 24.0 (s, 1C, *C*H$_3$, on backbone), 24.5 (s, 1C, *C*H$_3$, on backbone), 28.4 (s, 2C, *C*H(CH$_3$)$_2$), 100.0 (s, 1C, γ-*C*), 124.9 (s, 1C, Ar*C*), 125.7 (s, 1C, Ar*C*), 128.1 (s, 1C, Ar*C*), 128.8 (s, 1C, Ar*C*), 130.0 (s, 1C, Ar*C*), 135.4 (s, 1C, Ar*C*), 140.5 (s, 1C, Ar*C*), 143.9 (s,

1C, Ar*C*), 173.5 (s, 1C, *C*N), 174.9 (s, 1C, *C*N). ^{27}Al NMR (104 Hz, DCM, 25 °C): δ 66 (sharp, s). ^{19}F NMR (376 Hz, DCM, 25 °C): δ -77.40 (sharp, s).

Synthesis of 3f. Complex **3f** was prepared by treatment of **2f** (0.53 g, 1.16 mmol) and AgOTf (0.62 g, 2.41 mmol) following the same procedure described for **3a**. Yield: 0.44g, 56%. ^{1}H NMR (400 MHz, $CDCl_3$, 25 °C): δ 1.15 (d, 6H, J_{H-H} = 6.84, CH(CH_3)$_2$), 1.19 (d, 6H, J_{H-H} = 6.84, CH(CH_3)$_2$), 1.99 (s, 3H, CH_3 on backbone), 2.01 (s, 3H, CH_3 on backbone), 2.26 (s, 6H, ArCH_3), 2.97 (sept, 2H, J_{H-H} = 6.84, CH(CH$_3$)$_2$), 5.74 (s, 1H, γ-*H*), 7.14-7.33 (m, 6H, Ar*H*). ^{13}C NMR (100 MHz, $CDCl_3$, 25 °C): δ 18.4(s, 2C, Ar*C*H$_3$), 23.3(s, 2C, CH(*C*H$_3$)$_2$), 23.8 (s, 2C, CH(*C*H$_3$)$_2$), 24.3 (s, 1C, *C*H$_3$, on backbone), 24.5 (s, 1C, *C*H$_3$, on backbone), 28.2 (s, 2C, *C*H(CH$_3$)$_2$), 100.7 (s, 1C, γ-*C*), 124.9 (s, 1C, Ar*C*), 127.8 (s, 1C, Ar*C*), 128.7 (s, 1C, Ar*C*), 128.9 (s, 1C, Ar*C*), 129.4 (s, 1C, Ar*C*), 133.5 (s, 1C, Ar*C*), 138.9 (s, 1C, Ar*C*), 144.0 (s, 1C, Ar*C*), 180.0 (s, 1C, *C*N), 180.5 (s, 1C, *C*N). ^{27}Al NMR (104 Hz, DCM, 25 °C): δ 64 (sharp, s). ^{19}F NMR (376 Hz, DCM, 25 °C): δ -77.01 (sharp, s).

General procedure for the formation of LAl(OTf)$_2$/NaBAr$^{Cl}_4$.

15 mg (0.024 mmol) of NaBAr$^{Cl}_4$ was dissolved in 1 mL of DCM-d$_2$ in a J. Young NMR tube followed by the addition of1 equiv of LAl(OTf)$_2$. Multinuclear NMR was recorder right away. Even though these systems showed to be quite stable in DCM they appear to be extremely air/moisture sensitive and the most efficient results are achieved if used in situ. A small batch of crystals was obtained by layering this solution with hexane.

3b + NaBAr$^{Cl}_4$. ^{1}H NMR (400 MHz, CD_2Cl_2, 25 °C): δ 1.91 (s, 6H, CH_3 on backbone), 2.14 (s, 12H, ortho-CH_3), 5.69 (s, 1H, γ-*H*), 6.97 (m, 6H, Ar*H*), 7.03 (m, 12H, BAr$^{Cl}_4$*H*). ^{13}C NMR (100 MHz, CD_2Cl_2, 25 °C): δ 17.6 (s, *C*H$_3$ on backbone), 22.8 (s, *C*H$_3$ on R), 101.1 (s,

γ-*C*), 123.1 [BAr^{Cl}_4 (p-*C*H)], 128.7 (s, Ar*C*), 129.5 (s, Ar*C*), 132.9 (q, $^3J_{BC}$ = 4 Hz, BAr^{Cl}_4), 133.0 [BAr^{Cl}_4 (m-*C*H)], 134.0 (s, Ar*C*), 137.0(s, Ar*C*), 163.9 (q, $^1J_{BC}$ = 49 Hz, BAr^{Cl}_4) , 176.7(s, *C*N). ^{19}F NMR (376 Hz, DCM, 25 °C): *δ* -75.93 (sharp, s). ^{11}B NMR (128 Hz, DCM, 25 °C): *δ* -6.9.

3c + $NaBAr^{Cl}_4$.^{1}H NMR (400 MHz, CD_2Cl_2, 25 °C): *δ* 1.88 (s, 6H, C*H*$_3$ on backbone), 2.09 (m, 18H, Ar-C*H*$_3$), 5.68 (s, 1H, γ-*H*), 6.82 (m, 3H, BAr^{Cl}_4*H*), 6.97 (m, 4H, Ar*H*), 7.04 (m, 9H, BAr^{Cl}_4*H*). ^{13}C NMR (100 MHz, CD_2Cl_2, 25 °C): *δ* 17.5 (s, p-*C*H$_3$), 20.5 (s, ortho-*C*H$_3$), 22.7 (s, *C*H$_3$ on backbone), 101.1 (s, γ-*C*), 123.1 [BAr^{Cl}_4 (p-*C*H)], 130.1 (s, Ar*C*), 132.9 (q, $^3J_{BC}$ = 4 Hz, BAr^{Cl}_4), 133.3 [BAr^{Cl}_4 (m-*C*H)], 134.6 (s, Ar*C*), 138.8 (s, Ar*C*), 163.8 (q, $^1J_{BC}$ = 49 Hz, BAr^{Cl}_4), 176.8 (s, *C*N). ^{19}F NMR (376 Hz, DCM, 25 °C): *δ* -75.90 (sharp, s). ^{11}B NMR (128 Hz, DCM, 25 °C): *δ* -6.9.

3d + $NaBAr^{Cl}_4$. ^{1}H NMR (400 MHz, CD_2Cl_2, 25 °C): *δ* (d, 12H, J_{H-H} = 7.00, CH(C*H*$_3$)$_2$), 1.30 (d, 12H, J_{H-H} = 6.32, CH(C*H*$_3$)$_2$), 2.00 (s, 6H, C*H*$_3$ on backbone), 2.87 (m,4H, J_{H-H} = 6.52, C*H*(CH$_3$)$_2$), 5.74 (s, 1H, γ-*H*) , 7.04-7.10 (m, 12H, BAr^{Cl}_4*H*) , 7.43-7.45 (m, 6H, Ar*H*). ^{13}C NMR (100 MHz, Cd2Cl2, 25 °C): *δ* 24.2 (s, *C*H$_3$ on backbone), 24.4 (s, CH(*C*H$_3$)$_2$), 24.6 (s, CH(*C*H$_3$)$_2$), 28.7 (s, *C*H(CH$_3$)$_2$), 101.1 (s, γ-*C*), 123.1 [BAr^{Cl}_4 (p-*C*H)], 125.3 (s, Ar*C*), 129.2 (s, Ar*C*), 132.9 [BAr^{Cl}_4 (m-*C*H)], 133.0 (q, $^3J_{BC}$ = 4 Hz, BAr^{Cl}_4), 135.8 (s, Ar*C*), 144.1 (s, Ar*C*), 163.9 (q, $^1J_{BC}$ = 49 Hz, BAr^{Cl}_4), 176.8 (s, *C*N). ^{19}F NMR (376 Hz, DCM, 25 °C): *δ* -76.50 (sharp, s). ^{11}B NMR (128 Hz, DCM, 25 °C): *δ* -7.0.

3b + $LiBC_6F_5$. ^{1}H NMR (400 MHz, CD_2Cl_2, 25 °C): *δ* 1.05(t, 12H, J_{H-H} = 7.32, CH_2CH_3), 1.91(s, 6H,Ar*CH*$_3$), 2.18 (s, 6H, C*H*$_3$ on backbone), 3.38 (q, 8H, J_{H-H} = 7.32, C*H*$_2$CH$_3$), 5.71 (s, 1H, γ-*H*) , 7.19(m, 6H, Ar*H*). ^{13}C NMR (100 MHz, CD2Cl2, 25 °C): *δ* 14.4 (CH_2CH_3), 17.6 (*C*H$_3$ on backbone), 22.7 (Ar*C*H$_3$), 65.5 (*C*H$_2$*C*H$_3$), 100.7 (γ-*C*), 128.5(Ar*C*),

129.5(Ar*C*), 133.6(Ar*C*), 135.1 (BAr^F_4), 137.1 (s, Ar*C*), 137.5 (BAr^F_4), 147.0 (BAr^F_4), 149.3 (BAr^F_4), 176.3 (*C*N). ^{11}B NMR (128 Hz, DCM, 25 °C): δ –17.6.

References

1 (a) *Acid Catalysis in Modern Organic Synthesis, Vol. 1 and 2* (Eds.: H. Yamamoto, K. Ishihara), Wiley-VCH, Weinheim, **2008**; (b) *The Diels – Alder Reaction: Selected Practical Methods*, (Eds.: F. Fringuelli, A. Taticchi), John Wiley and Sons, Ltd, Chichester, **2002**; (c) *Cycloaddition Reactions in Organic Synthesis* (Eds.: S. Kobayashi, K.-A. Jorgensen), Wiley-VCH, Weinheim, **2001**.

2 Dove, A. P.; Gibson, V. C.;* Marshall, E. L.; White, A.J. P.; Williams, D. J. *Dalton Trans.*, **2004**, 570.

3 Lappert, M. F.; Liu, D. S. J. *Organomet. Chem.* **1995**, *500*, 203.

4 Clegg, W.; Cope, E. K.; Edwards, A. J.; Mair, F. S. *Inorg. Chem.* **1998**, *37*, 2317.

5 Yang, Y.; Li, H.; Wang, C.; Roesky, H. W. *Inorg. Chem.* **2012**, *51*, 2204.

6 Stender, M.; Eichler, B. E.; Hardman, N. J.; Power, P. P. *Inorg. Chem.***2001**, *40*, 2795.

7 Felix, A. M.; Dickie,D. A.; Horne, I. S.; Page, G.; Kemp, R. A. *Inorg. Chem.* **2012**, *51*, 4650.

8 Aeilts, S. L.; Coles, M. P.; Swenson, D. C.; Jordan R. F. *Organometallics* **1998**, *17*, 3265.

9 Romain, C.; Fliedel, C.; Laponnaz,´S. B.; Dagorne, S. *Organometallics* **2014**, *33*, 5730.

10 Zheng, W.; Mösch-Zanetti, N. C.; Blunck, Y.; Roesky, H. W.; Noltemeyer, M.; Schmidt, H. G. *Organometallics* **2001**, *20*, 3299.

11 Lawrance, G. A. *Chem. Rev.* **1986**, *86*, 17.

12 It is generally accepted that the signal for non-coordinated triflate anion is observed at around δ_F = -79 ppm, whereas the coordinated anion is found at about 1-2 ppm downfield shifted from this value. See for example: Hayashida, T.; Kondo, H.; Terasawa, J.; Kirchner, K.; Sunda, Y.; Nagashima, H. *J. Organomet. Chem*. **2007**, *692*, 382.

13 Vidovic, D.; Findlater, M.; Reeske, G.; Cowley, A. H. *J. Organomet. Chem.* **2007**, *692*, 5683.

14 Stender, M.; Eichler, B. E.; Hardman, N. J.; Power, P. P.; Prust, J.; Noltemeyer, M.; Roesky, H. W. *Inorg. Chem.* **2001**, *40*, 2794.

15 (a) Ward, B.; Qian, D. L.; Smith III, R. R. *Organometallics* **1998**, *17*, 3070; (b) Courtenay, S.; Walsh, D.; Hawkeswood, S.; Wei, P.; Das, A. K.; Stephan, D. W. *Inorg. Chem.* **2007**, *46*, 3623; (c) Ohashi, M.; Saijo, H.; Arai, T.; Ogoshi, S. *Organometallics* **2010**, *29*, 6534; (d) Kazem, N.; Stoll, S.; Britt, R. D.; Shanmugam, M.; Berben, L. A. *J. Am. Chem. Soc.* **2011**, *133*, 8662.

16 Liu, P. N.; Zhou, Z. Y.; Lau, C. P. *Chem. Eur. J.* **2007**, *13*, 8610.

17 Liu, J.; Petit, L. V.; Linden, A.; Luan, X.; Dorta, R. *J. Organomet. Chem.* **2012**, *719*, 80.

Chapter 3

Application in organic transformations

Ever since the elegant applications in the total synthesis of a large range of complex natural products in the 1950s, Diels-Alder cycloadditions have been at the frontline in organic synthesis for its power and effectiveness.[1] It was considered to be a useful and powerful synthetic reaction as it can increase the molecular complexity (molecular size, topology, stereochemistry, functionality, and appendages) and widely used to synthesize numerous natural products and biologically active molecules.[2-5] The reactivity of normal Diels-Alder reaction depends on the energy difference between the HOMO of the diene and the LUMO of dienophile.[6] The most common dienphiles usually contain electron withdrawing substituents such as carbonyl, cyano or nitro groups as they can lower the corresponding LUMO energy. This effect can be dramatically enhanced by coordinating to Lewis acids, which are the most widely used catalysts for Diels-Alder reaction. Herein, we examined the β-diketiminate supported Al bis(triflate) systems which were discussed in Chapter 2 as Lewis acid catalysts for a series of Diels-Alder reactions involving three dienes and several dienophiles.

3.1 Diels-Alder reactions involving 2,3-dimethylbutadiene.

As mentioned in Chapter Ⅱ, when activated by 1 equiv of $NaBAr^{Cl}_4$, $^{Dip}LAl(OTf)_2$ (**3d**) (5 mol%) is capable of efficiently catalyzing the Diels-Alder reaction between 2,3-dimethylbutadiene (**4**) and chalcone (**5**) in dichloromethane where 2 equiv of diene was used (entry 2, Table 3.1). After that, other species including $KBAr^{Cl}_4$, $NaBAr^{CF3}_4$ and $LiB(C_6F_5)_4 \cdot Et_2O$ were also used to activate the aluminum bistriflate complex in order to increase the catalytic activity. As shown in Table 3.1, $KBAr^{Cl}_4$ and $NaBAr^{CF3}_4$ showed similar ability to activate the aluminum bistriflate complex while introducing $LiB(C_6F_5)_4 \cdot Et_2O$ led to decreased activity presumably due to the presence of coordinating Et_2O .

Table 3.1 Diels-Alder reaction by different catalytic systems

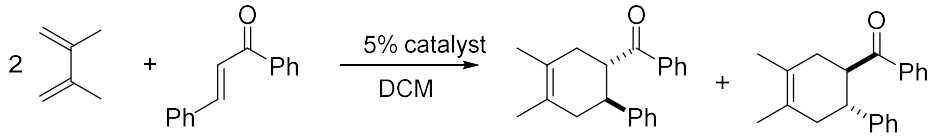

4 **5** endo **8** exo

#	Catalyst	Time (h)	Yield (%)	Endo/exo
1	**3d**	24	-	-
2	**3d** + $NaBAr^{Cl}_4$	6	80	99 : 1
3	**3d** + $KBAr^{Cl}_4$	6	78	99 : 1
4	**3d** + $KBAr^{CF3}_4$	6	80	99 : 1
5	**3d** + $LiB(C_6F_5)_4 \cdot Et_2O$	24	22	99 : 1

With all this information in hand, we decided to furthermore expand the catalytic properties of this series of aluminum bistriflate complexes. Complexes **3b**-**3d** combined with $NaBAr^{Cl}_4$ were used to catalyze the Diels-Alder cycloadditions between **4** and several different dienophiles as summarized in Table 3.2. When enones 3-buten-2-one (**9**) and ethyl vinyl ketone (**10**) were used, all the three catalytic systems were proved to be excellent catalysts for the cycloadditions with the corresponding trans adducts (where applicable) as the only observable isomers (entry 1, 2, Table 3.2). To be noticed, decent yields were also gained when the catalyst loadings were reduced to 1 mol%. When benzalacetone (**11**) was used for the cycloaddition, **3d** still acted as a good catalyst while catalyst loadings of 15% were required for **3b** and **3c** to afford decent yields (entry 3, Table 3.2). To our surprise, a quite different result was observed when **5** was examined as a dienophile, because **3b** and **3c** can complete the catalysis in 3h while **3d** required more than 18h to achieve good conversion.

After that we decided to examine whether these catalytic systems can also catalyze the Diels-Alder cycloaddtion reactions involving cyclic enones. Similar to the runs involving dienophiles **5** and **11**, when cyclic dienophiles were used for the Diels-Alder cycloadditions, **3b**/**3c** also performed quite differently in comparison to **3d**. A higher catalyst loading was required to catalyze the Diels-Alder reaction between diene **4** and 2-cyclopenten-1-one (**12**) for the system containing **3d**, affording good isolated yield of the desired cycloadduct (entry 5, Table 3.2). In contrast, when **3b** or **3c** was used for this particular transformation, no cycloadduct formation was observed even when 15 mol% catalyst loading was used. However, the reaction mixture became jelly, suggesting an occurance of a different transformation. After workup with methanol a white solid was successfully isolated and analyzed by multinuclear NMR spectroscopy. The ^{1}HNMR spectra revealed that this unexpected product resembled oligomeric/polymeric meterial. This part of work will be discussed in more detail in section **3.3**. Furthermore, Diels-Alder cycloaddition involving 2-cyclohexen-1-one (**13**) can also be catalyzed by **3d** resulting in the formation of the desired adduct in good yields (87% in 24h). Nevertheless, when **3b** or **3c** was used, a dramatically decrease in activity was observed (~20% in 24h, entry 6, Table 3.2). In addition, large amount of white precipitate was observed during the reaction, which also seemed to be of a polymeric character. All these three catalytic systems were also compatible with the Diels-Alder cycloadditions involving crotonaldehyde in good isolated yields (> 80% in 24h, entry 7, Table 3.2). A catalyst loading of 10% in the case of **3d** and additional amount of diene were required for cycloaddition reaction involving ethyl crotonate which is considered to be a much less reactive dienophile. On the other hand, **3b** and **3c** did not show any activity for this transformation under same reaction conditions (entry 8, Table 3.2).

Table 3.2 Diels-Alder reactions involving 2,3-dimethylbutadiene

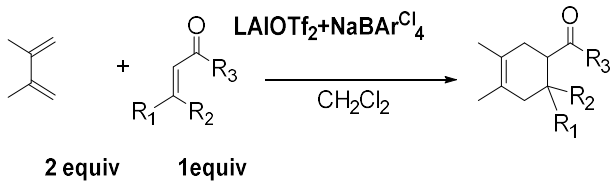

Entry	Dienophile	Adduct	3**b**/NaBAr$^{Cl}_4$	3**c**/NaBAr$^{Cl}_4$	3**d**/NaBAr$^{Cl}_4$	HBA
1	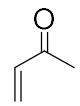 **9**	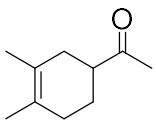 **16**	5% 1h 98% -	5% 1h 94% -	5% 1h 96% -	1% 1h 90% -
2	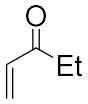 **10**	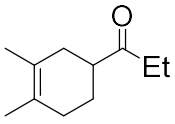 **17**	5% 1h 91% -	5% 2h 92% -	5% 1h 96% -	1% 1h 89% -
3	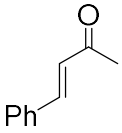 **11**	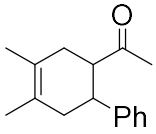 **18**	15% 12h 86% 99: 1	15% 12h 80% 99: 1	5% 12h 93% 99: 1	1% 24h 58% 99: 1
4	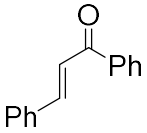 **5**	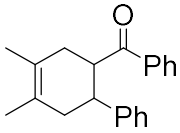 **8**	5% 3h 97% 99: 1	5% 3h 96% 99: 1	5% 18h 86% 99: 1	1% 24 33% 99: 1
5	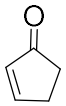 **12**	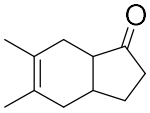 **19**	10% 24h -	10% 24h -	10% 1h 91% 99: 1	1% 12h -
6	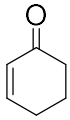 **13**	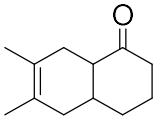 **20**	5% 24h 23% 99: 1	5% 24h 21% 99: 1	5% 24h 87% 99: 1	1% 12h -
7	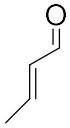 **14**	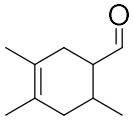 **21**	5% 24h 83% 96:4	5% 24h 85% 97:3	5% 24h 81% 96:4	1% 24h 60% 91:9
8	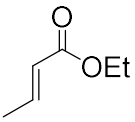 **15**	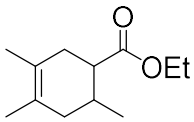 **22**	10% 24h -	10% 24h -	5% 24h 81%[a] 96:4	1% 24h -

[a] 4 equiv of diene was used.

As more and more evidences revealed that various organic transformations catalyzed by Lewis acids can also be catalyzed by HBA, which usually generated by the hydrolysis of

the metal compounds, it is necessary to perform additional experiments to demonstrate that the catalytic activity was afforded by the aluminum bistriflate compound rather than an HBA. The most prominent approaches to gather evidence against HBA catalysis are (i) investigation of the same transformations using an in-situ generated source of HOTf by mixing AgOTf and ^{t}BuCl, and (ii) addition of a proton source (e.g. dbpy: 2,6-^{t}Bu$_2$-py) to the examined catalytic systems. Therefore, rigorous steps have to be taken in order to minimize the possibility of the presence and subsequent reactivity of an HBA.

As already mentioned, an HBA was prepared by mixing AgOTf and 1 equiv of ^{t}BuCl in CD_2Cl_2 following the procedure described by Hintermann[7] *et al.* It was also suggested that 1 mol % of the HBA system was more than enough for this purpose as higher amounts and the use of triflic acid could result in false negative observations. Although the target Diels-Alder transformations involving 3-buten-2-one (**9**) and ethyl vinyl ketone (**10**) occurred with same reaction rates, the transformations involving other dienophiles were dramatically different with respect to the aluminum-based Lewis acid systems as shown in Table 3.2 (longer reaction times and lower yields). For instance, when the less reactive dienohplies were used, only the swift polymerization of 2,3-dimethylbutadiene was observed (entry 5, 6 and 8, Table 3.2).

Table 3.3 Selected Diels–Alder transformations in the presence of a pyridine base.

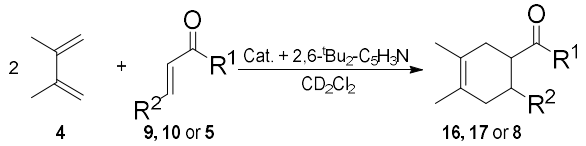

4 9, 10 or 5 16, 17 or 8

Entry	Dienophile	Catalytic system	Adduct	Time/yield/ trans:cis
1	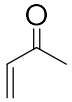 **9**	^{t}BuCl/AgOTf (1 mol %)	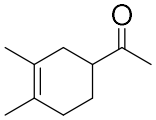 **16**	1 h traces -
2	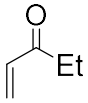 **10**	^{t}BuCl/AgOTf (1 mol %)	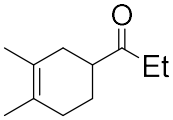 **17**	2 h traces -
3	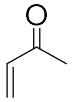 **9**	^{Dip}LAl(OTf)$_2$/ Na[BAr$^{Cl}_4$] (5 mol %)	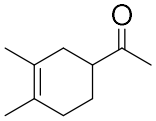 **16**	1 h 83 % -
4	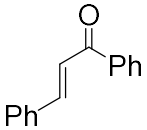 **5**	^{Dip}LAl(OTf)$_2$/ Na[BAr$^{Cl}_4$] (5 mol %)	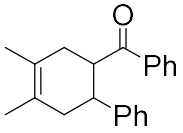 **8**	6 h 73 % 99:1

As anticipated, introducing equimolar amounts of the proton source (dbpy) to the HBA system completely quenched its catalytic activity (entry 1 and 2, Table 3.3) and stoichiometric amounts of pyridinium cation ([dbpy-H]$^+$) were formed . On the other hand, when **3d**/NaBAr$^{Cl}_4$ and equimolar amounts of dbpy were mixed in DCM-d_2 solution the formation [dbpy-H]$^+$ was limited to less than 10 %. The formed system showed only subtle effect on the isolated yields when used to catalyze the reactions between diene **4** and **9**presumably due to the dienophile-to-enolate side reaction (Schem 3.1).[8]

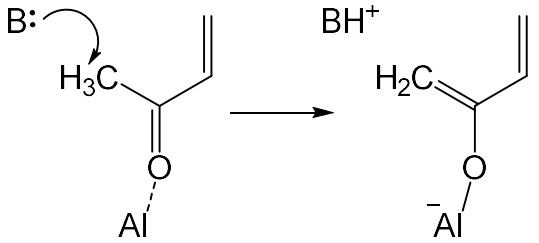

Schem 3.1 Proposed dienophile-to-enolate side reaction

Therefore, the aforementioned evidence strongly indicated that the investigated Diels-Alder cycloadditions were most likely catalyzed by our aluminum-based Lewis acid systems rather than an HBA.

3.2 Diels-Alder reactions of 1,3-cyclohexadiene and isoprene

Inspired by these achievements, we decided to investigate the Diels-Alder reactions involving less reactive dienes, 1,3-cyclohexadiene (**23**) and isoprene (**32**). The results were summarized in Table 3.4 and Table 3.5. When 1,3-cyclohexadiene was used, the high reactive dienophiles **9** and **10** were also quite suitable for the targeted Diels-Alder cycloaddtions resulting good isolated yields (entries 1 and 2, Table 3.4). However, the less reactive dienphiles demanded higher catalyst loadings or longer reaction times in order to obtain decent yields. For example, in the case of **11** 15 mol% of **3d** was required in order to obtain quantitative yield, while **3b** and **3c** did not show good catalytic activities for this reaction. Only about 40% yields were obtained even after 15 mol% of catalyst loadings were used and the reaction times were extended to 24h (entries 3, Table 3.4). In contrast, **3b** and **3c** showed better activities for the cycloaddition involving **5** than **3d** (84% in 12h, 60% in 12h and 16% in 60h respectively, entries 4, Table 3.4). In most of the cases, the cyclic dienophiles showed no activities under the investigated reaction conditions. Only when catalyzed by **3d** and extra amount of diene were used, cycloaddition product of **13** can be

obtained (81% in 24h, entries 5,6, Table 3.4). For **14** all the three catalytic systems showed mild activities and selectivities (entries 7, Table 3.4). There was then no surprise that no activity was observed for the quite unreactive dienophile **15** even when extra amounts of the diene and higher catalyst loading were used (entries 8, Table 3.4).

Table 3.4 Diels-Alder reactions involving 1,3-cyclohexadiene

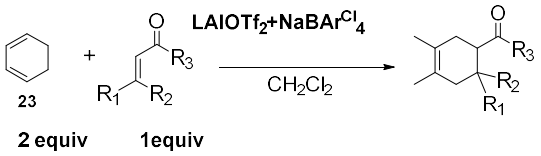

Entry	Dienophile	Adduct	3**b**/NaBAr$^{Cl}_4$	3**c**/NaBAr$^{Cl}_4$	3**d**/NaBAr$^{Cl}_4$	HBA
1	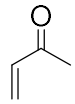 **9**	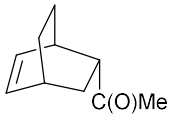 **24**	5% 1h 96% -	5% 1h 92% -	5% 1h 98% -	1% 1h 92% -
2	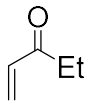 **10**	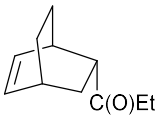 **25**	5% 1h 94% -	5% 2h 90% -	5% 1h 98% -	1% 2h 90% -
3	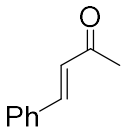 **11**	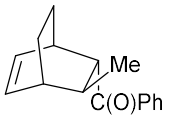 **26**	15% 24h 40% 99: 1	15% 24h 37% 99: 1	15% 7h 94% 99: 1	1% 24h 25% 99: 1
4	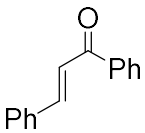 **5**	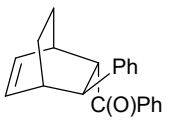 **27**	5% 12h 84% 98: 2	5% 12h 60% 99: 1	5% 60h 16% 99: 1	1% 24 16% 99: 1
5	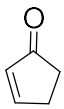 **12**	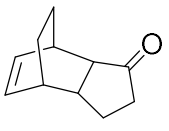 **28**	15% 24h -	15% 24h -	15% 24h -	1% 24h -
6	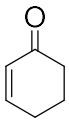 **13**	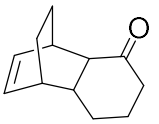 **29**	15% 24h -	15% 24h -	5% 24h 81%[a] 99:	1% 24h -
7	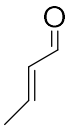 **14**	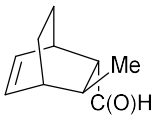 **30**	5% 24h 75% 95:5	5% 24h 70% 95:5	5% 24h 66% 95:5	1% 24h -

8	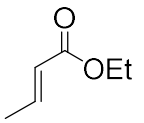 **15**	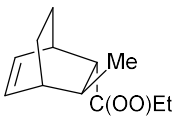 **31**	15% 24h -[a]	15% 24h -[a]	15% 24h -[a]	1% 24h -[a]

[a] 4 equiv of diene was used.

Similar results were obtained when isoprene (**32**) was examined to react with these dienophiles. For the reactive dienophiles **9** and **10**, all the catalytic systems including HBA can afford acceptable isolated yields in 2h with para : meta ratios > 97 : 3 (entries 1,2, Table 3.5). 10 mol% of **3d** was required to obtain cycloaddition product **35** while **3b** and **3c** did not show any activity at all (entry 3, Table 3.5). In contrast, **3b** and **3c** showed much higher activities than **3d** in the cycloaddtion reaction between **5** and isoprene. For this reaction HBA also showed some catalytic activity but much lower para : meta ratio (88 : 12, entry 4, Table 3.5). For cyclic dienophiles **12**, **13** and less reactive ethyl crotanate **15**, no cycloaddition product was obtained via the catalysis of all these catalytic systems even when extra amount of diene and catalyst loadings were used (entries 5, 6 and 8, Table 3.5). For aldehyde **14** all the catalytic systems showed mild activities with para : meta ratios > 96 : 4 (entry 7, Table 3.5).

Table 3.5 Diels-Alder reactions involving isoprene

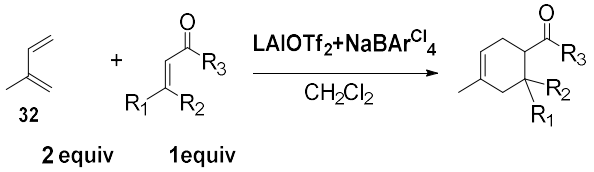

Entry	Dienophile	Adduct	3**b**/NaBAr$^{Cl}_4$	3**c**/NaBAr$^{Cl}_4$	3**d**/NaBAr$^{Cl}_4$	HBA
1	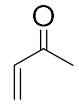	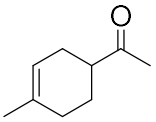	55%	5%	55%	11%
			2h	2h	2h	2h
			82%	84%	77%	83%
	9	**33**	99:1	99:1	99:1	97:3
2	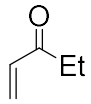	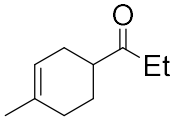	5%	5%	55%	1%
			2h	2h	2h	2h
			82%	74%	78%	82%
	10	**34**	98:2	97:3	98:2	97:3
3	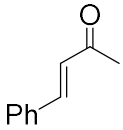	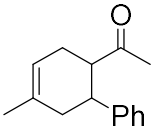	15%	15%	10%	1%
			24h	24h	12h	10h
			-	-	97.%	53%
	11	**35**			99:1	97:3
4	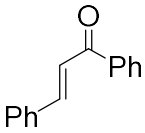	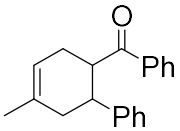	5%	5%	5%	1%
			20h	10h	20h	10h
			76%	98%	39%	29%
	5	**36**	99:1	99:1	99:1	88:12
5	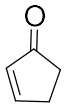	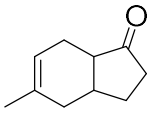	15%	15%	15%	1%
			24h	24h	24h	24h
			-	-	-	-
	12	**37**				
6	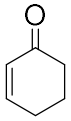	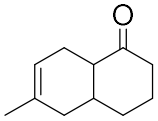	15%	15%	5%	1%
			24h	24h	24h	24h
			-	-	-	-
	13	**38**				
7	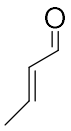	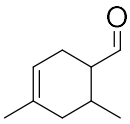	5%	5%	5%	1%
			24h	24h	24h	24h
			82%	69%	80%	28%
	14	**39**	96:4	96:4	96:4	96:4
8	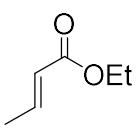	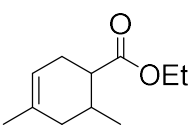	15%	15%	15%	1%
			24h	24h	24h	24h
			-[a]	-[a]	-[a]	-[a]
	15	**40**				

[a]4 quiv of diene was used.

In order to increase the para : meta ratios of the cycloaddtion products, we decided to use the asymmetric aluminum bistriflate compounds to catalyze the Diels-Alder reactions involving isoprene. As shown in Table 3.6, compounds **3e** ($^{Dip\text{-}Ph}LAl(OTf)_2$)/$NaBAr^{Cl}{}_4$ and **3f** ($^{Dip\text{-}Xyl}LAl(OTf)_2$)/$NaBAr^{Cl}{}_4$ were examined. However, for the reactive dienophiles **9** and **10**, no significant increase in para : meta ratios were observed while the activities were acceptable (entries 1 and 2, Table 3.6). In contrast, for the less reactive dienophiles **5** and **11**, para : meta ratios slightly increased but resulting dramatically decrease in activities (entries 3 and 4, Table 3.6). Thus, as these asymmetric compounds did not show promising improvements with respect to selectivity and reaction rates we decided not to further investigate their catalytic activity.

Table 3.6 Dies-Alder reactions involving isoprene by asymmetric catalysts

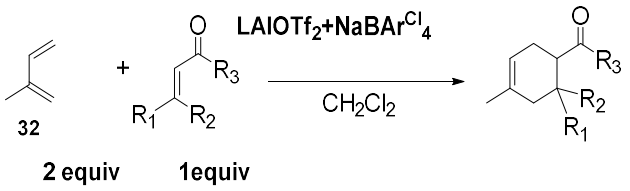

Entry	Dienophile	Adduct	3e/$NaBAr^{Cl}{}_4$	3f/$NaBAr^{Cl}{}_4$	HBA
1	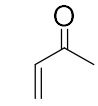 **9**	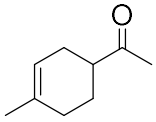 **33**	5% 1h 77% 98:2	5% 1h 77% 98:2	11% 2h 83% 97:3
2	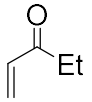 **10**	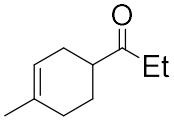 **34**	5% 2h 82% 98:2	5% 1h 82% 98:2	1% 2h 82% 97:3
3	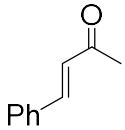 **11**	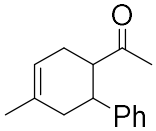 **35**	15% 24h -	15% 24h -	1% 10h 53% 97:3
4	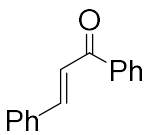 **5**	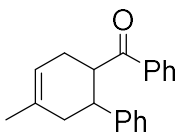 **36**	15% 24h -	5% 12h 50% 99:1	1% 10h 29% 88:12

3.3 Michael polymerizations involving dienophiles.

As aforementioned, when **3b** and **3c** were used to catalyze the Diels-Alder reactions involving 2-cyclopenten-1-one (**12**), the reaction mixture became jelly without any cycloaddition product formed. However, according to the initial ^{1}H NMR spectrum it was quite evident that **12** was actually consumed while diene **4** was not. Indeed, excluding **4** from the reaction mixture had no influence on the consumption of dienophile **12**. Closer examination of the ^{1}H NMR spectrum revealed the presence of a set of broad peaks from 1.0 to 3.5 ppm suggesting the formation of an oligomeric or polymeric material. This also occurred when 2-cyclohexen-1-one (**13**) was used for Diels-Alder reaction, where large amount of precipitate was formed during the reaction. However, when **3d** was used to catalyze these reactions, Diels-Alder adducts were obtained as the only products. In summary, as shown in Table 3.7, there is a competition between Diels-Alder cycloaddition and dienophile polymerization. For 5 membered ring dienophile **12**, the reaction was dominated by polymerization when catalyzed by **3b** or **3c**, while Diels-Alder cycloaddition played the dominant role when catalyzed by **3d** (entry 1, Table 3.7). This might be due to the higher steric hindrance of isopropyl groups at **3d** with respect to the methyl groups found at *ortho* positions at **3b**/**3c.** It is thought that due to these steric factors the dienophile can be more activated by **3b**/**3c** than by **3d** leading to self-polymerization of the substrate. In the case of **3d** the dioneophile might not be as strongly bound to the central Al but effectively enough for the Diels-Alder cycloaddition. When less reactive six-membered ring dienophile 2-cyclohexen-1-one (**13**) was used, both polymerization and Diels-Alder cycloaddition were obtained under the catalysis of **3b** and **3c**. but only Diels-Alder transformation was observed when **3d** was used as catalyst. The fact that the use of **13** resulted in both polymerization and cycloaddition suggest that the higher ring strain of **12** in comparison to **13** plays an important role in the observed polymerization.

Table 3.7 Competition between Diels-Alder cycloaddition and dienophile polymerization

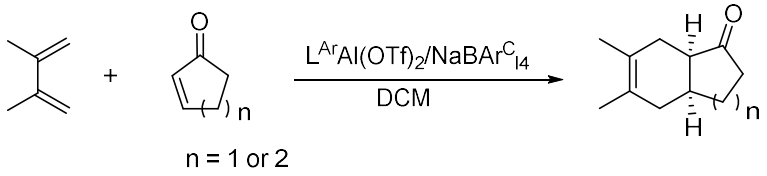

Entry	Dienophile	**3b**	**3c**	**3d**
1	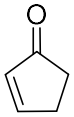 **12**	Dienophile polymerization	Dienophile polymerization	2h[a] 92% 99:1
2	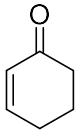 **13**	24h 23% 99:1	24h 21% 99:1	24h 87% 99:1

[a]10% of catalyst used.

As shown in Table 3.4 and 3.5, entries 5 and 6, when 1,3-cyclohexadiene or isoprene was used for these Diels-Alder reactions, polymerization was also favored under the catalysis of **3b** or **3c**/$NaBAr^{Cl}{}_{4}$. Hence, we want to study whether a more reactive diene would favor Diels-Alder cycloaddition rather than dienophile polymerization. For this purpose we chose cyclopentadiene, which is 500 more reactive than 1,3-cyclohexadiene. Under the same reaction conditions already described in Table 3.7, ^{1}H NMR clearly revealed the formation of Diels-Alder adduct and the absence of polymerization of **12** when cyclopentadiene was introduced in the reaction mixture. Thus, based on the nature of the diene it is possible to control whether Diels-Alder cyclization or dienophile polymerization will occur for **12**.

In order to gather more information on the polymer properties and the mechanism insights of this reaction a clean polymer sample(s) was required. This was achieved by combining compound **3b** with 1 equiv of $NaBAr^{Cl}_4$ in DCM following by the addition of 20 equiv of 2-cyclopenten-1-one or 2-cyclohexen-1-one. After several hours methanol was added to the reaction mixture in order to precipitate the product and remove the catalyst and unreacted starting materials. After filtration and dryness under vacuum, individual polymers (poly-**12** (polymer based on **12**) and poly-**13** (polymer based on **13**)) were obtained as white solids in moderate yields (56% in 3h for poly-**12** and 50% in 6h for poly-**13**). Unfortunately, complete conversion cannot be reached by extending the reaction times or increasing the catalyst loadings. Poly-**12** was analyzed by gel permeation chromatography (GPC) and multinuclear NMR spectroscopy. Apart from IR spectroscopy poly-**13** was not further characterized due to its insolubility in common organic solvents. As shown in Figure 3.1, ^{1}H NMR of the polymer is quite different with its monomer or cyclopentanone. The HC=CH signal at 6.1 and 7.7 ppm disappeared while the alkyl peaks were replaced by broad peaks around 1.0 to 3.5 ppm. More evidence for the existence of an oligomeric/polymeric material was acquired from the ^{13}C NMR spectrum as it also contained broad signals. In fact, a broad signal at δ_C 220 ppm suggested that the carbonyl group was still intact as shown in Figure 3.2. More evidence for the presence of a carbonyl fragment was gathered from IR spectroscopy which revealed the presence of a strong band at ~ 1730 cm^{-1}. On the other hand, the absence of any signals associated with an alkene group implied that the C=C double bond of the monomeric dienophile was presumably involved in the formation of this new material. This was also supported by the observation that cyclopentanone (**41**) and cyclohexanone (**44**) lacking of C=C, cannot polymerize under the same reaction conditions. To examine the molar mass of the prepared and purified polymeric material, gel permeation chromatography (GPC) was employed. This analysis indicated that the average molecular weight of the purified polymers ranged from 30-40

kDa with polydispersity index of 1.5-2. Finally, to further investigate the chemical structure (i.e. the repeating unit) of the polymer, MALDI-TOF mass spectrometry was used. This study indicated that the polymer chains were composed of a structural repeat unit with molar mass of 82 g/mol. Considering the nature of the monomer and structural knowledge acquired from other analyses, this weight fits very well to the proposed structure of the polymer repeat unit (C_5H_6O) presented in Scheme 3.4.

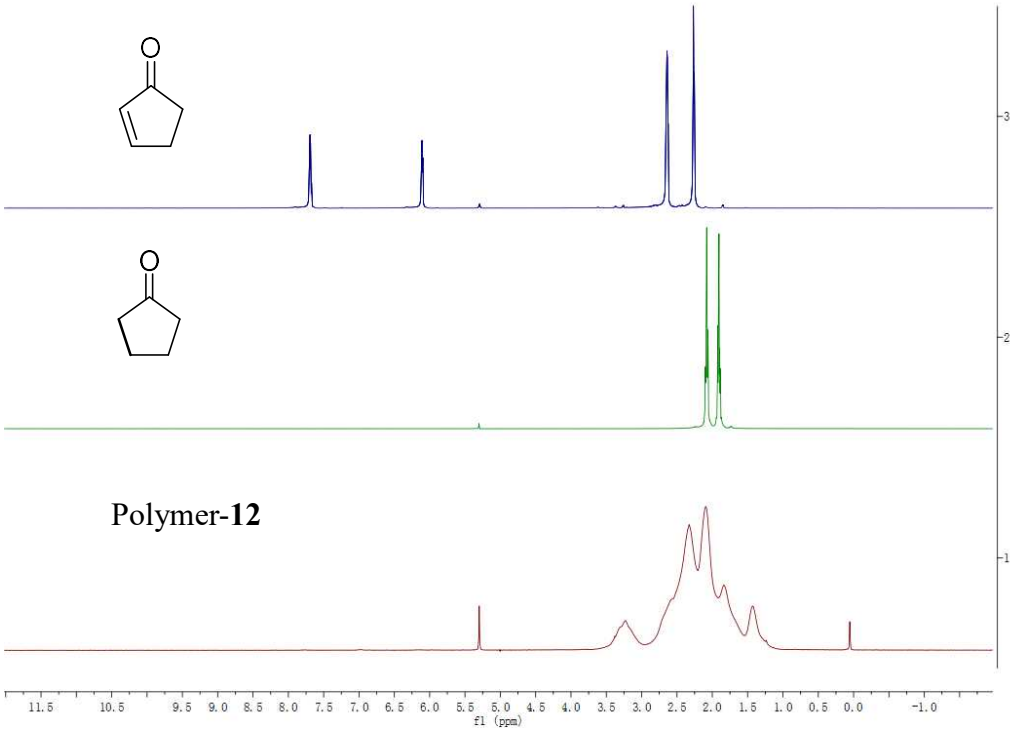

Figure 3.1 ^{1}H NMR of **13, 41** and poly-**12**

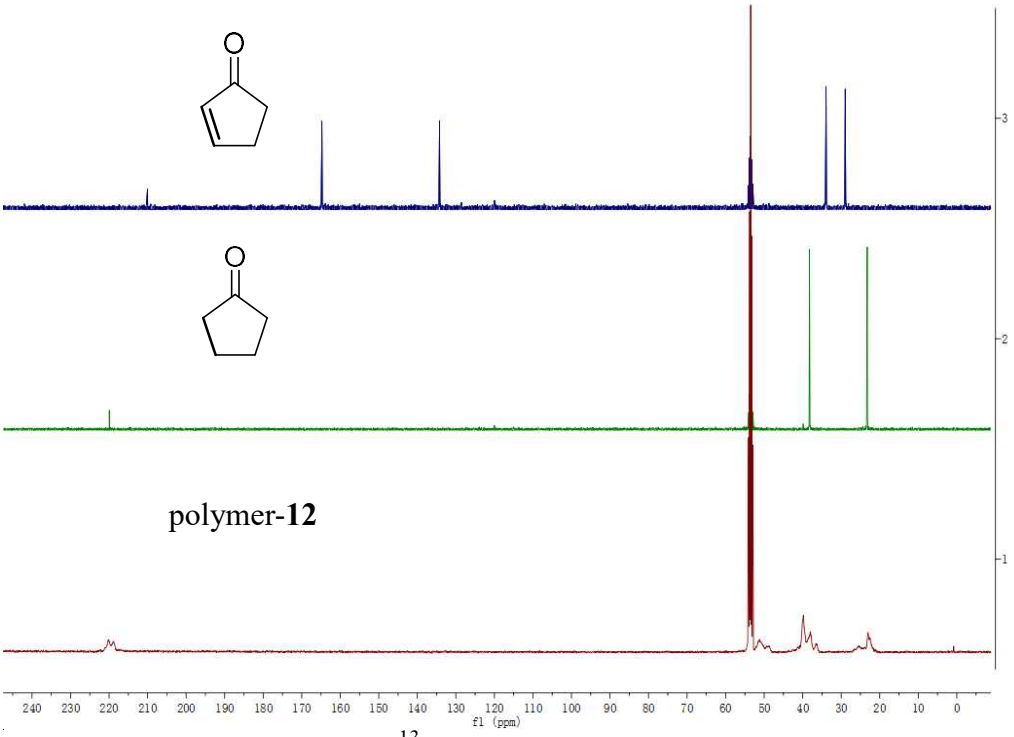

Figure 3.2 ^{13}C NMR of **13, 41** and poly-**12**

Based on our knowledge this appears to be the first time that cyclopentenone was polymerized via Michael addition polymerization. In other to gather more information on the mechanism, polymerization of **13** was attempted with several different reagents. Firstly, in the absence of $NaBAr^{Cl}_4$ compound **3b** succeeded in polymerizing this substrate but slow conversion rates were observed (36% of the substrate converted in 3h). This is in agreement that the addition of $NaBAr^{Cl}_4$ dramatically enhances the Lewis acidity of these aluminium bistriflate compounds. Then, most common Lewis acids, such as $AlCl_3$, $B(C_6F_5)_3$ and BF_3OEt_2, were not adequate catalysts for polymerization of **13** as no conceivable transformation of cyclopentenone was detected under the reaction conditions used for **3b**/$NaBAr^{Cl}_4$. The same inactivity was observed when a soluble source of HOTf (^{t}BuCl/AgOTf) was mixed with cyclopentenone.

Since we did not find another type of catalyst capable to catalyze this polymerization, we decided to figure out the optimized reaction conditions using **3b**/$NaBAr^{Cl}_4$ system. First, we

examined the influence of different catalyst loadings on the reaction activity. It was not surprised when 1 mol% of catalyst loading was used, the Al-dienophile coordination did occur, but no polymerization product was obtained. However, to our surprise, when the catalyst loading was increased to 10 mol%, a decrease in isolated yield (28%, 3h) was obtained. Meanwhile, the obtained polymer has a lower molecule weight of about 23000. This could be possibly due to a higher catalyst/monomer ratio resulting in lower molecule weights and higher content of oligomer, which is washed away by methanol. We were also interested in investigating the solvent influence to the catalysis. We found that beside of DCM, non-coordinate solvents such as chloroform, fluorobenzene and 1,2-difluorobenzene were also quite suitable for the polymerization. It is also worth mentioning that polymerization cannot occur when the catalyst was mixed with neat 2-cyclopenten-1-one.

It was strange that the quite reactive 3-buten-2-one (**9**) did not afford any polymeric material when catalyzed by **3b**/$NaBAr^{Cl}_4$ system as self-polymerization can readily occur when fresh distilled 3-buten-2-one was stored at room temperature. Then, we attempted to polymerize several different substrates using **3b**/$NaBAr^{Cl}_4$ to investigate the role of the carbonyl and the alkene groups as well as the importance of the cyclic nature of substrate **13**. As shown in Scheme 3.2, other non-cyclic dienphiles **10**, **11**, **5**, **14**, **15** were not suitable to the polymerization, which indicated a strained framework was possibly required for the polymerization. As aforementioned, cyclopentanone and cyclohexanone cannot be polymerized due to lack of C=C double bond. Then, we examined another substrate cyclopentene (**42**), which possesses both strained framework and C=C double bond, but lack of a carbonyl group. Yet again, even this substrate was not polymerized by the catalytic system. With this information in hand, we decided to expand the scope of substrates for polymerization. However, replacing one of the vinylic protons with a methyl group at of 2-cyclopenten-1-one resulted in the catalytic inertness of this new substrate (**43**) with

respect to the desired polymerization. On the other hand, introducing cyclohexenone (**13**) or cycloheptenone (**45**) into a DCM solution containing 5% (mol) of **3b**/NaBAr$^{Cl}_4$ resulted in the consumption of the substrate, albeit longer reaction times were required, and the formation of an oligomeric/polymeric material in the yields of 50% and 23%, respectively. Unfortunately, high insolubility of these materials in most common organic solvents prevented their further characterization. Nevertheless, the sole formation of these presumably oligomeric/polymeric materials suggested that, besides the presence of the carbonyl and alkene groups, the cyclic nature of the substrate played a pivotal role in their ability to form polymeric materials with catalytic amounts of **3b**/NaBAr$^{Cl}_4$. One can only assume that alleviation of ring strain as these materials are polymerized (e.g. cyclopentenone →polymeric cyclopentanone) is one of the most prominent driving forces behind the observed reactivity of cyclic dienophiles. This would also explain slower reaction rates and lower isolated yields for transformation of **13** and **45** due to a lesser degree of ring strain in comparison to **12**.

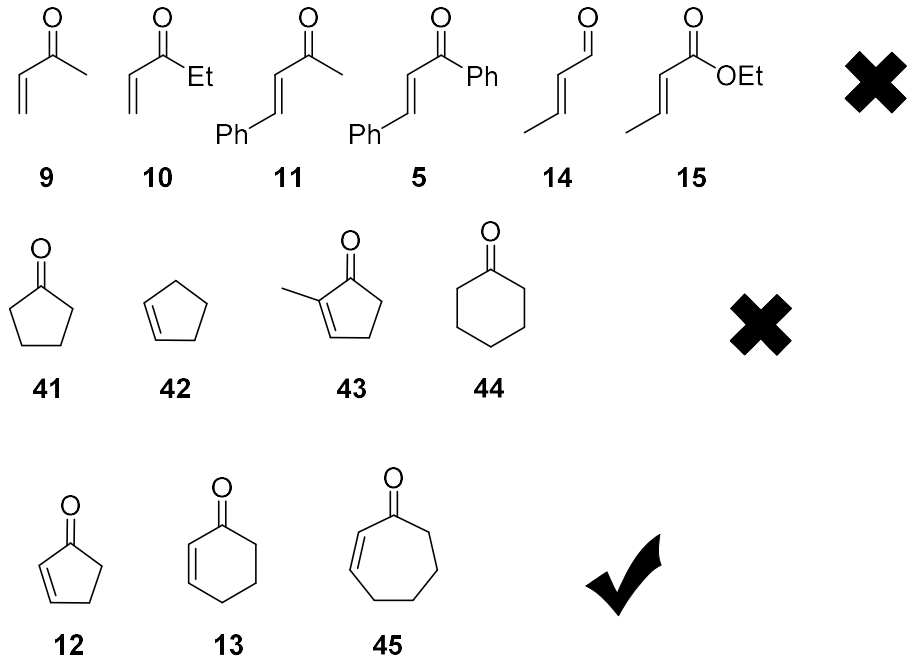

Scheme 3.2 Scope of substrates for polymerization

Considering the abovementioned evidence it was proposed that the polymerization of cyclic dienophiles, or at least of **12**, occurs via the Michael addition polymerization mechanism that is summarized in Scheme 3.3. Once the first molecule of substrate coordinates to the aluminium centre its β position becomes electrophilic enough (**A**, Scheme 3.4) for an attack by another molecule of **12**. The substrate polarization i.e. the site of the nucleophilic attack is consistent with several examples of Michael addition, which mechanism involved an Al-activated cyclopentenone. However, in this case **12** is dramatically more activated by the Al system than in the case of the most common Lewis and Brønsted acids allowing the subsequent molecule of the same substrate to act as a Michael donor. This would presumably yield the formation of a very reactive carbocation (**B**, Scheme 3.3) that would then sequentially react with other molecules of the dienophile leading to the observed polymerization. It is also noteworthy that the reason for inability of **3b**/$NaBAr^{Cl}_4$ to perform similar polymerization could be found in the fact that the ^{i}Pr substituents on **3d** prevent as strong coordination of **12** as in the case of **3b**. This would then lead to less polarized substrate **12** when **3d** was used in comparison to **3b**, which is not sufficient for the polymerization but is adequate for the Diels Alder cycloaddition.

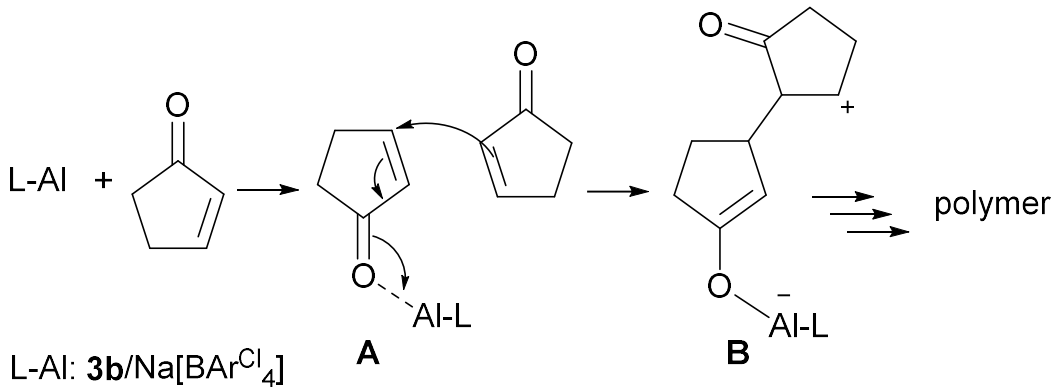

Scheme 3.3 Proposed mechanism for Michael polymerization

Our next aim was to investigate whether this polymer can be possibly modified in order to afford potential applications. The presence of carbonyl group provided the polymer the possibility to react with amines. As shown in Scheme 3.5, 1.2 equiv of benzylamine was mixed with the polymer in dry DCM with 4Å molecule sieves. The reaction mixture was set up to reflux overnight. After removal of the volatiles, the residue was examined by ^{1}H NMR. To our disappointment, the lack of aromatic signal suggested that the polymer cannot be modified by this method.

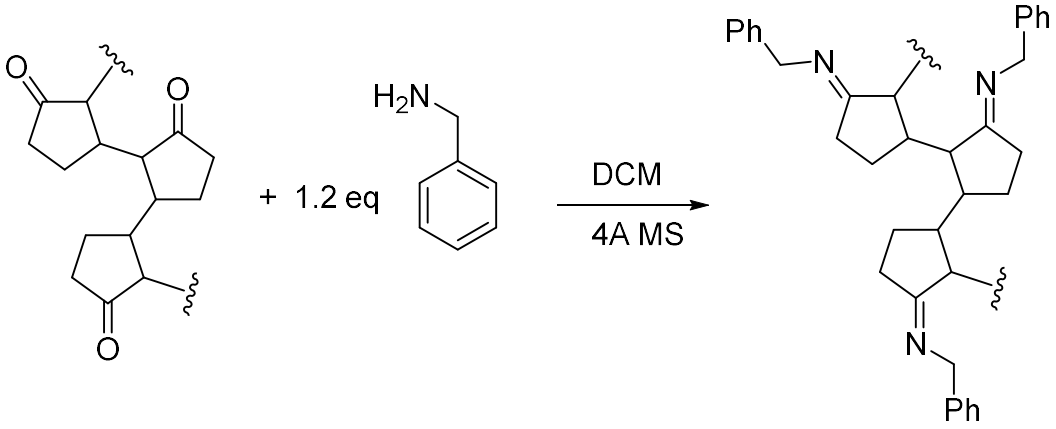

Scheme 3.4 Reactivity of poly-**12**

3.4 Summary

In summary, when combined with $NaBAr^{Cl}_4$ β-diketiminate-supported aluminum bistriflate complexes **3b**-**3d**, can form quite active Lewis acid systems capable of performing a series of Diels-Alder reactions. Several additional experiments were also performed to demonstrate that these cycloadditions were indeed catalyzed by the Lewis acid systems rather than an HBA. A subtle reduction in steric hindrance of Lewis acid catalyst **3d**, achieved by replacing the ^{i}Pr substituents with Me groups, to form catalyst **3b** resulted in unprecedented chemistry of cyclic dienophiles. **3b**/ $NaBAr^{Cl}_4$ was unexpectedly shown to polymerize cyclic dienophiles. After several experimental studies it is believed that the

Michael addition polymerization mechanism most adequately describes the polymer formation.

3.5 Experimental section

General procedure for aluminum-catalyzed Diels-Alder reactions

3d (12 mg, 0.016 mmol) and $NaBAr^{Cl}_4$ (10 mg, 0.016 mol) was dissolved in 1 mL DCM-d_2 in a J. Young NMR tube. To this solution the diene 2,3-dimethyl-1,3-butadiene (52 mg, 72 µL, 0.64 mmol) and a dienophile (0.5 equiv with respcet to the diene) was added. The reaction mixture was left for the time indicated in Tables 3.1-3.6 in the main text. After reaction completion, the corresponding products were purified by flash column chromatography on silica gel using hexane/ethyl acetate mixtures affording analytically pure Diels-Alder products. The trans/cis ratio (if applicable) was determined by ^{1}H NMR.

General procedure for ^{t}BuCl/AgOTf-catalyzed Diels-Alder reactions

The acid system was generated based on the reported procedure to which system 100 equiv of the dienophile and 200 equiv of the diene were added. The reaction mixture was left for the time indicated in Table 3.2 and 3.4-3.6 in the main text before purifying the products using already described technique(s).

General procedure for the catalytic reactions with 2,6-^{t}Bu$_2$-C_6H_3N

These reactions were conducted in the exactly same manner as already described for aluminium- and ^{t}BuCl/AgOTf-catalyzed reactions except for the addition of 1 equiv of the pyridine base before addition of the organic substrates. The reaction mixture was left for the time indicated in Table 3.3 in the main text before purification step(s).

General procedure for aluminum-catalyzed Michael polymerization

3b (56 mg, 0.088 mmol) and 1 equiv of $NaBAr^{Cl}_4$ (56 mg, 0.088 mmol) was dissolved in 2 mL DCM in a 10 mL round-bottomed flask containing a stir bar in glovebox. To this solution 2-cyclopenten-1-one (150 μL, 1.78 mmol) was added. The reaction mixture was left to stir for 3h before added in to 20 mL methanol to precipitate the polymer. After filtration the crude product was re-dissolved in 0.5 mL THF and then precipitated with another 20 mL methanol. Repeat twice. The obtained polymer was dried under vacuum at 40 ºC overnight. Yield: 87 mg, 59%. ^{1}H NMR (400 MHz, CD_2Cl_2, 25 °C): δ 1.0 -3.5 ppm (broad, aliphatic). ^{13}C NMR (100 MHz, CD_2Cl_2, 25 °C): δ 20-25, 38-40, 49-51 (all aliphatic), 119-121 (carbonyl). FTIR (KBr pellets): 1728 cm^{-1}(C=O stretch). GPC: *M*n = 26000, *M*w = 36000, *M*w/*M*n(PDI) =1.38.

The polymerization of 2-cyclohexen-1-one and 2-cyclohepten-1-one have been attempted using the same procedure yielding insoluble materials in the yields of 50% (6 h) and 23% (24 h), respectively. Due to poor solubilitythese materials have been characterized by FTIR only.

2-cyclohexen-1-one: FTIR (KBr pellets): 1707cm-1(C=O stretch).

2-cyclohepten-1-one: FTIR (KBr pellets): 1681cm-1(C=O stretch).

NMR data for Diels-Alder products

1-(3,4-Dimethylcyclohex-3-en-1-yl)ethanone (16)

^{1}H NMR (400 MHz, $CDCl_3$): δ 1.49-1.57 (m, 1H), 1.60 (s, 3H), 1.62 (s, 3H), 1.87-1.94 (m, 1H), 1.98-2.12 (m, 4H), 2.17 (s, 3H), 2.52-2.58 (m, 1H) ppm. ^{13}C NMR (100 MHz, $CDCl_3$): δ 18.9, 19.1, 25.4, 28.0, 31.3, 33.4, 48.4, 124.1, 125.5, 212.0 ppm. The analytical and spectroscopic data are in accordance with those reported.[9]

1-(3,4-Dimethylcyclohex-3-en-1-yl)ethanone (17)

^{1}H NMR (400 MHz, $CDCl_3$): δ 1.03 (t, J = 7.3 Hz, 3H), 1.45-1.58 (m, 1H), 1.59 (s, 3H), 1.62 (s, 3H), 1.82-1.90 (m, 1H), 1.95-2.17 (m, 4H), 2.49 (dq, $J_{H\text{-}H}$ = 7.2 Hz, J = 4.0 Hz, 2H), 2.54-2.61 (m, 1H) ppm. ^{13}C NMR (100 MHz, $CDCl_3$): δ 7.9, 18.9, 19.2, 25.7, 31.4, 33.5, 33.9, 47.5, 124.2, 125.5, 214.6 ppm. The analytical and spectroscopic data are in accordance with those reported.[9,10]

1-(3,4-Dimethyl-6-phenylcyclohex-3-en-1-yl)ethanone (18)

^{1}H NMR (400 MHz, $CDCl_3$): δ 1.61 (s, 3H), 1.63 (s, 3H), 1.81 (s, 3H), 2.03-2.12 (m, 1H), 2.13-2.21 (m, 2H), 2.22-2.30 (m, 1H), 2.87-3.00 (m, 2H), 7.10-7.17 (m, 3H), 7.21-7.26 (m, 2H) ppm. ^{13}C NMR (100 MHz, $CDCl_3$): δ 18.8, 18.8, 29.7, 35.1, 40.5, 43.6, 54.1, 123.9, 125.6, 126.7, 127.5, 128.7, 144.3, 212.3 ppm. The analytical and spectroscopic data are in accordance with those reported.[11]

(3,4-Dimethyl-6-phenylcyclohex-3-en-1-yl)phenylmethanone (8)

^{1}H NMR (400 MHz, $CDCl_3$): δ 1.70 (bs, 6H), 2.24-2.38 (m, 4H), 3.31 (ddd, J = 14.4 Hz, J = 9.6 Hz, J = 7.1 Hz, 1H), 4.02 (dt, J = 10.7 Hz, J = 5.6 Hz, 1H), 7.04-7.10 (m, 1H), 7.13-7.25 (m, 4H), 7.35-7.42 (m, 2H), 7.46-7.51 (m, 1H), 7.81-7.87 (m, 2H) ppm. ^{13}C NMR (100 MHz, $CDCl_3$): δ 18.8, 18.9, 37.1, 40.8, 43.2, 47.5, 124.2, 125.8, 126.3, 127.5, 128.2, 128.4, 128.6, 132.8, 137.5, 144.8, 203.6 ppm. The analytical and spectroscopic data are in accordance with those reported.[12]

5,6-dimethyl-2,3,3a,4,7,7a-hexahydro-1H-inden-1-one (19)

^{1}H NMR (400 MHz, $CDCl_3$): δ 1.57 (bs, 3H), 1.60 (bs, 3H), 1.66-1.78 (m, 3H), 1.95-2.33 (m, 6H), 2.40-2.466 (m, 1H). ^{13}C NMR (100 MHz, $CDCl_3$): δ 18.9, 19.4, 26.4, 27.9, 32.8, 33.0, 34.4, 47.8, 123.5, 124.1, 220.1 ppm.

6,7-Dimethyl-3,4,4a,5,8,8a-hexahydro-2H-naphthalen-1-one (20)

^{1}H NMR (400 MHz, $CDCl_3$): δ 1.59 (bd, J = 1.6 Hz, 3H), 1.62 (bd, J_{H-H} = 0.7 Hz, 3H), 1.68-1.78 (m, 2H), 1.81-1.94 (m, 4H), 1.97-2.06 (m, 1H), 2.20-2.22 (m, 1H), 2.31-2.46 (m, 3H), 2.68 (m, 1H) ppm. ^{13}C NMR (100 MHz, $CDCl_3$): δ 18.9, 19.3, 24.2, 28.4, 30.2, 34.1, 36.6, 39.9, 49.3, 122.9, 123.6, 213.3 ppm. The analyticaland spectroscopic data are in accordance with those reported.[13]

4,6-dimethylcyclohex-3-ene-1-carbaldehyde (21)

^{1}H NMR (400 MHz, $CDCl_3$): δ 0.99 (d, J = 6.2 Hz, 3H), 1.56 (s, 3H), 1.59 (s, 3H), 1.63 (m, 1H), 2.01 (m, 3H), 2.17 (m, 2H), 9.61 (s, 1H). ^{13}C NMR (100 MHz, $CDCl_3$): δ 18.7, 18.9, 19.6, 28.8, 30.4, 39.0, 53.6, 122.6, 125.2, 205.4 ppm.

ethyl 3,4,6-trimethylcyclohex-3-ene-1-carboxylate (22)

^{1}H NMR (400 MHz, $CDCl_3$): δ 0.92 (d, J = 6.3 Hz, 3H), 1.24 (t, J = 7.1 Hz, 3H), 1.59 (bs, 6H), 1.71-1.73 (m, 1H), 1.88-2.27 (m, 5H), 4.10-4.18 (m, 2H). ^{13}C NMR (100 MHz, $CDCl_3$): δ 14.4, 18.6, 18.8, 19.6, 31.5, 35.1, 40.1, 48.0, 60.1, 123.6, 125.0, 176.3ppm.

endo-1-(Bicyclo[2.2.2]oct-5-en-2-yl)ethanone (24)

^{1}H NMR (400 MHz, $CDCl_3$): δ 1.18-1.38 (m, 2H), 1.44-1.55 (m, 1H), 1.57-1.61 (m, 1H), 1.62-1.68 (m, 2H), 2.12 (s, 3H), 2.51-2.63 (m, 1H), 2.71 (ddd, J_{H-H} = 8.7 Hz, J = 6.9 Hz, J = 2.1 Hz, 1H), 2.88-2.92 (m, 1H), 6.11 (ddd, J_{H-H} = 8.3 Hz, J = 6.5 Hz, J = 1.1 Hz, 1H), 6.26 (ddd, J = 8.5 Hz, J = 6.8 Hz, J = 1.1 Hz, 1H) ppm. ^{13}C NMR (100 MHz, $CDCl_3$): δ 24.6, 26.0, 28.4, 28.8, 29.7, 32.2, 51.7, 131.2, 135.3, 209.9 ppm. The analytical and spectroscopic data are in accordance with those reported.[14]

endo-1-(Bicyclo[2.2.2]oct-5-en-2-yl)propan-1-one (25)

^{1}H NMR (400 MHz, $CDCl_3$): δ 1.02 (t, J_{H-H} = 7.3 Hz, 3H), 1.21-1.35 (m, 2H), 1.44-1.53 (m, 1H), 1.54-1.62 (m, 1H), 1.62-1.67 (m, 2H), 2.33-2.51 (m, 2H), 2.55-2.61 (m, 1H), 2.68 (dt, J = 7.7 Hz, J = 2.1 Hz, 1H), 2.84-2.89 (m, 1H), 6.10 (ddd, J = 7.9 Hz, J = 6.5 Hz, J = 1.0 Hz, 1H), 6.27 (ddd, J = 8.0 Hz, J = 6.7 Hz, J = 1.1 Hz, 1H) ppm. ^{13}C NMR (100 MHz, $CDCl_3$): δ 8.2, 24.6, 26.1, 29.0, 29.7, 32.3, 34.0, 50.6, 131.3, 135.1, 212.6 ppm. The analytical and spectroscopic data are in accordance with those reported.[10]

endo-1-(3-Phenylbicyclo[2.2.2]oct-5-en-2-yl)ethanone (26)

^{1}H NMR (400 MHz, $CDCl_3$): δ 0.97-1.10 (m, 1H), 1.43-1.49 (m, 1H), 1.67-1.79 (m, 2H), 2.02 (s, 3H), 2.50-2.56 (m, 1H), 2.94 (dd, J = 6.8 Hz, J = 1.8 Hz, 1H), 2.99-3.05 (m, 1H), 3.12 (ddd, J = 6.7 Hz. J = 2.0 Hz, J = 2.0 Hz, 1H), 6.12 (ddd, J = 7.6 Hz, J = 6.8 Hz, J = 0.9 Hz, 1H), 6.48 (ddd, J = 8.0 Hz, J = 6.8 Hz, J = 1.2 Hz, 1H), 7.22-7.40 (m, 5H) ppm. ^{13}C NMR (100 MHz, $CDCl_3$): δ 18.5, 26.1, 28.5, 32.7, 37.3, 45.6, 56.6, 126.5, 128.2, 128.6, 131.6, 136.1, 142.8, 209.0 ppm. The analytical and spectroscopic data are in accordance with those reported.[15]

endo-Phenyl-(3-phenylbicyclo[2.2.2]oct-5-en-2-yl)methanone (27)

^{1}H NMR (400 MHz, $CDCl_3$): δ 1.08-1.18 (m, 1H), 1.47 (dddd, J = 11.3 Hz, J = 11.3 Hz, J = 3.4 Hz, J = 3.4 Hz, 1H), 1.80-1.95 (m, 2H), 2.55-2.71 (m, 1H), 2.96-3.01 (m, 1H), 3.48 (ddd, J = 6.5 Hz, J = 4.0 Hz, J = 2.0 Hz, 1H), 3.80 (dd, J = 6.5 Hz, J = 1.6 Hz, 1H), 6.11 (ddd, J = 8.9 Hz, J = 7.7 Hz, J = 0.8 Hz, 1H), 6.58 (ddd, J = 9.1 Hz, J = 8.0 Hz, J = 1.0 Hz, 1H), 7.19-7.24 (m, 1H), 7.27-7.36 (m, 4H), 7.36-7.43 (m, 2H), 7.48-7.53 (m, 1H), 7.85-7.90 (m, 2H) ppm. ^{13}C NMR (100 MHz, $CDCl_3$): δ 18.6, 26.6, 34.7, 36.6, 44.8, 51.1, 126.3, 128.3, 128.6, 128.6, 130.8, 132.8, 136.4, 136.6, 143.0, 200.9 ppm. The analytical and spectroscopic data are in accordance with those reported.[15]

4,4a,6,7,8,8a-hexahydro-1,4-ethanonaphthalen-5(1H)-one (29)

^{1}H NMR (400 MHz, $CDCl_3$): δ 1.28 (m, 1H), 1.45-1.59 (m, 3H), 1.71-1.80 (m, 4H), 2.05-2.09 (m, 1H), 2.34-2.45 (m, 4H), 3.08 (m, 1H), 6.11 (m, 1H), 6.24 (m, 1H) pppm. ^{13}C NMR (100 MHz, $CDCl_3$): δ 20.8, 24.0, 26.0, 29.6, 31.2, 35.9, 38.8, 42.2, 52.9, 133.1, 134.5, 214.5 ppm.

3-methylbicyclo[2.2.2]oct-5-ene-2-carbaldehyde (30)

^{1}H NMR (400 MHz, $CDCl_3$): δ 1.08 (d, J_{H-H} = 6.92 Hz, 3H), 1.25-1.32 (m, 1H), 1.53-1.55 (m, 2H), 1.75-1.94 (m, 3H), 2.32 (m, 1H), 2.81 (m, 1H), 6.08 (m, 1H), 6.40 (m, 1H), 9.40 (d, J = 2.00 Hz, 1H) ppm. ^{13}C NMR (100 MHz, $CDCl_3$): δ 18.4, 19.7, 25.6, 31.4, 32.3, 35.6, 59.7, 130.2, 137.8, 203.7 ppm.

1-(4-methylcyclohex-3-en-1-yl)ethan-1-one (33)

^{1}H NMR (400 MHz, $CDCl_3$): δ 1.57 (m, 1H), 1.65 (s, 3H), 1.94-1.98 (m, 3H), 2.15 (bs, 5H), 2.51 (m, 1H), 5.38 (m, 1H) ppm. ^{13}C NMR (100 MHz, $CDCl_3$): δ 23.4, 25.0, 27., 28.0, 29.5, 47.3, 119.3, 133.9, 211.9 ppm.

1-(4-methylcyclohex-3-en-1-yl)propan-1-one (34)

^{1}H NMR (400 MHz, $CDCl_3$): δ 1.02 (t, J_{H-H} = 7.3 Hz, 3H), 1.56-1.61 (m, 1H), 1.64 (bs, 3H), 1.90-1.99 (m, 3H), 2.11-2.1 (m, 2H), 2.45-2.54 (m, 3H), 5.38 (m, 1H) ppm. ^{13}C NMR (100 MHz, $CDCl_3$): δ 7.8, 23.4, 25.2, 27.3, 29.6, 33.9, 46.3,119.4, 133.8, 214.5 ppm.

1-(5-methyl-1,2,3,6-tetrahydro-[1,1'-biphenyl]-2-yl)ethan-1-one (35)

^{1}H NMR (400 MHz, $CDCl_3$): δ 1.69 (s, 3H), 1.84 (s, 3H), 2.20-2.26 (m, 4H), 2.96-3.04 (m, 2H), 5.46 (m, 1H), 7.18-7.30 (m, 5H) ppm. ^{13}C NMR (100 MHz, $CDCl_3$): δ 23.1, 28.8, 29.7, 38.6, 43.0, 53.0, 118.9, 126.5, 127.4, 128.6, 133.8, 144.1, 121.2 ppm.

(5-methyl-1,2,3,6-tetrahydro-[1,1'-biphenyl]-2-yl)(phenyl)methanone (36)

^{1}H NMR (400 MHz, $CDCl_3$): δ 1.74 (s, 3H), 2.28-2.38 (m, 4H), 3.32 (m, 1H), 3.93 (m, 1H), 5.50 (m, 1H), 7.04-7.10 (m, 1H), 7.16-7.19 (m, 4H), 7.36-7.42 (m, 2H), 7.46-7.52 (m, 1H), 7.79-7.81 (m, 2H) ppm. ^{13}C NMR (100 MHz, $CDCl_3$): δ 23.2, 30.8, 38.9, 42.8, 46.6, 119.3, 126.2, 127.5, 128.0, 128.4, 128.5, 132.7, 134.1, 137.4, 144.7, 203.7 ppm.

4,6-dimethylcyclohex-3-ene-1-carbaldehyde (39)

^{1}H NMR (400 MHz, $CDCl_3$): δ 1.00 (d, J_{H-H} = 6.3 Hz, 3H), 1.62 (s, 3H), 1.66-1.69 (m, 1H), 2.00-2.20 (m, 5H), 5.35 (m, 1H), 9.60 (s, 1H), ^{13}C NMR (100 MHz, $CDCl_3$): δ 19.7, 23.4, 24.1, 28.4, 37.0, 52.4, 117.8, 133.5, 205.4 ppm.

References

1 Anand, N.; Bindra, J. S.; Ranganathan, S. *Art in Organic Synthesis*, Holden-Day, Inc. San Francisco, 1970; 2nd. Edition, John Wiley & Sons, New York, 1988.

2 Takao, K.-i.; Munakata, R.; Tadano, K.-i. *Chem. Rev.* **2005,** *105*, 4779.

3 Jørgensen, K. A. *Eur. J. Org. Chem*. **2004**, 2093.

4 Nicolaou, K. C.; Snyder, S. A.; Montagnon, T.; Vassilikogiannakis, G. *Angew. Chem. Int. Ed.* **2002,** *41*, 1668.

5 Stocking, E. M.; Williams, R. M. *Angew. Chem. Int. Ed.* **2003,** *42*, 3078.

6 Cazeau, P.; Duboudin, F.; Moulines, F.; Babot, O.; Dunogues, J. *Tetrahedron* **1987,** *43*, 2089.

7 Dang, T. T.; Boeck, F.; Hintermann, L. *J. Org. Chem.* **2011,** *76*, 9353.

8 Taarning, E.; Madsen, R. *Chem. Eur. J.* **2008,** *14*, 5638.

9 Rickerby, J.; Vallet, M.; Bernardinelli, G.; Viton, F.; Kündig, E. P. *Chem. Eur. J.* **2007,** *13*, 3354.

10 Nakashima, D.; Yamamoto, H. *Org. Lett.* **2005,** *7*, 1251.

11 Schmidt, R. K.; Müther, K.; Mück-Lichtenfeld, C.; Grimme, S.; Oestreich, M. *J. Am. Chem. Soc*. **2012,** *134*, 4421.

12 Cong, H.; Ledbetter, D.; Rowe, G. T.; Caradonna, J.P.; Porco, Jr., J. A. *J. Am. Chem. Soc.* **2008**, *130*, 9214.

13 Ryu, D. H.; Corey, E. J. *J. Am. Chem. Soc.* **2003**, *125*, 6388.

14 Klare, H. F. T.; Bergander, K.; Oestreich, M. *Angew. Chem. Int. Ed.* **2009**, *48*, 9077.

15 Kinsman, A. C.; Kerr, M. A. *Org. Lett.* **2000**, *2*, 3517.

Chapter 4

Pursuing the active species in an NCN pincer aluminum-based Lewis acid system for catalytic Diels-Alder cycloadditions

After identifying a series of well-defined β-diketiminate-stabilized alumnium bis(triflate) systems capable of catalyzing several difficult Diels Alder transformations we decided to investigate the role of the ligand on the overall catalytic activity. Various pincer ligands have been extensively used to support numerous transition metal complexes including Ru, Os, Ni, Pd and Pt.[1–6] Theses complexes showed good stability and were widely investigated as Heck-coupling and C–C bond formation catalysts. More recently, a series of lanthanide complexes based on bis(imino)aryl NCN pincer ligands were reported as efficient catalysts for diene polymerization with excellent cis-1,4 selectivities.[7] However, with respect to the aluminum chemistry, there is only a single report describing the preparation of diethylaluminum complexes stabilized by these NCN pincer ligands and their role as L-lactide polymerization catalysts.[8] Besides which, Beck and Schmidt[9] reported that monodentate analogues of the current ligand family can used to support aluminum halide derived Lewis acids. Hence, we decide to prepare an aluminum bistriflate complex based on this type of pincer ligand and extend its potential applications in catalysis.

4.1 Synthesis of bis(imino)aryl NCN pincer ligand

At the beginning, pincer ligand $C_6H_3[CHNC_6H_3(i\text{-}Pr)_2]_2Br$ (**45**) was synthesized following the procedure reported by Elsevier[10] as shown in Scheme 4.1.This procedure involved condensation of $C_6H_3(CHO)_2Br$ and excess of 2,6-diisopropylaniline in reflux toluene in the presence of 4Å molecular sieves for 16h, which was then followed by THF extraction. However, this method required long reaction time and harsh reaction conditions. Moreover, the final product obtained with this method contained few impurities causing the appearance of a green color.

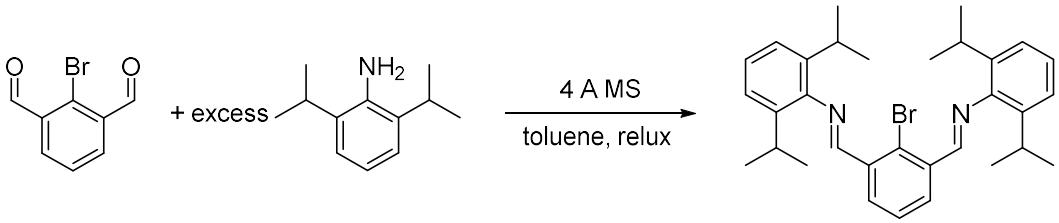

45

Scheme 4.1 General synthesis of Ligand **45**

Thus, we tried another method provided by Cui's[7] group as shown in Scheme 4.2. This reaction was performed at room temperature by mixing the two reagents in methanol with catalytic amount of formic acid. Pure product (yellow color) can be easily obtained by simple filtration resulting in excellent isolated yields (> 90%) and, more importantly, the entire procedure takes around 2 h.

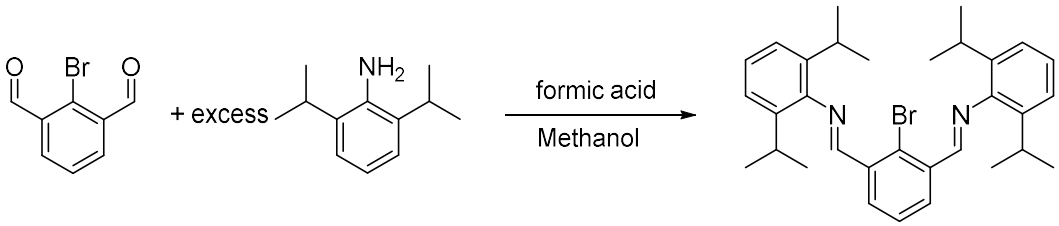

45

Scheme 4.2 General synthesis of Ligand **45**

4.2 Synthesis of NCN pincer ligand supported aluminum complexes

In order to synthesize the target aluminum bistriflate complex, the corresponding aluminum dichloride precursor needed to be prepared first. The initial synthetic procedure was similar to that used in synthesis of the nacnac $LAlCl_2$ in Chapter Ⅱ. The free ligand (**45**) was debrominated by $^{n}BuLi$ in toluene at -78°C followed by addition of 1 equiv of $AlCl_3$ as shown in Scheme 4.3. However, after several tries we unable to isolate pure samples.

According to ^{1}H NMR spectroscopy numerous species were present in the reaction mixture and it was impossible to determine whether the dicholoride aluminum compound was actually formed. Then, we tried other non-coordinating solvents, such as benzene and hexane, but no improvement in terms of purity was achieved. This might be due to the low solubility of the lithium salt, formed in the initial step, in these solvent media. Thus, we decided to use coordinating solvents to perform this reaction in order to stabilize and solubilize the lithium salt, although the introduction of a coordinating molecule might cause the decrease in Lewis acidity of the target aluminum complex. We first chose diethyl ether as a solvent for this reaction. However, we still could not isolate a pure sample of the desired aluminum dichloride compound. Then we tried another commonly used coordination solvent THF, which to our delight, was quite suitable for this reaction. As shown in Scheme 4.3, after removing all volatiles under reduced pressure and extraction with DCM, the target dichloride aluminum complex **46** was isolated, as a THF adduct. The presence of bound THF was confirmed by ^{1}H NMR spectroscopy as a set of signals at 1.89 and 3.92 ppm was downfield shifted from the same signals observed for free THF (1.85 and 3.76 ppm). ^{27}Al NMR spectroscopic identification of this dichloride complex revealed the presence of a signal at δ_{Al} ~ 97 ppm. The coordinated THF can be easily removed by exposing **46** under reduced pressure overnight affording THF-free analogue **47**. The ^{1}H NMR spectrum of **47** was quite similar to that of **46** except for the absence of THF signals. The formation of **47** can also be confirmed by ^{27}Al NMR spectroscopy as the aluminum signal shifted downfield to δ_{Al} ~ 106 ppm. Crystals of **47** suitable for single crystal X-ray diffraction were obtained from a toluene/hexane solvent mixture. Molecular structure is shown in Figure 4.1 with the crystallographic data summarized in Table 4.1. It is worth noting that a crop of crystals obtained from a toluene/hexane solvent mixture of **46** revealed the same structure as **47**, which suggested a weak coordination between of THF at the aluminum center.

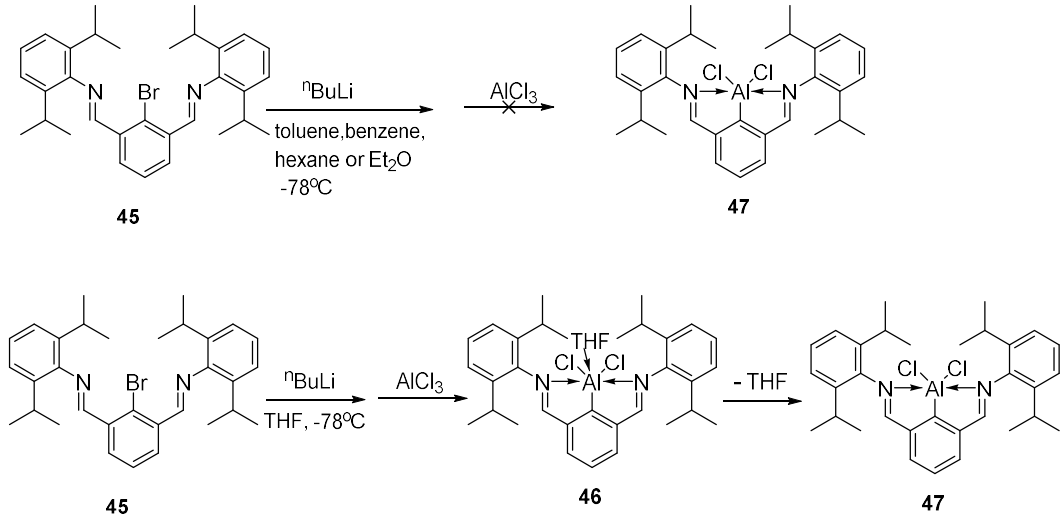

Scheme 4.3 Synthetic approaches to $LAlCl_2$ compounds

As shown in Figure 4.1, the monoanionic bis(imino)aryl NCN pincer ligand coordinates to the aluminum atom in a tridentate fashion. The geometry around the central Al atom can be described as a distorted trigonal bipyamid with one carbon atom and two chloride atoms in the equatorial position and two nitrogen atoms in the apical position. The Al-C bond length 1.943(3) Å is shorter than those observed in diethylaluminum complex $(2,6\text{-}(2,6\text{-}i\text{-}Pr_2C_6H_3N{=}CH)_2C_6H_3)AlEt_2$ (1.977(7) Å) stabilized by the same NCN pincer ligand but similar to those observed in cationic aryl aluminum complex $[(2,6\text{-}Mes_2C_6H_3)_2Al]^+[B(C_6F_5)_4]^-$ (1.9412(12) Å).[11] The two Al-N bonds have quite different lengths even though only one set of proton and carbon signals were observed in the NMR experiments in solution. The value for the short Al-N bond length of 2.139(2) Å is comparable to the same bond distance of 2.1862(19) Å for $(2,6\text{-}(2,6\text{-}i\text{-}Pr_2C_6H_3NCH)_2C_6H_3)AlEt_2$ but considerably longer than that reported for $\{3,5\text{-}Bu^t_2\text{-}2\text{-}(O)C_6H_2CH{=}N\text{-}2,6\text{-}Me_2C_6H_3\}AlMe_2$ (1.972(3) Å).[12] On the other hand the long Al-N bond distance of 2.502 Å is apparently longer than typical Al-N coordination bonds. Nevertheless, this bond distance is shorter than the sum of the van der Waals radii for N and Al atoms [$r_v(N) + r_m(Al)$ =1.55 +1.43 = 2.98 Å], suggesting that the imine N

atom indeed coordinates to the Al atom.[13] The Al-Cl bond lengths of 2.1250(11) and 2.1384(11) Å are similar with that for compound **2c** (2.1299(6) and 2.1295(6) Å) and **2f** (2.124(7) and 2.116(9) Å) discussed in Charpter 2, which are stabilized by β-diketiminato ligands.

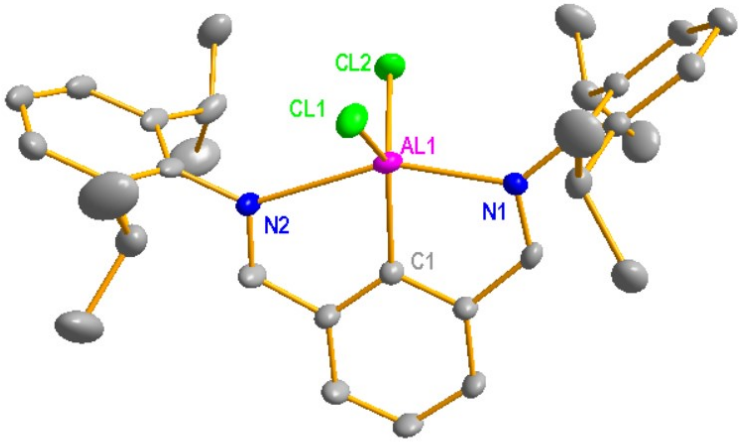

Figure 4.1 Molecular structure for **47**.

Thermal ellipsoids have been drawn at 50% probability level. All hydrogen atoms have been omitted for clarity. Selected bond lengths (Å) and angles (°): Al1-C1 1.943(3), Al1-N1 2.139(2), **Al1-N2 2.1637**, Al1-Cl1 1.943(3), Al1-Cl2 2.1250(11), C1-Al1-N1 80.37(10), Cl1-Al1-N1 102.72(7), Cl1-Al1-Cl2 109.78(5).

Our next aim was to prepare bistriflate aluminum compound by replacing the Cl ligands with OTf in order to enhance the Lewis acidic properties of the aluminum center.[14] For this purpose, dichloride precursor **46** or **47** was mixed with AgOTf in DCM or 1,2-difluorobenzene in the absence of light as shown in Scheme 4.4. However, after numerous tries no clean sample of the target bistriflate compound was obtained even though the formation of AgCl precipitate was observed. According to ^{1}H and ^{19}F NMR

spectroscopy numerous species were present in the reaction mixture and it was difficult to determine whether the bistriflate aluminum compound has actually formed. On one occasion, before we even isolated **46** (or **47**) we added AgOTf to the reaction mixture in THF, left it to stir overnight and layered the resulting solution with hexane after filtration. Fortunately several crystals suitable for single crystal X-ray diffraction were obtained and the resulting molecular structure is shown in Figure 4.2 with the crystallographic data summarized in Table 4.1.

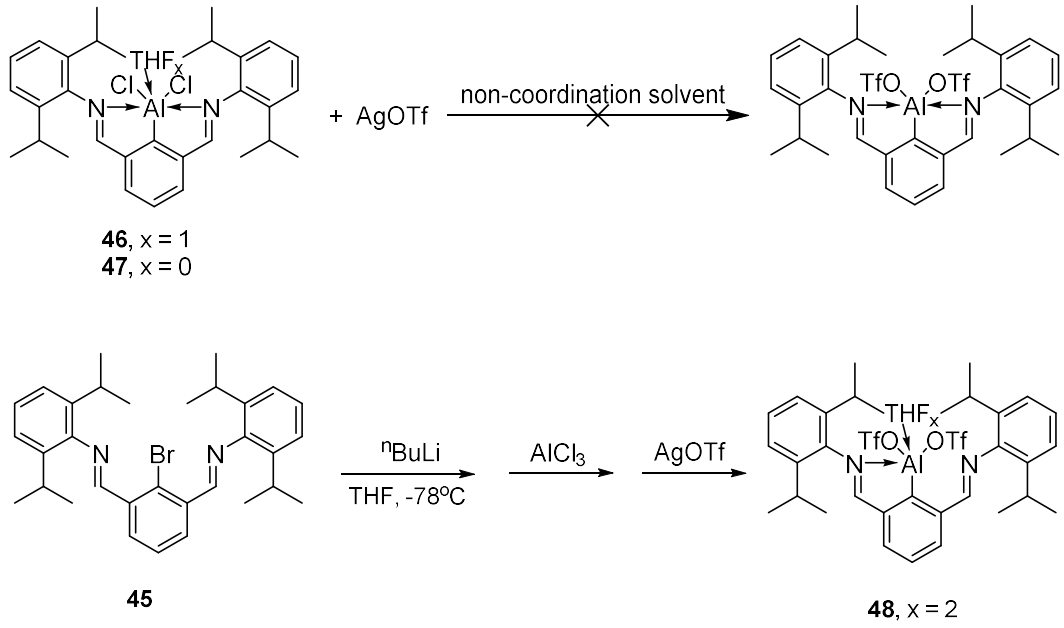

Scheme 4.4 Synthetic approaches to $LAl(OTf)_2$ compounds

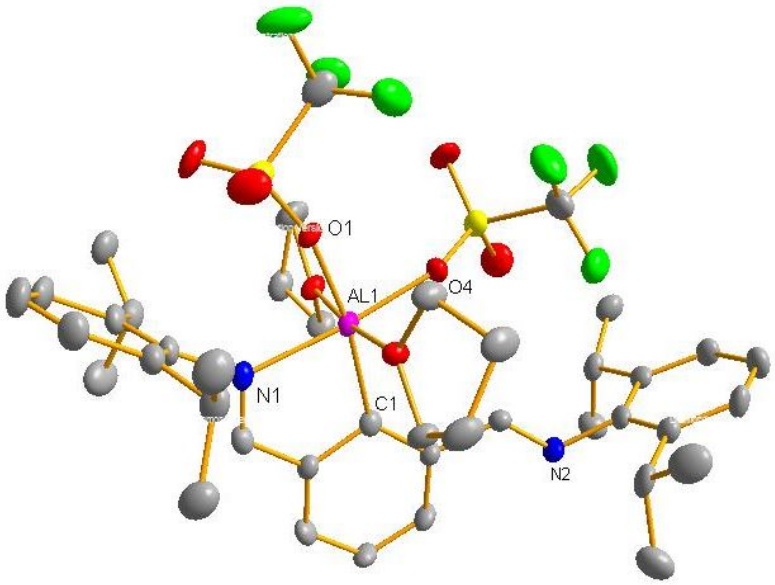

Figure 4.2 Molecular structure for **48**.

Thermal ellipsoids have been drawn at 50% probability level. All hydrogen atoms have been omitted for clarity. Selected bond lengths (Å) and angles (°): Al1-C1 2.052(4), Al1-N1 2.122(3), Al1-O1 1.882(3), Al1-O4 1.920(3), Al1-O7 1.977(3), Al1-O8 1.960(3), O1-S1 1.479(3), O4-S2 1.477(3), C1-Al1-N1 82.03(14), Cl1-Al1-O1 169.54(14), Cl1-Al1-O4 103.60(14).

Table 4.1 Summary of crystallographic data for **47** – **50**

	47	**48**	**49**	**50**
Formula	C_{32} H_{39} Al Cl_2 N_2	$C_{96}H_{134}Al_2F_{12}$ $N_4O_{19}S_4$	$C_{92}H_{98}Al_2BCl_2$ $_0N_4Na$	$C_{64.36}H_{68.91}AlB$ $Cl_{11.82}N_2O$
Formula weight	549.53	2058.26	2056.50	1343.31
Crystal system	Monoclinic	monoclinic	monoclinic	triclinic
Space group	P2(1)/n	P 1 21/c 1	C 1 2/c 1	P -1
a /Å	9.5204(11)	9.7628(8)	16.9979(7)	14.2999(7)
b /Å	25.954(3)	27.367(2)	27.9699(11)	16.7422(9)
c /Å	12.6419(16)	19.2292(14)	20.6231(9)	17.0542(9)
β/°	98.612(5)	101.133(3)	92.6642(16)	104.6772(19)
V / Å3	3088.5(6)	5040.9(7)	9794.2(7)	3280.3(3)
Z	4	2	4	2
Dc/ g cm-3	1.182	1.356	1.395	1.360

F(000)	1168	2176	4240	1392
Crystal size/ mm	0.20 x 0.16 x 0.12	0.140 x 0.160 x 0.200	0.220 x 0.320 x 0.360	0.390 x 0.400 x 0.420
θ range/°	2.26 to 29.00	2.48 to 26.48	1.40 to 29.19	1.46 to 27.13°
No. of reflns collected	35460	60773	31329	106602
No. of indep reflns	8162	10354	13109	14392
R1 [I >2σ (I)]	0.0619	0.0650	0.0792	0.0510
wR2 (all data)	0.1754	0.1876	0.2458	0.1380
Peak and hole/e $Å^{-3}$	0.324 and -0.349	0.800 and -0.537	1.462 and -1.397	1.628 and -0.817

As shown in Figure 4.2, the central aluminum is six-coordinate, adopting a distorted octahedral geometry. The monoanionic bis(imino)aryl NCN pincer ligand coordinates to the aluminum atom in a bidentate fashion with only one imine N atom forming a coordination bond. Besides the two triflate ligands, the metal center is further supported by two THF molecules. The Al-N bond length of 2.122(3) Å is a bit shorter than the shorter Al-N bond length of its precursor **46** (2.139(2) Å), potentially hinting at a decrease in electron density at the aluminum center after the ligand exchange. The Al-OTf bond lengths of 1.882(3) and 1.920(3) Å were longer than those observed for bistriflate aluminum complexes **3a** - **3f** (1.755(4) to 1.769(3) Å) stabilized by Nacnac ligands which is presumably due to the presence of coordinated THF molecules which not only increase the electron density at the aluminum center but also increase the coordination number from 4 to 6. Unfortunately, we were never able to isolate enough pure samples of **48** in order to perform further analysis, such as multinuclear NMR spectroscopy, because this compound appeared to be extremely air/moisture sensitive. As a result we were not able investigate its catalytic properties for Diels Alder transformations.

4.3 Identification for the active species of Diels-Alder cycloadditions

Nevertheless, both **46** and **47** could potentially be used as Lewis acid catalysts simply because of the presence of the aluminum center. Hence, we then focused our attention on investigating the potential catalytic properties of **46** or **47** for Diels Alder reaction between 2,3-dimethylbutadiene (**4**) and 1,3-diphenyl-2-propenone (**5**) which has already been proven to be quite suitable for the β-diketiminate bistriflate aluminum catalytic systems. Unfortunately, both **46** and **47** showed no catalytic activity with respect to the target cycloaddition as no formation of adduct **8** or consumption of the starting materials was observed (entry 1, Table 4.2). In our experience the addition of borates such as $NaBAr^{Cl}_4$ could dramatically increase the catalytic properties of the aluminum compounds. As a result when **47** was mixed with 1 equiv of $NaBAr^{Cl}_4$ in CD_2Cl_2, we did observe the formation of the target Diels-Alder cycloadduct via ^1H NMR spectroscopy as 22% conversion of the starting materials could be achieved in 3h at room temperature (entry 3, Table 4.2). This is, however, a much slower conversion rate than in the case of β-diketiminate bistriflate aluminum compounds as discussed in chapter 3. Nevertheless, the slower catalytic performance was understandable as OTf was less nucleophilic and a much better leaving group than Cl. Due to the presence of THF coordination at aluminum center, **46** is also thought to be less Lewis acidic than **47**, and potentially even a worst catalyst than its THF-free analogue. However, to our surprise, when **46** was mixed with 1 equiv of $NaBAr^{Cl}_4$ and used for the catalysis, it showed a much higher catalytic activity than **47** under the same reaction conditions. Complete conversion of starting materials was achieved in 3h (entry 2, table 4.2) which was comparable to the β-diketiminate aluminum catalytic systems. This suggested that the reactions between **46** or **47** and $NaBAr^{Cl}_4$ form different species due to the presence of THF. It was then meaningful to investigate the role of THF in this particular catalytic process.

Table 4.2. Screening of potential (pre)catalysts for Diels Alder cycization between 2,3-dimethylbutadiene and 1,3-diphenyl-2-propenone.

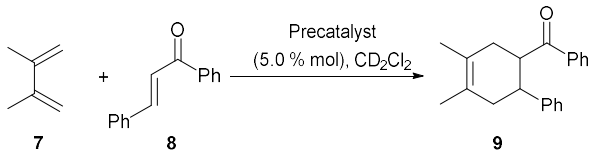

7 8 9

#	Pre-catalyst	Time (h)	Yield (%)	Trans/cis
1	**46** or **47**	3	-	-
2	**46**/$NaBAr^{Cl}_4$	3	99	99:1
3	**47**/$NaBAr^{Cl}_4$	3	22	99:1
4	**47**/THF/$NaBAr^{Cl}_4$	3	30	99:1
5	**47**/THF/$NaBAr^{Cl}_4$[a]	3	97	99:1
6	**49**	4	11	99:1
7	**49**/THF[a]	1	12	99:1
8	**50**	3	99 [b]	99:1

[a] heat up to 50°C for 6h before adding $NaBAr^{Cl}_4$ or substrates. [b]The same % conversion was observed even with the addition of 1 equiv (with respect to the catalyst) of dbpy.

Since the only difference between **46** and **47** was the presence of a bound THF, it seems that **47** can readily converted to **46** by simple addition of 1 equiv of THF. However no coordinated THF signal was observed by ^{1}H NMR spectroscopy when 1 equiv of THF was added to the CD_2Cl_2 solution of **47** and even more surprisingly was the fact that this resulting mixture did not show any increase in catalytic activity when 1 equiv of $NaBAr^{Cl}_4$ was added. Furthermore, the catalytic activity still remained quite sluggish even when THF was used as solvent. This indicated that THF could not coordinate to aluminum center by simply mixing the aluminum compound and THF together. This might be due the fact that

in order for THF to coordinate to the dichloroaluminum moiety in **47** one of the imine N must de-coordinate. As **46** (precursor to **47**) is formed in THF it might be possible that THF coordination precedes the formation of the bonds between central Al and the pincer NCN ligand resulting in only one imine N coordination as in the case of **48**. Even though there is no spectroscopic evidence to suggest asymmetric coordination of the pincer ligand in **46** this simply could be explain by rapid (on the NMR time scale) coordination/de-coordination between the two imine N atoms. This hypothesis is further supported by the fact that the catalytic activity of the **47**/THF system can be increased by heating the reaction mixture to 60 °C for 6 h before the addition of $NaBAr^{Cl}_4$ (entries 4,5, Table 4.2). Different heating times were also examined as shown in Table 4.3 which showed longer heating time did not increase the reaction rates. As these reactions were performed in *situ* they do not give a clear picture about the true role of THF in the catalysis. Therefore, it was important to identify the major species of the two catalytic systems.

Table 4.3 Catalytic activity of **47**/THF system under different heating times

#	Temperature	Time(h)	Conversion(%)[a]
1	r.t.	6	13
2	60 °C	1	31
3	60 °C	6	48
4	60 °C	12	50
5	60 °C	24	52

[a] 5% of $LAlCl_2$ was mixed with 1 equiv of THF in CD2Cl2 following by heat up for x h and then added 1 equiv of $NaBAr^{Cl}_4$ before used for the Diels-Alder reaction between **4** and **5**, reaction time: 1 h.

As shown in Figure 4.3, when mixed with 1 equiv of $NaBAr^{Cl}_4$ in CD_2Cl_2, **46** and **47** acted quite differently. The ^1H NMR spectrum of the mixture of **47** and $NaBAr^{Cl}_4$ gave a set of quite broad signals, which is in the contrast in comparison to the most signals of the **46**/$NaBAr^{Cl}_4$ mixture. Besides, a new set of signals were observed at the aromatic region as well as at 2.58 ppm which should be identified as the ^{i}Pr protons. This suggested that a second species was formed which processed a quite different structure. The ^1H NMR spectru also clearly showed the presence of THF coordination as the signals for this molecule were downfield shifted (2.05 and 4.04 ppm) compared to free THF (1.82 and 3.69 ppm).

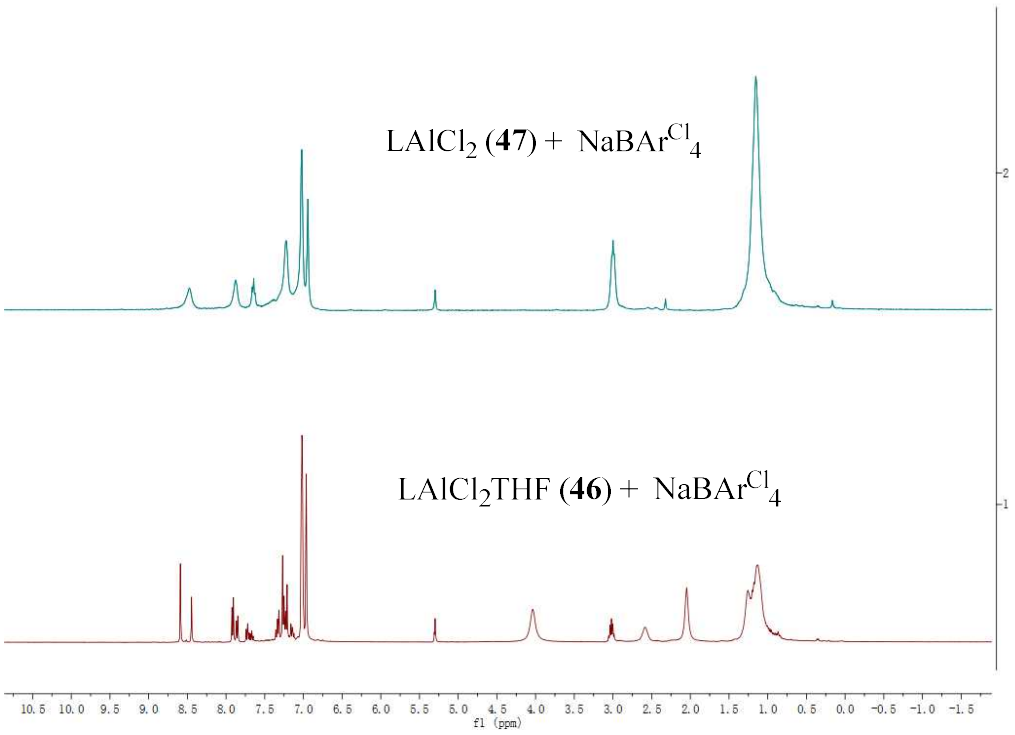

Figure 4.3 Reactions between **46** or **47** and $NaBAr^{Cl}_4$

With this information in hand, we tried to obtain crystalline samples for both reactions in order to figure out what exactly happened in these two cases. Stirring **47** and 1 equiv of $NaBAr^{Cl}_4$ in DCM for 5 min and layering the resulting solution with hexane afforded a crop of colorless crystals, suitable for single crystal X-ray diffraction, which were identified as

complex **49** (Scheme 4.5). Molecular structure is shown in Figure 4.4 with the crystallographic data summarized in Table 4.1. It is not surprising that both two Cl atoms were still bonded to aluminum center as this also occurred in the β-diketiminate case. This complex is essentially a dimer of **47** supported by a Na cation. The monoanionic bis(imino)aryl NCN pincer ligand coordinates to the aluminum atom in a tridentate fashion. Compared with **47**, **49** has a slightly shorter Al-C bond (1.936(3) Å) and longer Al-Cl bonds (2.1500(13) and 2.1583(13) Å). The most important distinction between **47** and **49** is that both nitrogen atoms in **49** coordinate to the aluminum center with similar bond lengths (2.182(3) and 2.237(3) Å), which are quite different in **47** (2.139(2) and 2.502 Å). This might be due to the presence of Na cation as it shifts electron density away from the $AlCl_2$ moiety causing the Al center to be more electron deficient, resulting in a more efficient Al-N bonding.

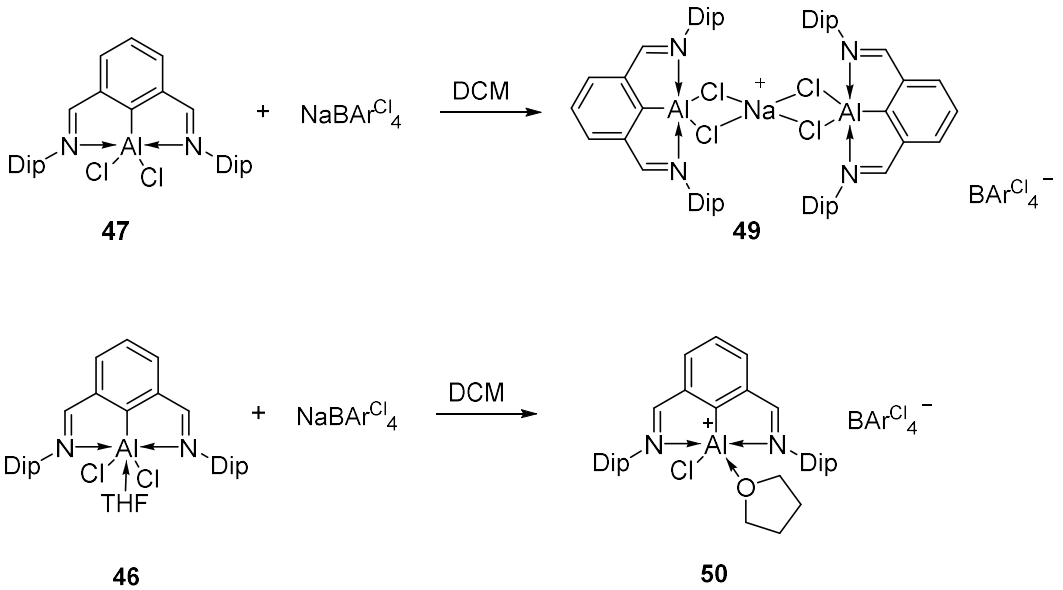

Scheme 4.5 Reactions between aluminum dichloride complexes and NaBAr$^{Cl}_4$

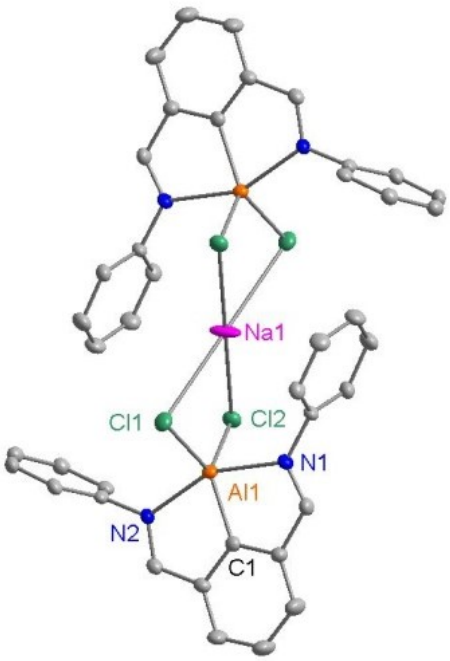

Figure 4.4 Molecular structure for **49**.

Thermal ellipsoids have been drawn at 50% probability level. All hydrogen atoms, the ^{i}Pr groups of the Dip substituents, the counter ion and solvent molecules have been removed for clarity. Selected bond lengths (Å) and angles (°): Al1-C1 1.936(3), Al-Na1 3.5707(10), Al1-N1 2.237(3), Al1-N2 2.182(3), Al1-Cl1 2.1500(13), Al1-Cl2 2.1583(13), Na1-Cl1 2.9622(9), Na1-Cl2 2.8838(9), N2-Al1-N1 155.29(11), C1-Al1-N1 76.71(13), Cl1-Al1-N1 95.42(9), Cl1-Al1-Cl2 103.13(5).

We then used the dimer **49** to investigate its catalytic properties towards the initial Diels Alder reaction, hoping to shed light on the active species. However, the activity of the new compound was the lowest (~ 11% conversion in 4h; entry 6, Table 4.2) with respect to all systems containing $NaBAr^{Cl}_4$. This suggested that **49** was not the active species in the **47**/$NaBAr^{Cl}_4$ system which is reported to produce high catalytic activity. When 1 equiv of THF was added into the DCM solution of **49** followed by heating the resulting solution to 60 °C for 6h, a slight promotion in catalytic activity was observed (~ 12% conversion in 1h; entry 7, Table 4.2). The lower increase in catalytic activity than that of the

$LAlCl_2$/THF/$NaBAr^{Cl}_4$ system might be due to the presence of Na cation resulting in difficulty in formation of the true active species which was still unknown.

On the other hand, when **46** reacted with 1 equiv of $NaBAr^{Cl}_4$ in DCM, another species **50** was obtained by layering the resulting solution with hexane. Crystal structure showed that the new species was a mononuclear cationic aluminum compound. As shown in Figure 4.5 the central aluminum was also five coordinate, with one of the Cl ligands replaced by a THF molecule. Both nitrogen atoms are coordinated to the aluminum center and the Al-N bond lengths were 2.182(3) and 2.237(3) Å. The Al-Cl bond length was 2.1185(11) Å, which were a bit shorter than that of **46** (1.943(3) and 2.1250(11) Å) and **49** (2.1500(13) and 2.1583(13) Å**)**, revealing a decrease in electron density at the aluminum center. The Al-C bond length 1.932(3) Å was also shorter than that of **46** (1.943(3) Å) and **49** (1.936(3) Å), which also suggested that the cationic aluminum complex was more Lewis acidic than its dichloride precursor. Consequently, complex **50** appears to be a better Lewis acid catalyst than **49**.

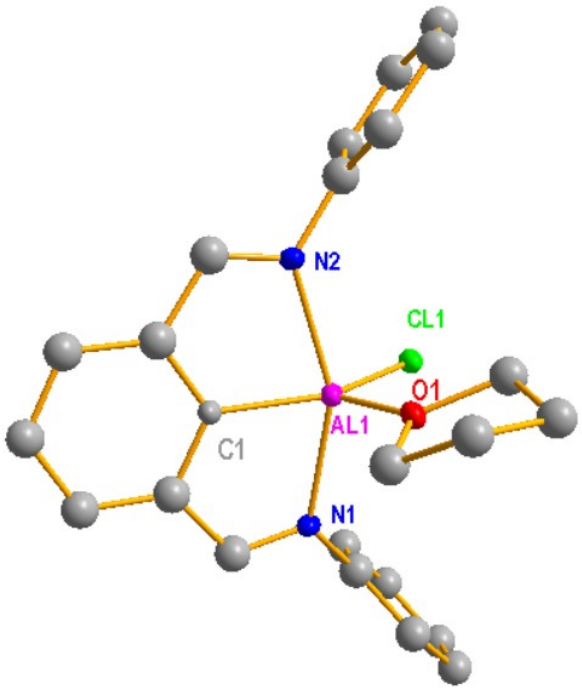

Figure 4.5 Molecular structure for **50**.

Thermal ellipsoids have been drawn at 50% probability level. All hydrogen atoms, the ^{i}Pr groups of the Dip substituents, the counter ion and solvent molecules have been removed for clarity. Selected bond lengths (Å) and angles (°): Al1-C1 1.932(3), Al1-N1 2.181(2), Al1-N2 2.213(2), Al1-Cl1 2.1185(11), A1-O1 1.844(2), N2-Al1-N1 154.69(9), C1-Al1-N1 78.32(10), Cl1-Al1-N1 96.81(7), O1-Al1-C1 112.23(11)

When **50** was used for the same Diels-Alder reaction, complete conversion of starting materials was observed in 3h, which was similar with the **46**/NaBAr$^{Cl}_4$ system. This suggested that we formed a more Lewis acidic system, in comparison to **46**/**47**/**49**. It was then important to investigate whether the coordinated THF played any role in the catalysis process or just stabilized the cationic species. For this purpose 5 equiv of 1,3-diphenyl-2-propenone (**5**) was mixed with **50** in CD_2Cl_2. ^{1}H NMR spectroscopy clearly revealed a complete de-coordination of THF and coordination of the dienophile (Scheme

4.6, Figure 4.6). This observation suggested that the active species was free cation $[LAlCl]^+$ (**51**) while **50** its pre-catalyst. When **47**/$NaBAr^{Cl}_4$ was mixed with **5** in CD_2Cl_2, the formation of **51** was also observed, but in a lower conversion (~30%). This might be the reason why **47**/$NaBAr^{Cl}_4$ system also showed some activity with respect to the attempted Diels-Alder transformation.

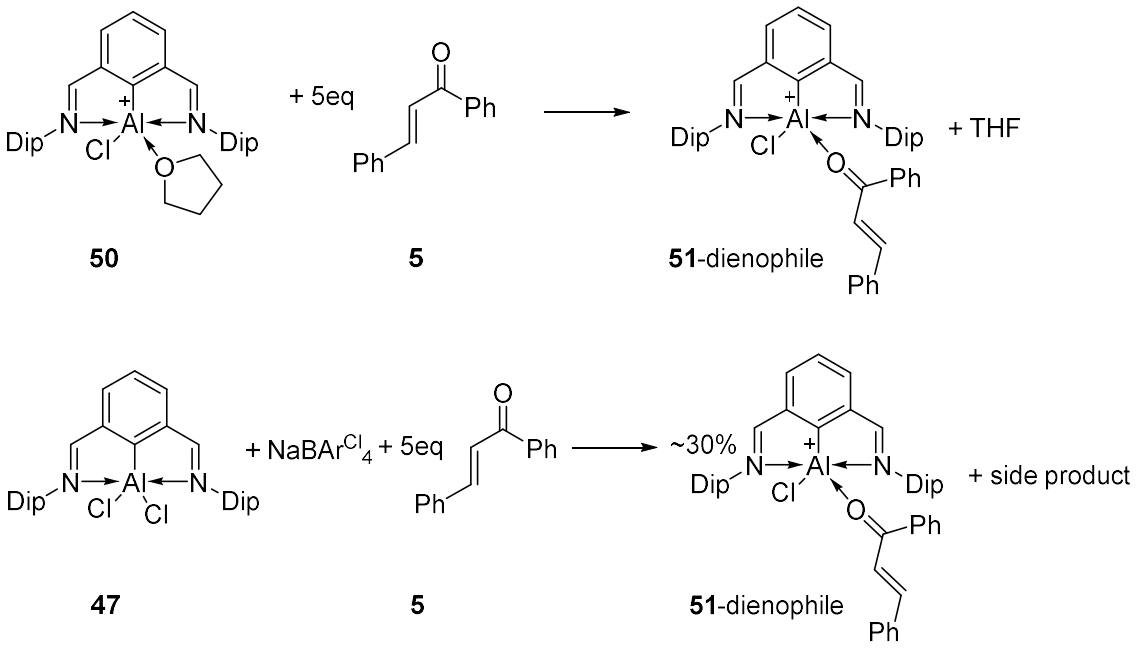

Scheme 4.6 Formation of active species

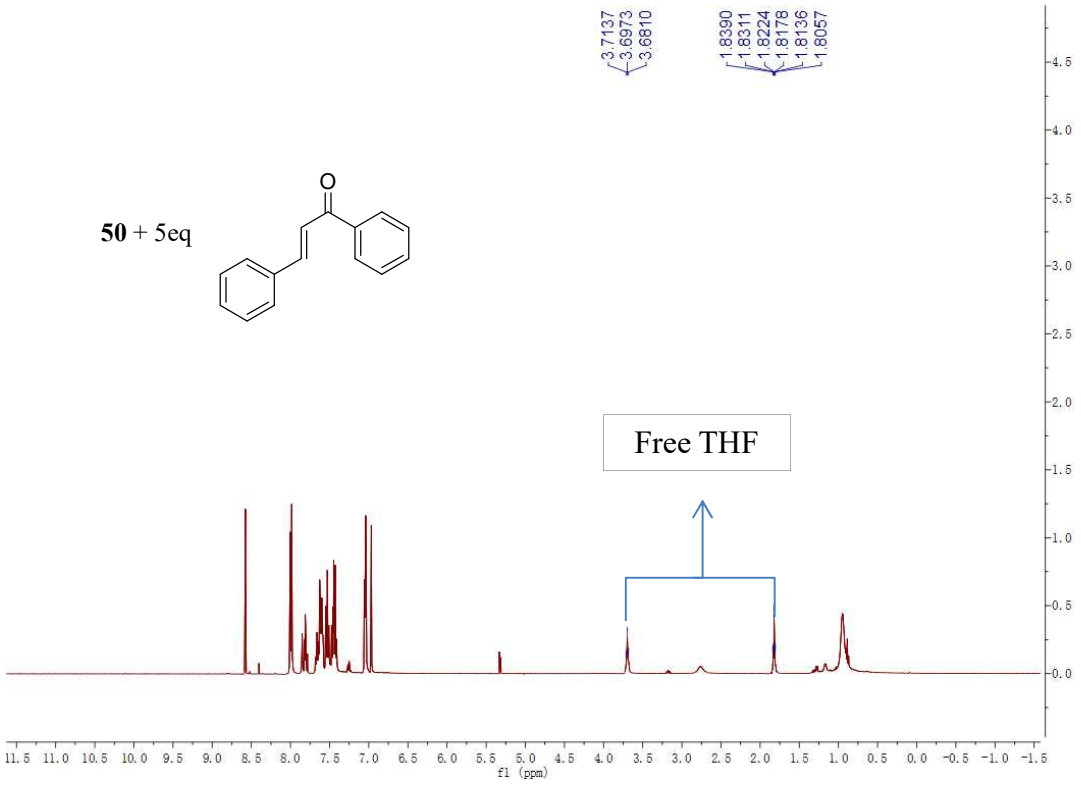

Figure 4.6 ^{1}H NMR for the formation of active species

4.4 Catalytic application in Diels-Alder cycloadditions

As monocationic aluminum complex **50** was determined to be the most prominent pre-catalyst, we decided to investigate its catalytic property for several other Diels Alder reactions as summarized in Table 4.4. Almost all dienophiles were quite suitable for the target Diels Alder reactions with diene **4**. For example, complete substrates conversion can be observed within 1h for the reactive dienophiles **9** and **10** when 5% of **50** was used (entries 1 and 2, Table 4.4). Longer reaction times were required for the difficult dienophiles such as **11**, **5** and **14** (entries 3, 4 and 7, Table 4.4). However, **50** showed lower catalytic activities for the cycloadditions involving cyclic dienophiles. Only 41% isolated yield was obtained for **13** in 24h while no formation of the target Diels Alder adduct was observed even though a 10% catalyst loading was used (entries 5 and 6, Table 4.4) for **12**. Unlike what happened in the Nacnac case, no formation of polymers was observed. For

much less reactive dienophile **15**, extra amount of diene and longer reaction times were required to approach decent conversion (entries 8, Table 4.4). Additionally, less reactive dienes (**23** and **32**) were also examined for Diels Alder transformations. For **9** complete substrate conversion was observed in 1 h while for **5** longer reaction times were required to achieve excellent isolated yieds of > 97% (entries 9-12, Table 4.4). Considering these observations the catalytic activity of cation **50** is comparable with those for the ferrocenyl-stabilized silylium cation[15] and β-diketiminate supported Al-based systems with respect to the attempted Diels Alder cycloadditions.

Table 4.4 **50** or HBA catalyzed Diels-Alder reactions of dienophiles **5** and **9**-**14** with dienes **4**, **23** or **32**. The results are listed as: time (h), yield (%), trans/cis or endo:exo, and/or para:meta ratios for each run.

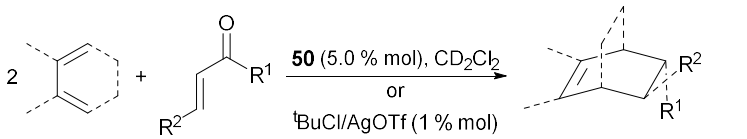

4, 23, 32 **5, 9-15** **8, 17-22,24,27,33,36**

#	Diene	Dienophile	Adduct	**50**	HBA
1	 **4**	 **9**	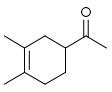 **16**	1 h 96 % - -	1 h 90 % - -
2	 **4**	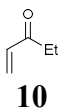 **10**	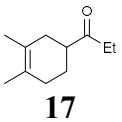 **17**	1 h 98 % - -	1 h 89 % - -
3	 **4**	 **11**	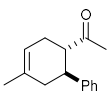 **18**	24 h 72 % 99:1 -	24 h 58 % 99:1 -
4	 **4**	 **5**	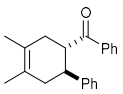 **8**	3 h 98 % 99:1 -	24 h[b] 33 % 99:1 -
5	 **4**	 **12**	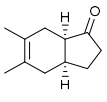 **19**	-	1 h[a]

6	 **4**	 **13**	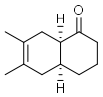 **20**	24 h 41 % 99:1 -	1 h[a]
7	 **4**	 **14**	 **21**	12 h 96 % 91:9 -	24 h 60 % 91:9 -
8	 **4**	 **15**	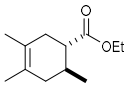 **22**	40 h[c] 89 % 99:1 -	1 h[a]
9	 **23**	 **9**	 **24**	1 h 97 % 99:1 -	1 h 92 % 99:1 -
10	 **23**	 **5**	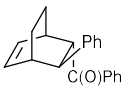 **27**	12 h 99 % 99:1 -	24 h[b] 16 % 99:1 -
11	 **32**	 **9**	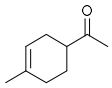 **33**	1 h 97 % - 99:1	2 h 83 % - 97:3
12	 **32**	 **5**	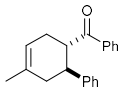 **36**	10 h 99 % 99:1 99:1	10 h[b] 29 % 99:1 88:12

[a]Diene polymerization occurred within the first hour with no evidence for the formation of the product. [b]% conversion as estimated by ^{1}H NMR spectroscopy. [c]4 equiv of the diene used.

Even though detailed investigations on the nature of the catalytic species were undertaken it still did not rule out the presence of an HBA. However, as discussed in Chapter Ⅲ, an HBA (HOTf generated by AgOTf/^{t}BuCl) showed quite different catalytic property for the abovementioned catalytic cycloadditions, suggesting the absence of HBA activity. Additionally, when **4** and **5** (entry 8, Table 4.2) were cyclized by **50** in the presence of 1 equiv of dbpy no loss of catalytic activity was observed, which provided additional evidence against HBA activity. Therefore, the investigated Diels Alder cycloadditions were indeed catalyzed by Lewis acidic complex **50** rather than an HBA. it is worth noting that

when **50** was mixed with equimolar amounts of dbpy in CD_2Cl_2, less than 10% (^{1}H NMR spectoscopy) of the corresponding pyridium cation [dbpy-H]$^+$ was formed as shown in Figure 4.7.This is important because if large amounts of the [dbpy-H]$^+$ are produced, especially if excess (with respect to catalyst) quantities of dbpy are used[16], then [dbpy-H]$^+$ could actually act as a proton source because the pKa value for [dbpy-H]$^+$ varies from 0.9 (DMSO) to 5 (H_2O) suggesting that this pyridinium cation could be a quite potent proton donor. Thus, we believe that when using dbpy to potentially gather evidence against an HBA activity it is crucial to determine the amount of [dbpy-H]$^+$ that has been produced under the established reaction conditions as large quantities of this pyridiium cation could, in fact, be the source of HBA activity.

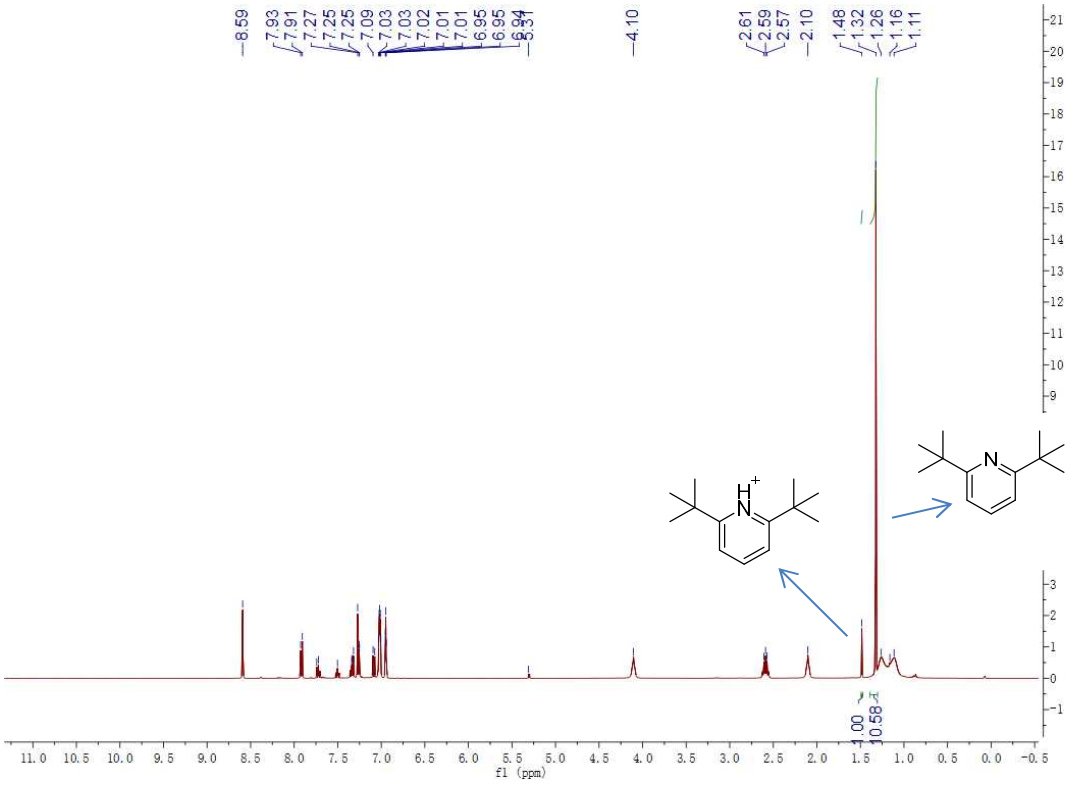

Figure 4.7 ^{1}H NMR for reaction of **50** and dbpy

In order to provide more evidence for this hypothesis, we prepared pyridium cation through the reaction between dbpy and HOTf in hexane and used it for the catalysis of a simple

Diels-Alder cycloaddition as shown in Scheme 4.7. Excess amount of dbpy was used for the preparation of pyridium in order to make sure one of the starting materials, HOTf was consumed completely as trace amount of HOTf might result in catalytic activity.

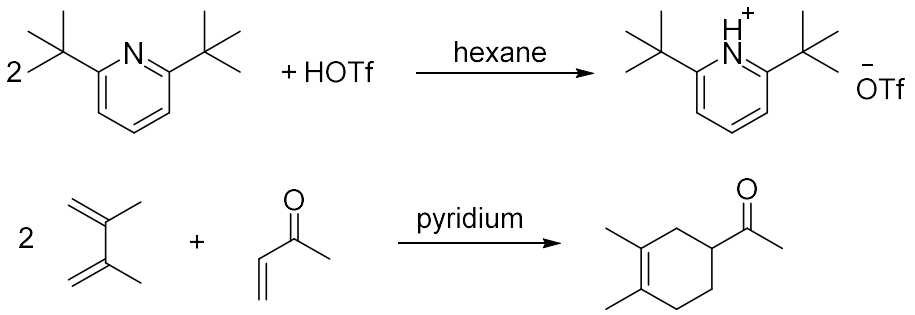

Scheme 4.7 Synthesis of pyridium cation and catalysis for Diels-Alder cycloaddition

As shown in Table 4.5, even the simplest Diels-Alder reaction did not occur at room temperature without any addition of catalyst (pyridium). When 10% of pyriudium was added into this reaction mixture, also no formation of cycloadduct was observed by ^{1}H NMR spectroscopy. This is in agreement to the conclusion that HBA activity can be avoided by the addition of dbpy with the formation of small amounts of the corresponding protonated pyridine. However, when 50% of pyridium of used for this reaction, about 50% starting materials conversion was observed in 6h, although the activity became much lower in the following reaction times (77% conversion in 24h, entries3, 4, Table 4.5). When stoichiometric amount of pyridium was used, about 67% conversion was obtained in 2h while it took 12h to achieve complete conversion (entries 5, 6, Table 4.5). Although we still have not figure out the reason for the dramatic decrease in activity, there is enough evidence to demonstrate that even this particular pyridinium cation could be considered as a source of protons. Thus, it is critical to consider the effect of the formation of pyridinium cation when carrying out such experiments for avoiding HBA activity.

Table 4.5 Pyridium catalyzed Diels-Alder reaction

#	Pyridium (%)	Time (h)	Conversion (%)
1	0%	12	-
2	10%	6	-
3	50%	6	51%
4	50%	24	77%
5	100%	2	67%
6	100%	12	>99

4.5 Summary

Several aluminum complexes stabilized by bis(imino)phenyl NCN pincer ligand were prepared, fully characterized and used for the catalysis of a series of Diels Alder transformations. The mononuclear cationic compound **50** appears to be the most prominent pre-catalyst. Several control experiments were performed to show that cation **51** is most likely to be the active species in the catalysis process rather than an HBA. . Lastly, the control experiment using dbpy should be carefully examined as the presence of large quantities of the corresponding pyridinium cation could serve as a proton source.

4.6 Experimental Section

All manipulations were carried out using standard Schlenk techniques and a dry-box. CH_2Cl_2, CD_2Cl_2 and $CDCl_3$ were destilled over CaH_2 while THF, toluene and *n*-hexane were distilled over sodium. All solvents were stored over 4 Å molecular sieves. Ligand **45** was prepared according to reported synthetic procedures. All other chemicals were purchased from commercial sources and used without further purification. The NMR spectra were recorded on a Bruker Avance III 400 or JEOL ECA400 (^{1}H NMR at 400 MHz; ^{13}C NMR at 100 MHz, ^{11}B NMR at 128 MHz and ^{27}Al NMR at 104 MHz) instrument. Tetramethysilane was used as reference for ^{1}H and ^{13}C NMR, while ^{11}B and ^{27}Al NMR spectra were recorded with respect to $Et_2O{\cdot}BF_3$, and $AlCl_3/D_2O$, respectively. Mass spectrometry was performed by Waters Q-Tof Premier Micromass instrument, using the electro spray ionization (ESI) mode.

Synthesis of ligand 45. 2-Bromobenzene-1,3-dialdehyde (10.0 g, 46.9 mmol) and 2,6-diisopropylaniline (22.1 mL, 117.3mmol) was dissolved in 200 mL methanol in a 500 mL round-bottomed flask with a stirrer bar. To this solution, 1 drop of formic acid was added. The reaction mixture was left to stir for 2h and then filtered. The obtained yellow solid was washed by cold methanol and dried under vacuum. Yield 23 g, 92%.^{1}H NMR (400 MHz, $CDCl_3$, 25 °C): δ 1.20 (d, $^3J_{H\text{-}H}$ = 6.92 Hz, 24H, CH(C*H*$_3$)$_2$), 2.95 (sept, $J_{H\text{-}H}$ = 6.92 Hz, 4H, C*H*(CH$_3$)$_2$), 7.12-7.21 (m, 6H, Ph), 7.58 (t, $^3J_{H\text{-}H}$ = 7.72 Hz, 1H, Ph), 8.39 (d, $^3J_{H\text{-}H}$ = 7.72 Hz, 2H, Ph), 8.70 (s, 2H, C*H*═N) ppm.

Synthesis of $LAlCl_2$(THF), 46. ^{n}BuLi (0.52 mL, 1.05 mmol, 2M in cyclohexane) was added dropwise to a THF (20 mL) solution of 2,6-(2,6-^{i}Pr$_2$-C$_6$H$_3$N=CH)$_2$-C$_6$H$_3$-1-Br (**45**) (0.53 g, 1.00 mmol) at – 78°C. The mixture was stirred for 30 min before $AlCl_3$ (0.13, 1.00

mmol) was added. The solution was allowed to warm to room temperature gradually and stir overnight. The solvent was removed under reduced pressure and the residue was extracted by dichloromethane. After evaporation of most of the dichloromethane, 10 mL *n*-hexane was added. The red powder formed was dried under vacuum for 5 min. Yield: 0.46g, (74%). ^{1}H NMR (400 MHz, $CDCl_3$, 25 °C): δ 1.16 (d, $^{3}J_{H\text{-}H}$ = 6.50 Hz, 24H, CH(CH_3)$_2$), 1.89 (b, 4H, THF), 3.16 (sept, 6.50 Hz, 4H, CH(CH$_3$)$_2$), 3.92 (b, 4H, THF), 7.19-7.24 (m, 6H, Ph), 7.60 (t, $^{3}J_{H\text{-}H}$ = 7.48 Hz, 1H, Ph), 7.74 (d, $^{3}J_{H\text{-}H}$ = 7.48 Hz, 2H, Ph), 8.34 (s, 2H, CH=N) ppm. ^{13}C NMR (100.5 MHz, $CDCl_3$, 25 °C): δ 24.5 (CH(CH$_3$)$_2$), 25.5 (THF), 28.2 (CH(CH$_3$)$_2$), 69.5 (THF), 123.7 (*p*-N-C$_6$H$_3$), 126.7 (*m*-N-C$_6$H$_3$), 131.0 (*p*-Al-C$_6$H$_3$), 132.3 (*m*-Al-C$_6$H$_3$), 139.7 (*o*-N-C$_6$H$_3$), 140.9 (C=N-*C*), 143.7 (*o*-Al-C$_6$H$_3$), 168.4 (*C*=N-C) ppm. ^{27}Al NMR (104.2 MHz, $CDCl_3$, 25 °C): δ 97 ppm. HRMS (ESI) calculated for $C_{36}H_{48}N_2OCl_2Al$ [M + H]: 621.2959; Found: 621.2927. MP: ~ 191°C (onset of decomposition).

Synthesis of LAlCl$_2$, 47. ^{n}BuLi (0.52 mL, 1.05 mmol, 2M in cyclohexane) was added dropwise to a THF (20 mL) solution of 2,6-(2,6-^{i}Pr$_2$-C$_6$H$_3$N=CH)$_2$-C$_6$H$_3$-1-Br (**45**) (0.53 g, 1.00 mmol) at –78°C. The mixture was stirred for 30 min before $AlCl_3$ (0.13, 1.00 mmol) was added. The solution was allowed to warm to room temperature gradually and stir overnight. The solvent was removed under reduced pressure and the residue was extracted by toluene. After evaporation of toluene, 10 mL *n*-hexane was added to wash the crude product. The red powder obtained was dried under vacuum for about 15h. Yield: 0.41g, (75%). Crystals were grown in toluene/*n*-hexane mixed solution. ^{1}H NMR (400 MHz, $CDCl_3$, 25 °C): δ 1.16 (d, $^{3}J_{H\text{-}H}$ = 6.52 Hz, 24H, CH(CH_3)$_2$), 3.16 (sept, $J_{H\text{-}H}$ = 6.52 Hz, 4H, CH(CH$_3$)$_2$), 7.19-7.23 (m, 6H, Ph), 7.60 (t, $^{3}J_{H\text{-}H}$ = 7.48 Hz, 1H, Ph), 7.74 (d, $^{3}J_{H\text{-}H}$ = 7.48 Hz, 2H, Ph), 8.34 (s, 2H, CH=N) ppm. ^{13}C NMR (100.5 MHz, $CDCl_3$, 25 °C): δ 25.5 (CH(CH$_3$)$_2$), 28.2 (CH(CH$_3$)$_2$), 123.7 (*p*-N-C$_6$H$_3$), 126.7 (*m*-N-C$_6$H$_3$), 131.0 (*p*-Al-C$_6$H$_3$),

132.3 (*m*-Al-C_6H_3), 139.8 (*o*-N-C_6H_3), 140.9 (C=N-*C*), 143.7 (*o*-Al-C_6H_3), 168.4 (*C*=N-C) ppm. ^{27}Al NMR (104.2 MHz, $CDCl_3$, 25 °C): δ 106 ppm. HRMS (ESI) calculated for $C_{32}H_{40}N_2Cl_2Al$ [M + H]: 549.2384; Found: 549.2371. MP: ~ 190°C (onset of decomposition).

Synthesis of LAl(OTf)$_2$(THF)$_2$, 48. ^{n}BuLi (0.52 mL, 1.05 mmol, 2M in cyclohexane) was added dropwise to a 20 mL THF solution containing **45** (0.53 g, 1.00 mmol) at – 78°C. The mixture was stirred for 30 min before $AlCl_3$ (0.13, 1.00 mmol) was added. The solution was gradually allowed to warm to room temperature and stir for 15h. This reaction mixture was then transferred to another flask that contained AgOTf (0.77 g, 3.0 mmol) and left to stir overnight in the absence of light. After filtration, the solution was concentrated and layered with *n*-hexane. Few yellow crystals were obtained at -15°C after 1 day. The product appeared to be generally unstable presumably due to high air/moisture sensitivity and, thus, it was possible only to obtain single crystal X-ray analysis.

Synthesis of [LAlCl$_2$NaCl$_2$AlL][NaBAr$^{Cl}_4$], 49. 47 (0.55g, 1.00 mmol) and NaBAr$^{Cl}_4$ (0.62g, 1.00 mmol) were dissolved in 5 mL of CH_2Cl_2 and left to stir for 5 min. After filtration, the solution was layered with 5 mL *n*-pentane. Colorless crystals were obtained after 1 day. Yield: 0.61g, 71%. ^{1}H NMR (400 MHz, CD2Cl2, 25 °C): δ 1.12 (broad, 48H, CH(C*H*$_3$)$_2$), 2.99 (sept, J_{H-H} = 6.84 Hz, 8H, C*H*(CH$_3$)$_2$), 6.97-7.21 (m, 24H, Ph), 7.64 (t, $^3J_{H-H}$ = 7.58 Hz, 2H, Ph), 7.83 (d, $^3J_{H-H}$ = 7.58 Hz, 4H, Ph), 8.42 (s, 4H, C*H*=N) ppm. ^{13}C NMR (100.5 MHz, CD2Cl2, 25 °C): δ 25.5 (CH(*C*H$_3$)$_2$), 28.4 (*C*H(CH$_3$)$_2$), 123.1 (*p*-N-C_6H_3), 124.2 (*p*-C, Ar^{Cl}), 127.6 (*m*-N-C_6H_3), 132.1 (*m*-Al-C_6H_3), 132.9 (*m-C,* Ar^{Cl}), 133.0 (*o*-C*,* Ar^{Cl}), 133.1 (*p*-Al-C_6H_3), 139.2 (*o*-N-C_6H_3), 140.9 (C=N-*C*), 142.2 (o-Al-C_6H_3), 164.0 (q, $^1J_{BC}$ = 49 Hz, B-C), 170.0 (*C*=N-C) ppm. ^{11}B NMR (128 MHz, CD2Cl2, 25 °C): δ -7.9 ppm. ^{27}Al NMR (104.2 MHz, CD2Cl2, 25 °C): no signal observed.

HRMS (ESI): (the only signal observed was actually for $LAlCl_2$) calculated for $C_{32}H_{40}N_2Cl_2Al$ [M + H]: 549.2384; Found: 549.2372. MP: ~ 254°C (onset of decomposition).

Synthesis of [LAlCl(THF)][BAr^{Cl}_4], 50. A fresh sample of **46** (0.62g, 1.00 mmol) was dissolved in 5 mL of CH_2Cl_2 followed by the addition of $NaBAr^{Cl}_4$ (0.62g, 1 mmol). After it was left to stir for 6 h, the solution was filtered and layered with 5 mL pentane. Colorless crystals were obtained after 1 day. Yield: 0.73g, 62%. ^{1}H NMR (400 MHz, CD2Cl2, 25 °C): δ 1.10 (broad, 24H, CH(CH_3)$_2$)), 2.10 (b, 4H, THF), 2.56 (sept, J_{H-H} = 6.88 Hz, 4H, CH(CH$_3$)$_2$), 4.07 (b, 4H, THF), 6.94-7.34 (m, 18H, Ph), 7.71 (t, $^3J_{H-H}$ = 7.32 Hz, 1H, Ph), 7.91 (d, $^3J_{H-H}$ = 7.32 Hz, 2H, Ph), 8.59 (s, 2H, CH=N) ppm. ^{13}C NMR (100.5 MHz, CD2Cl2, 25 °C): δ 25.2 (CH(CH$_3$)$_2$), 25.8 (THF), 29.1 (CH(CH$_3$)$_2$), 75.5 (THF), 123.0 (p-N-C$_6$H$_3$), 124.3 (p-C, Ar^{Cl}), 128.2 (m-N-C$_6$H$_3$), 132.9 (m-C, Ar^{Cl}), 133.1 (o-C, Ar^{Cl}), 134.0 (m-Al-C$_6$H$_3$), 134.4 (p-Al-C$_6$H$_3$), 139.0 (o-N-C$_6$H$_3$), 140.1 (C=N-C), 142.2 (o-Al-C$_6$H$_3$), 164.0 (q, $^1J_{BC}$ = 48 Hz, B-C), 173.3 (C=N-C) ppm. ^{11}B NMR (128 MHz, CD2Cl2, 25 °C): δ -7.9 ppm. ^{27}Al NMR (104.2 MHz, CD2Cl2, 25 °C): no signal observed. HRMS (ESI): (the only signal observed was due to ligand L) calculated for $C_{32}H_{41}N_2$ [M + H]: 453.3270; Found: 453.3269. MP: ~ 156°C (onset of decomposition).

Synthesis of pyridium. dbpy (0.86 mL, 2 equiv, 4.00 mmol) was dissolved in 100 mL hexane. To this solution a mixture of 300 mg HOTf and 5 mL hexane was added slowly while vigorous stirring. The reaction mixture was left to stir overnight. After filtration and dry under vacuum, pure product was obtained as white solid. Yield: 510 mg, 75%. ^{1}H NMR (400 MHz, $CDCl_3$, 25 °C): δ 1.16 (s, 18H, C(CH_3)$_3$), 7.77 (dd, $^3J_{H-H}$ = 8.24 Hz, 2H, m-ArH), 8.39 (t, $^3J_{H-H}$ = 8.24 Hz, 1H, p-ArH), 12.46 (br, 1H, NH) ppm. ^{13}C NMR (100.5

MHz, $CDCl_3$, 25 °C): δ 29.1 (C(CH_3)$_3$), 37.2 (C(CH_3)$_3$), 119.0 (CF_3), 122.1 (CH), 147.8 (CH), 164.9 (C) ppm. ^{19}F NMR (376.4 MHz, $CDCl_3$, 25 °C): δ -78.08 ppm.

General procedure for Diels-Alder cycloadditions. A precatalyst, usually **50**, (0.017 mmol, 0.05 equiv) was dissolved in 1 mL CD2Cl2 in a J. Young NMR tube. To this solution a diene (0.68 mmol, 2 equiv) and a dienophile (0.34 mmol, 1 equiv) was added. The reaction mixture was left for the time indicated in Table 4.2-4.5. Then, the crude mixture was purified by flash column chromatography on silica gel using *n*-hexane/ethyl acetate solvent mixture affording the corresponding Diels-Alder products. The *endo*:*exo* ratio is determined by GLC analysis of the reaction mixture prior to workup.

References

1 Albrecht, M.; Koten, G. *Angew. Chem., Int. Ed*. **2001**, *40*, 3750.

2 Beley, M.; Collin, J.; Sauvage, J. *Inorg. Chem*. **1993**, *32*, 4539.

3 Cámpora, J.; Palma, P.; del Río, D.; Conejo, M. M.; Álvarez, E. *Organometallics* **2004**, *23*, 5653.

4 Kjellgren, J.; Sundén, H.; Szabó, K. J. *J. Am. Chem. Soc*. **2005**, *127*, 1787.

5 Hoogervorst, W.; Koster, A.; Lutz, M. *Organometallics* **2004**, *23*, 1161.

6 Oakley, S.; Coogan, M.; Arthur, R. *Organometallics* **2007**, *26*, 2285.

7 Gao, W.; Cui, D. *J. Am. Chem. Soc.* **2008**, *130*, 4984.

8 Liu, Z.; Gao, W.; Zhang, J.; Cui, D.; Wu, Q.; Mu, Y. *Organometallics* **2010**, *29*, 5783.

9 Beck, J. F.; Schmidt, J A. R. *Dalton Trans.* **2012**, *41*, 860.

10 Hoogervorst, W. J.; Koster, A. L.; Lutz, M.; Spek, A. L.; Elsevier, C. J. *Organometallics* **2004**, *23*, 1161.

11 Young, J. D.; Khan, M. A.; Wehmschulte, R. J. *Organometallics* **2004**, *23*, 1965.

12 Cameron, P. A.; Gibson, V. C.; Redshaw, C.; Segal, J. A.; Solan, G. A.; White, A. J. P.; Williams, D. J. *J. Chem. Soc., Dalton Trans.* **2001**,1472.

13 Pauling, L. *The Nature of the Chemical Bond*, 3rd ed.; Cornell University Press: Ithaca, NY, 1960.

14 Liu, Z.; Lee, J. H. Q.; Ganguly, R.; Vidović, D. *Chem. Eur.-J.* **2015**, *21*, 11344.

15 Schmidt, R. K.; Müther, K.; Mück-Lichtenfeld, C.; Grimme, S.; Oestreich, M. *J. Am. Chem. Soc.***2012,** *134*, 4421.

16 Schneider, A. E.; Manolikakes , G. *J. Org. Chem*. **2015**, *80*, 6193.

Appendix

1. NMR Spectrum

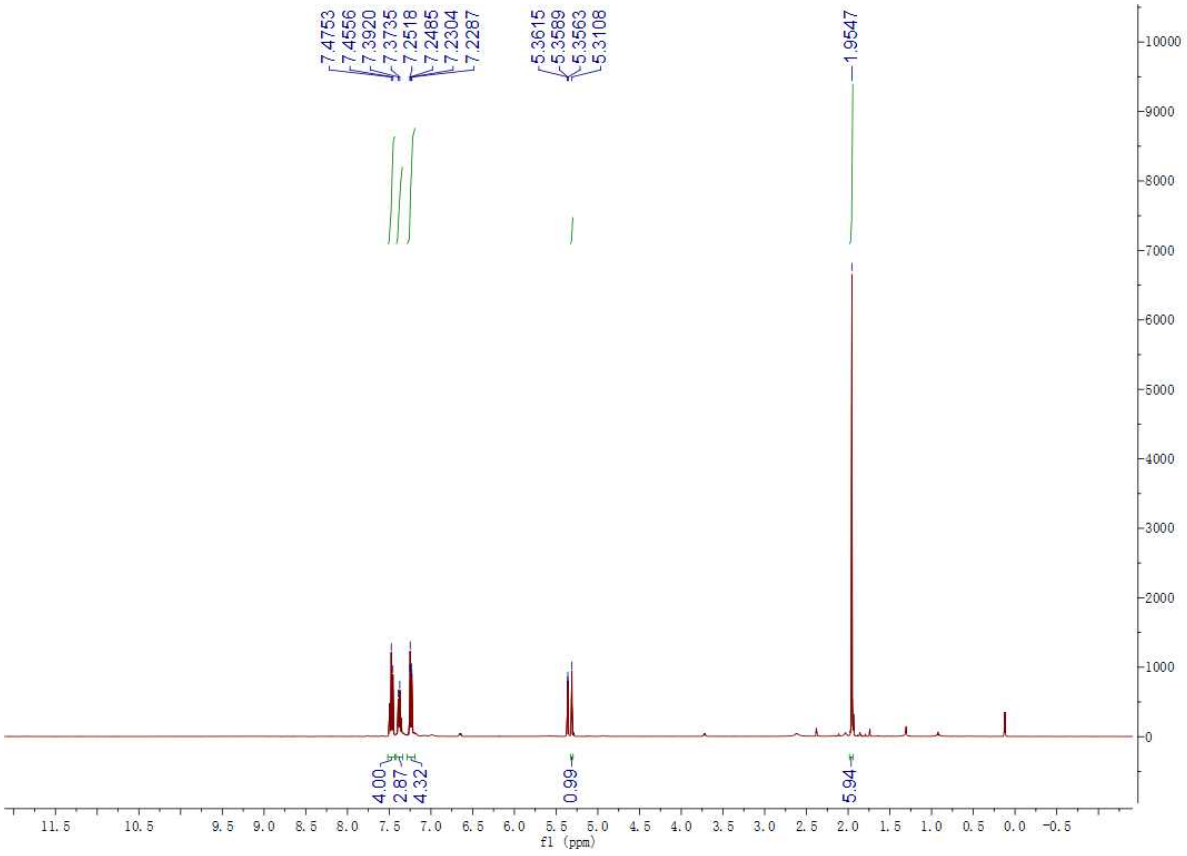

Figure S1. ^{1}H-NMR spectrum of **3a**.

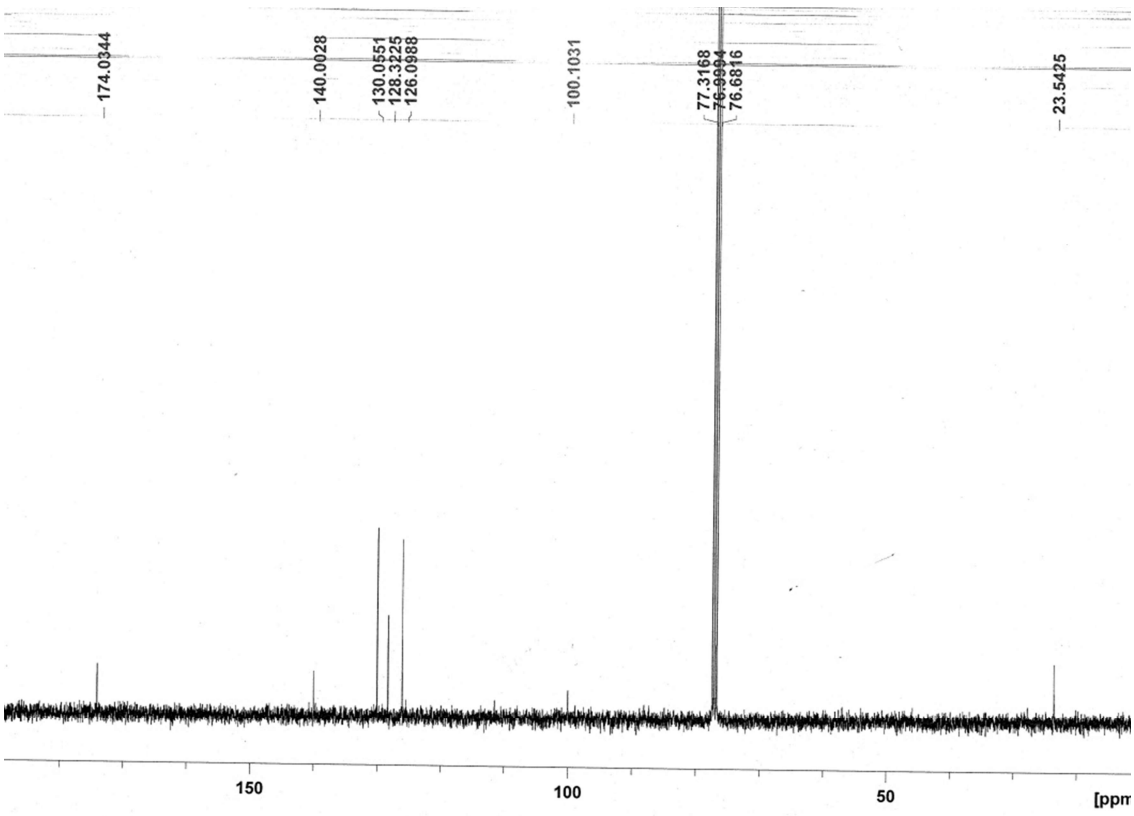

Figure S2. ^{13}C-NMR spectrum of **3a**.

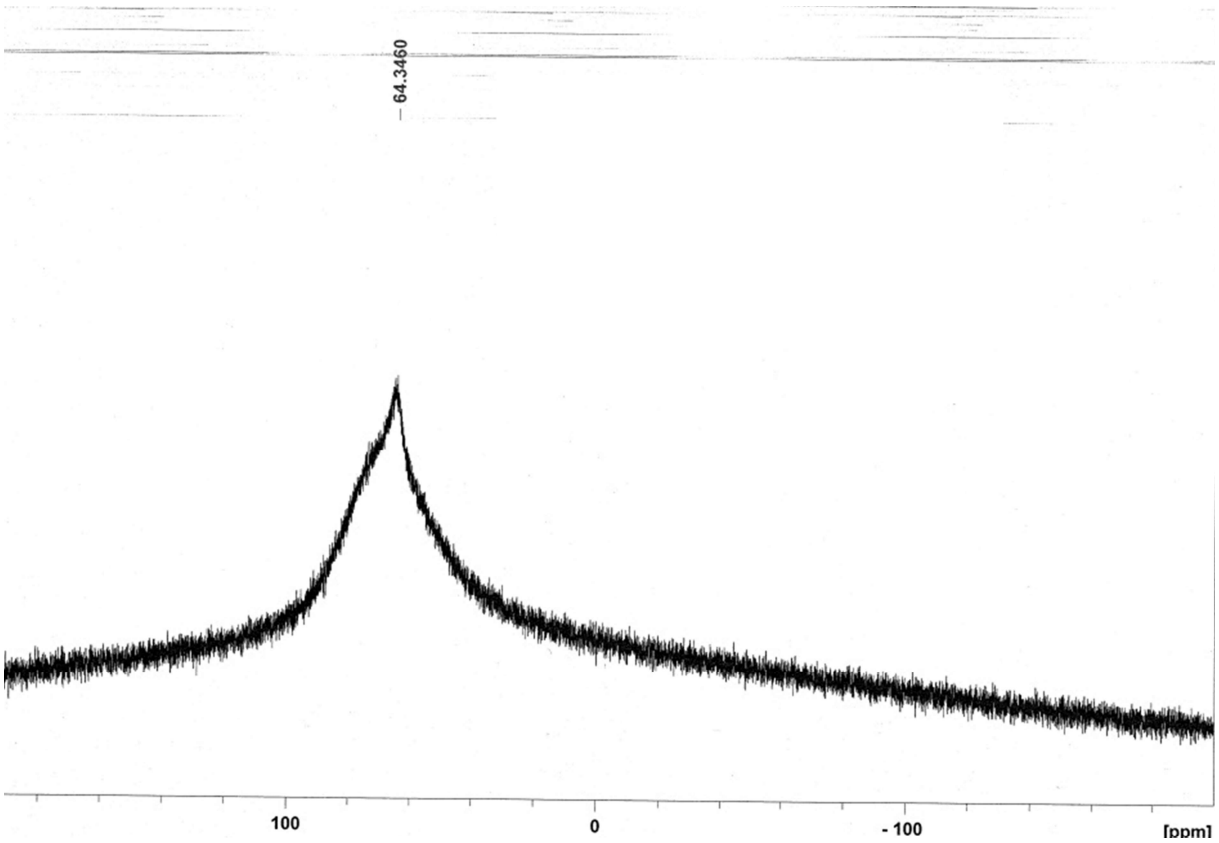

Figure S3. ^{27}Al-NMR spectrum of **3a**.

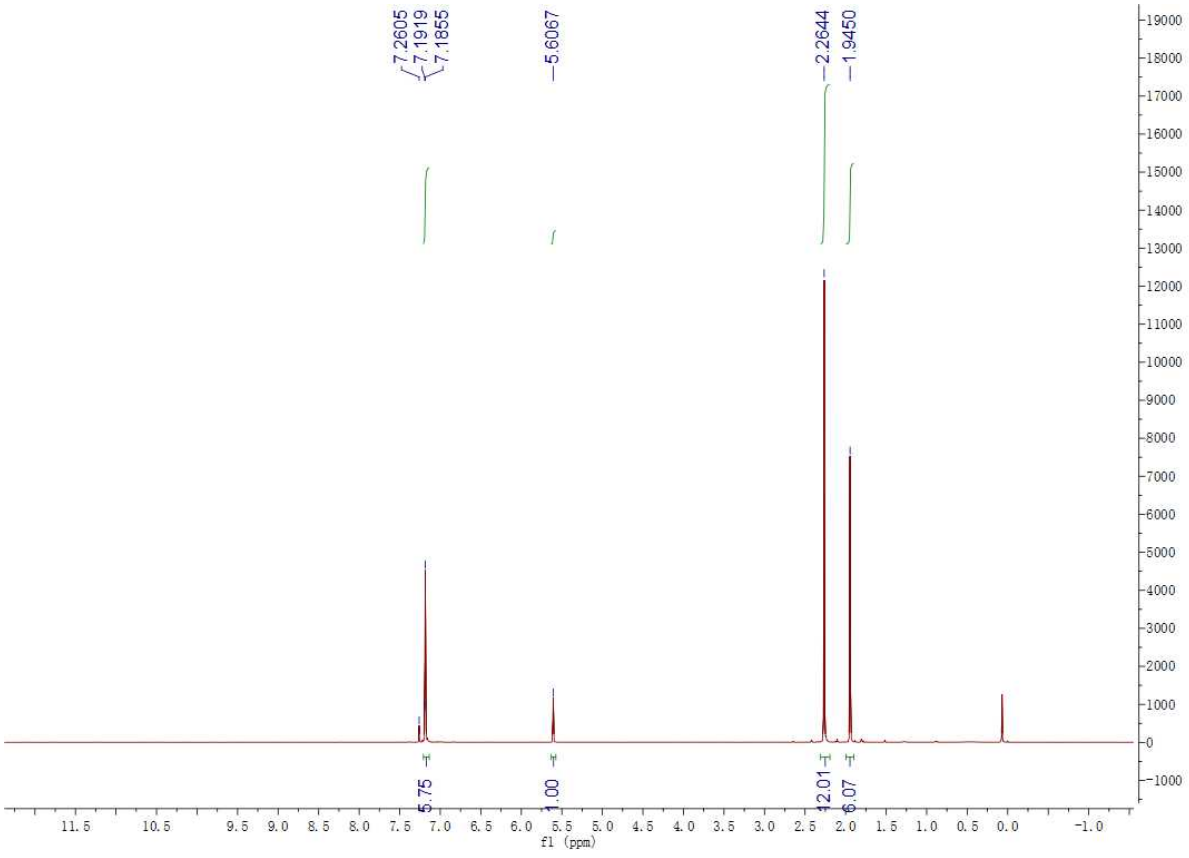

Figure S4. ^{1}H-NMR spectrum of **3b**.

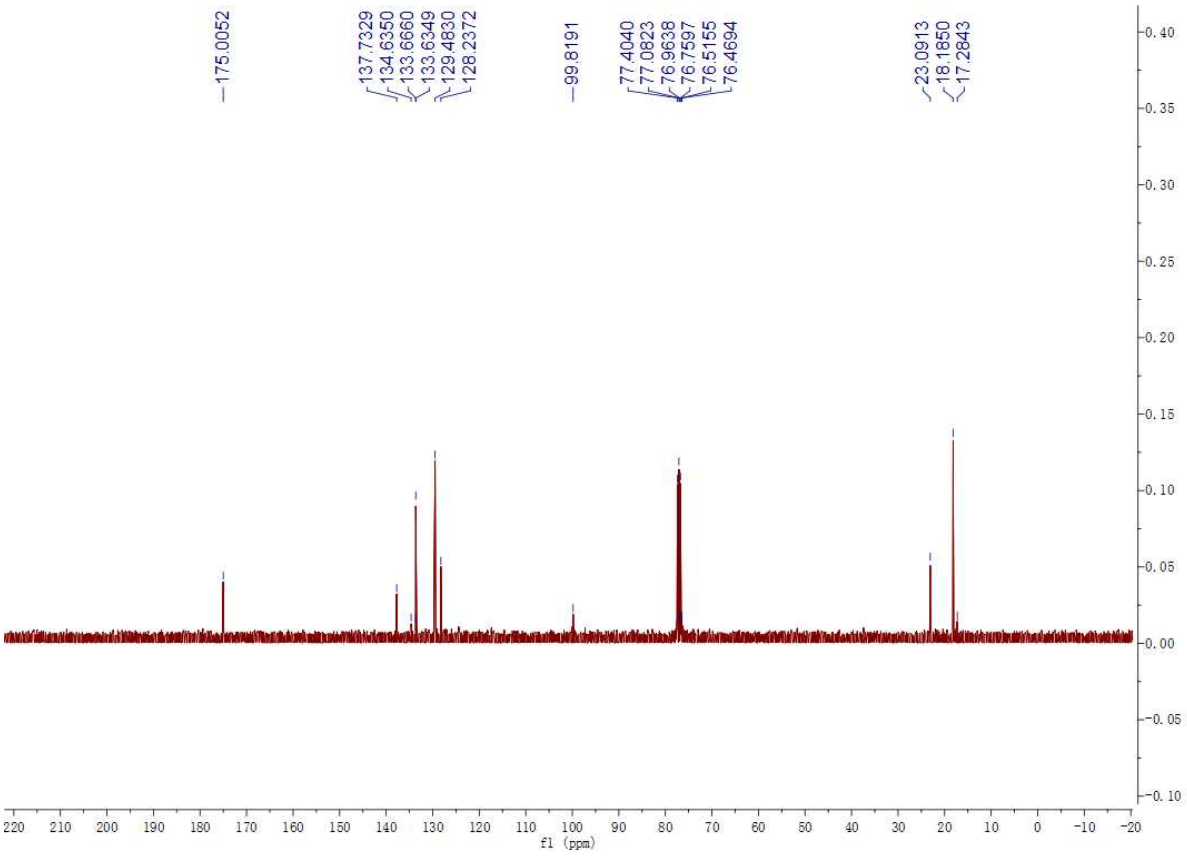

Figure S5. ^{13}C-NMR spectrum of **3b**.

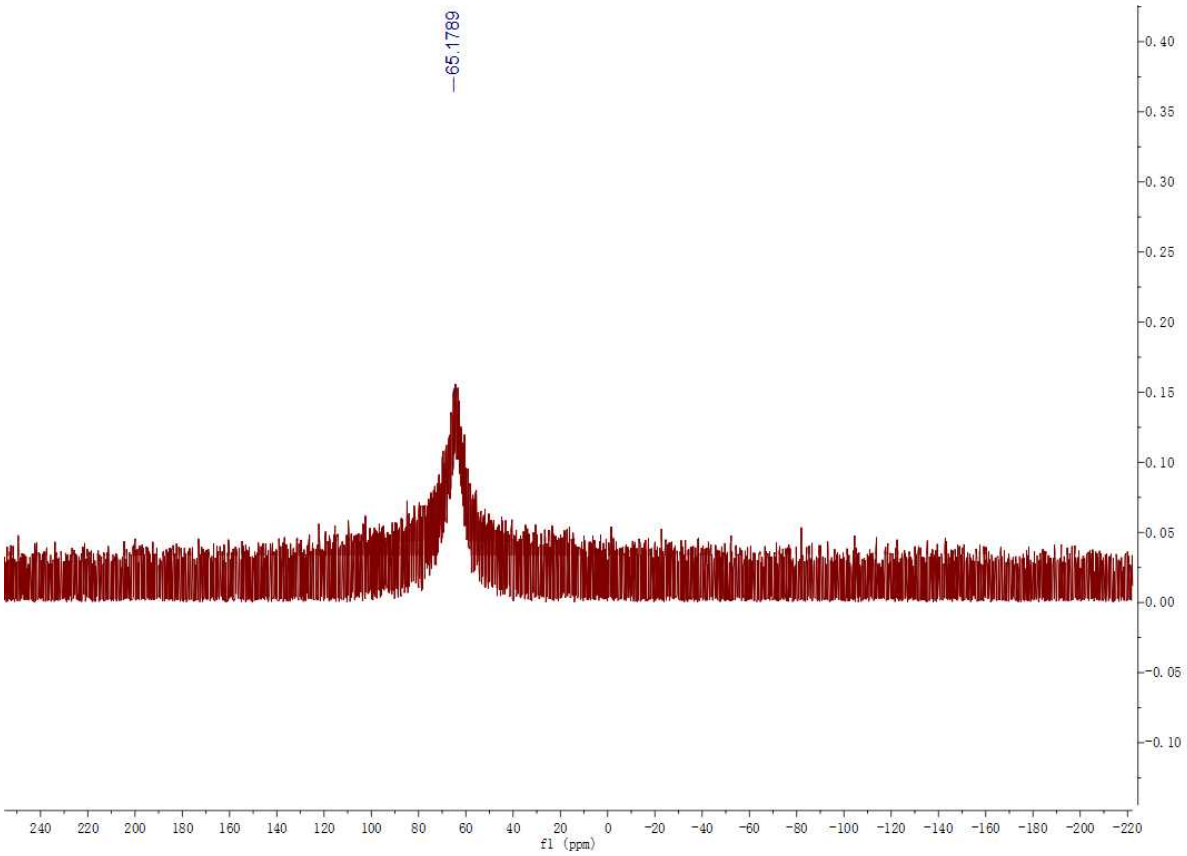

Figure S6. ^{27}Al-NMR spectrum of **3b**.

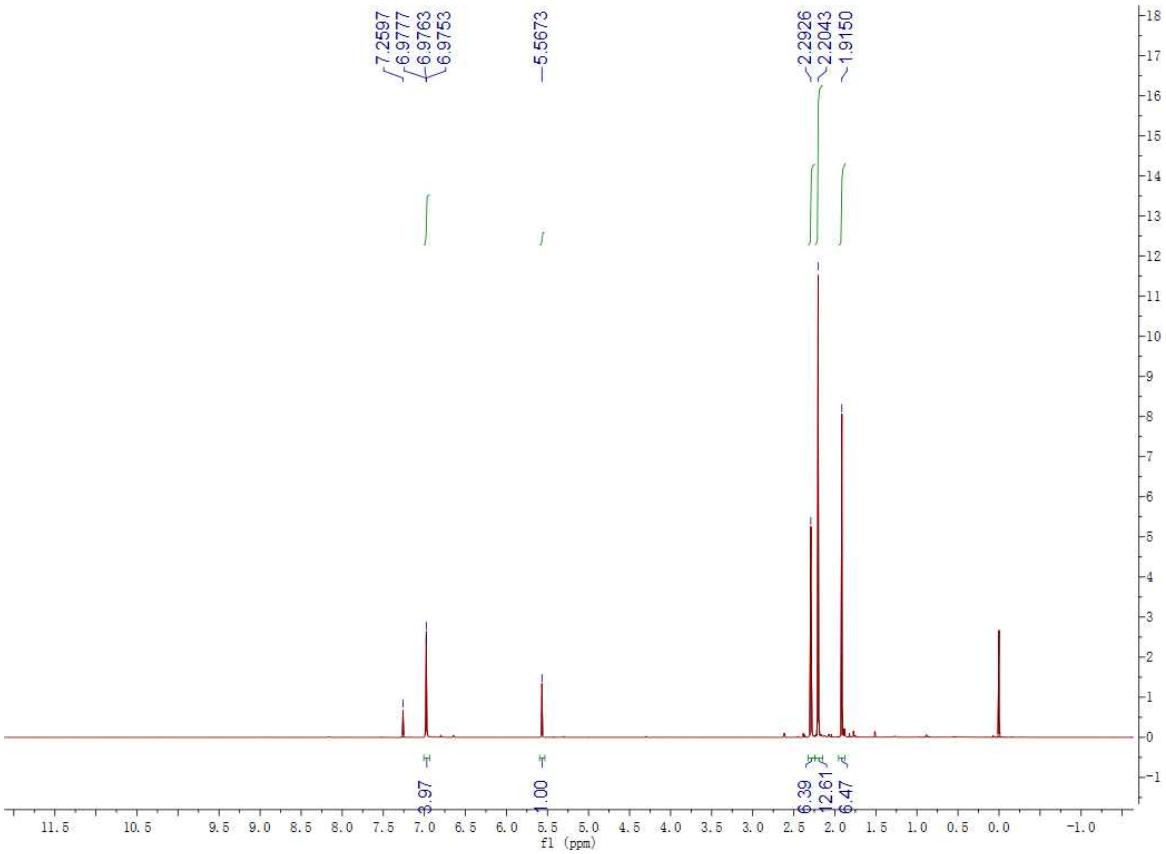

Figure S7. ^{1}H-NMR spectrum of **3c**.

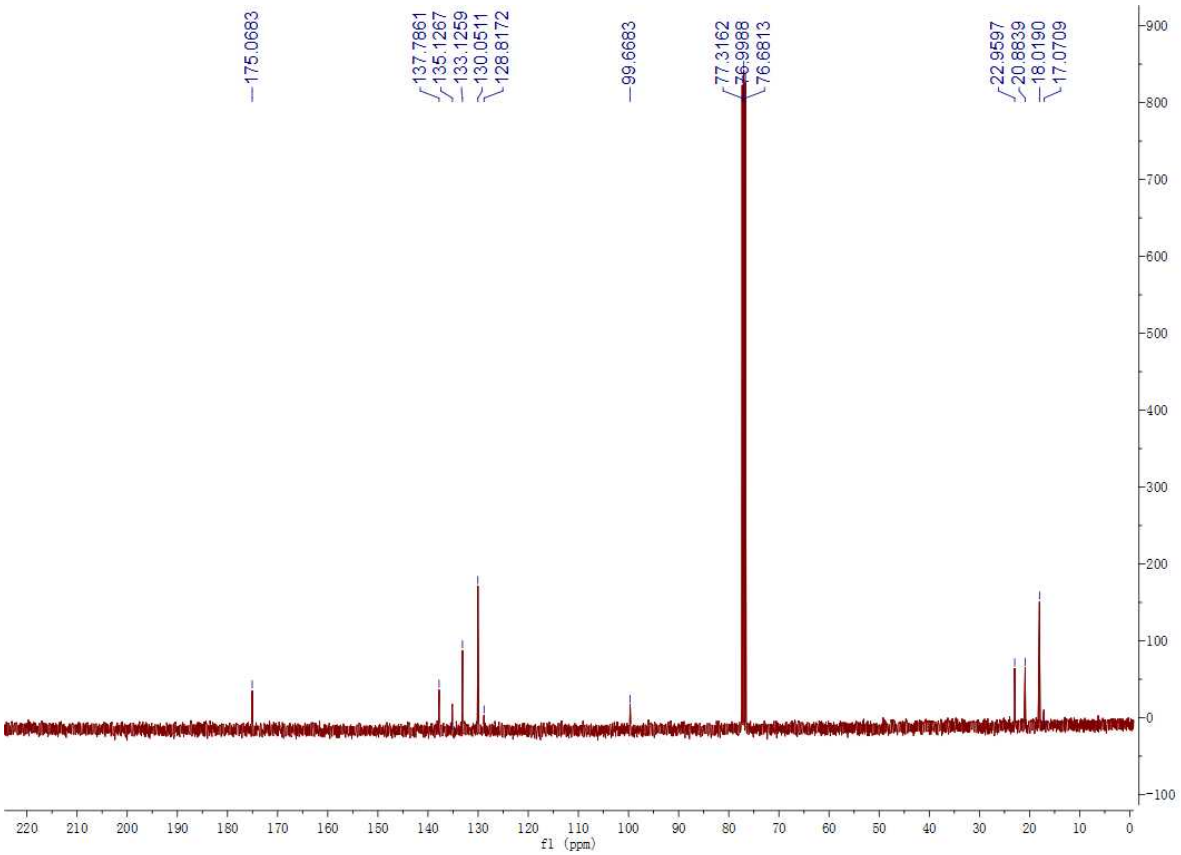

Figure S8. ^{13}C-NMR spectrum of **3c**.

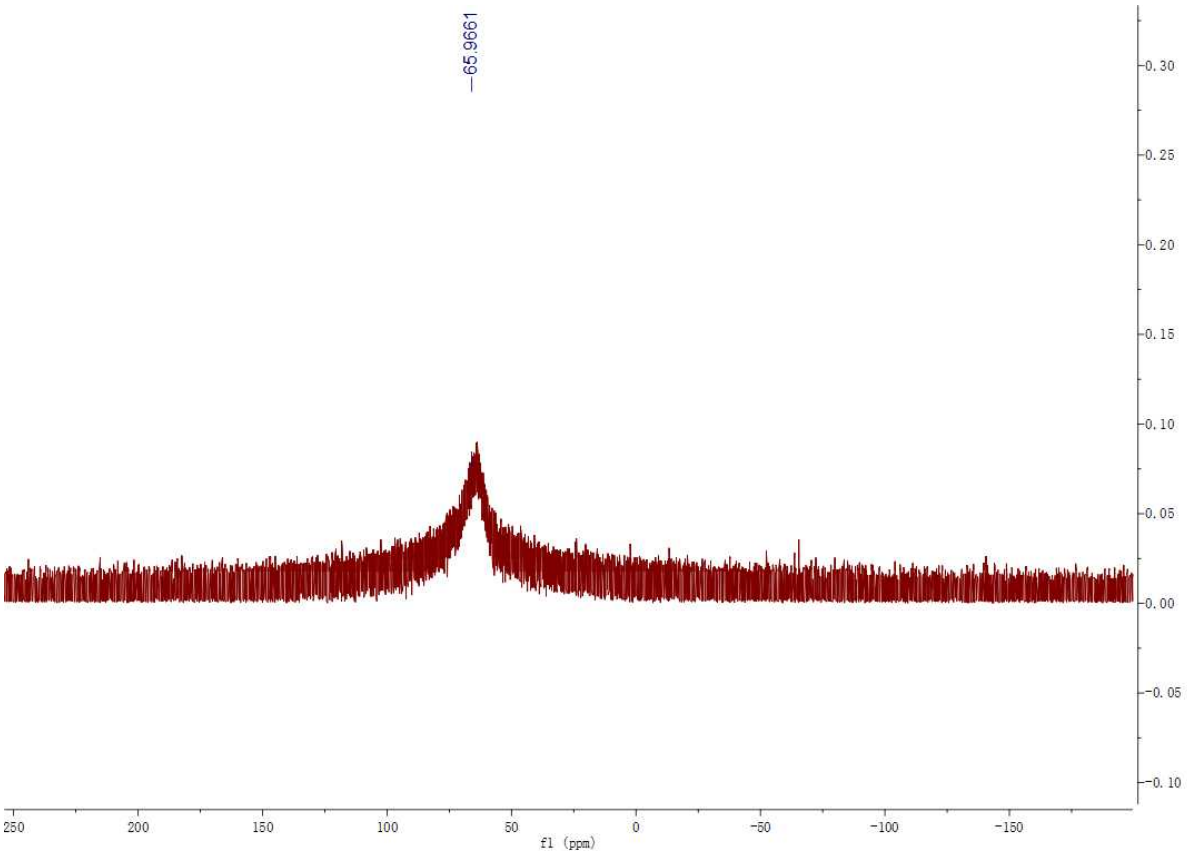

Figure S9. ^{27}Al-NMR spectrum of **3c**.

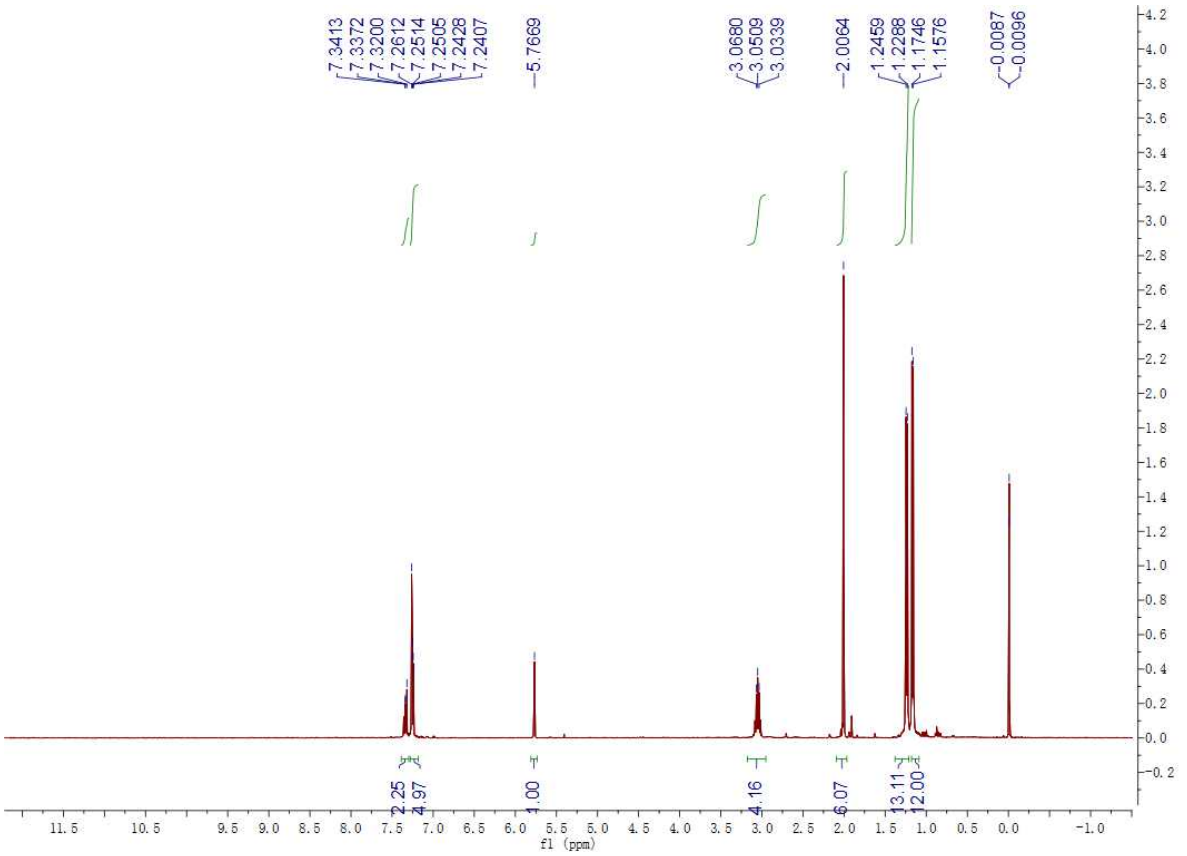

Figure S10. ^{1}H-NMR spectrum of **3d.**

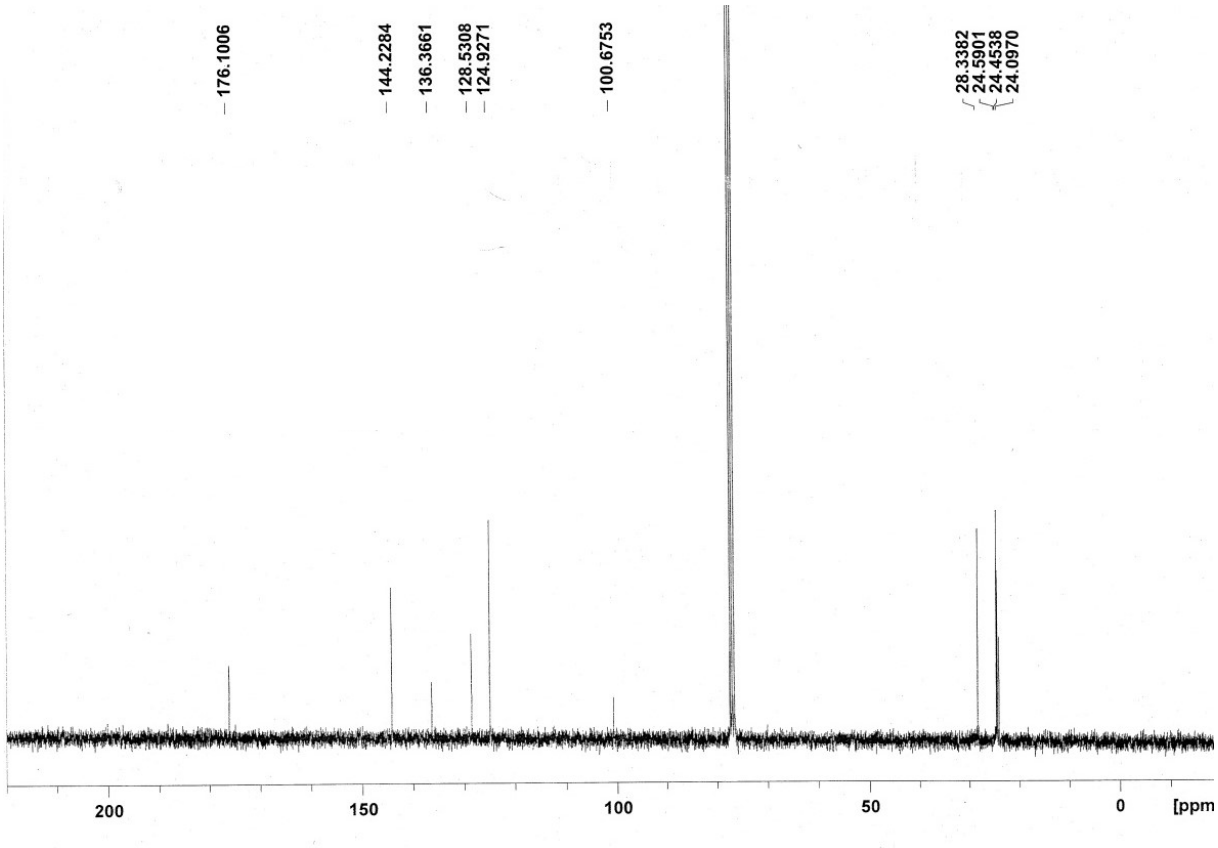

Figure S11. ^{13}C-NMR spectrum of **3d**.

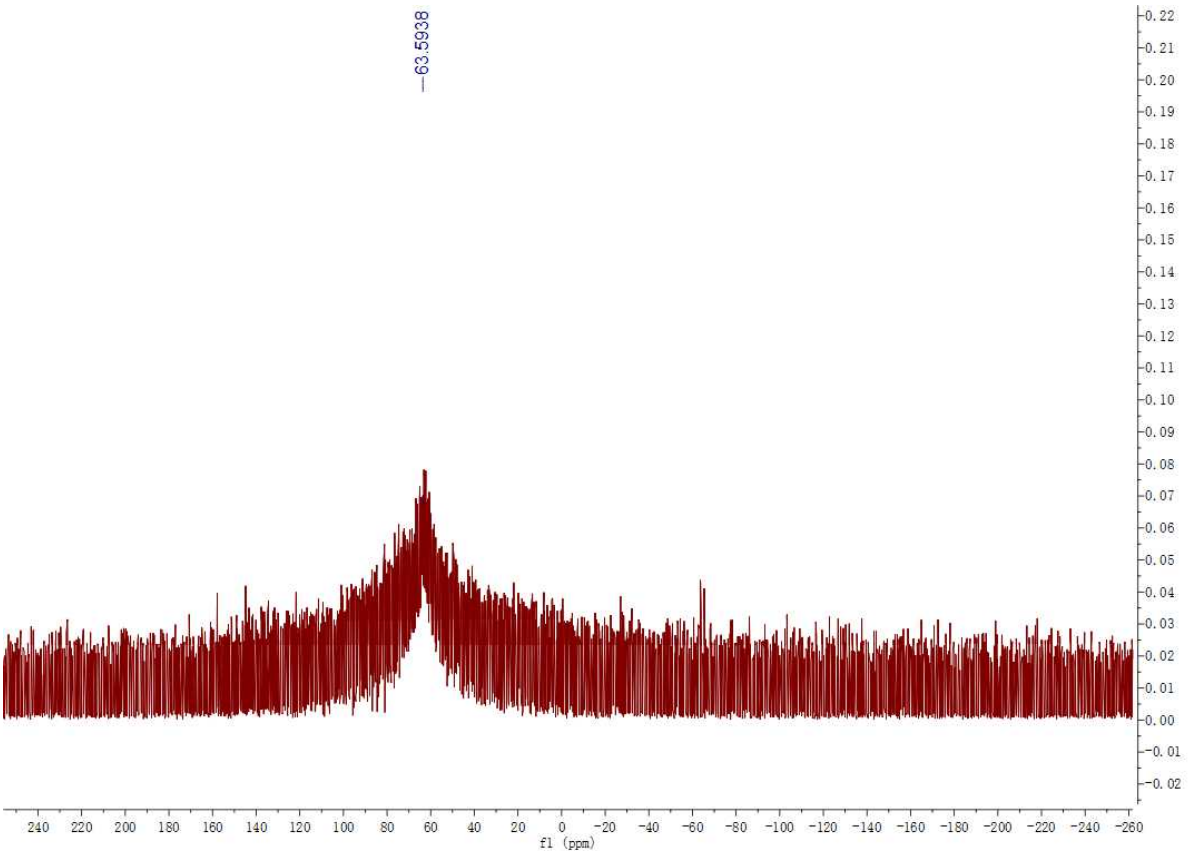

Figure S12. ^{27}Al-NMR spectrum of **3d**.

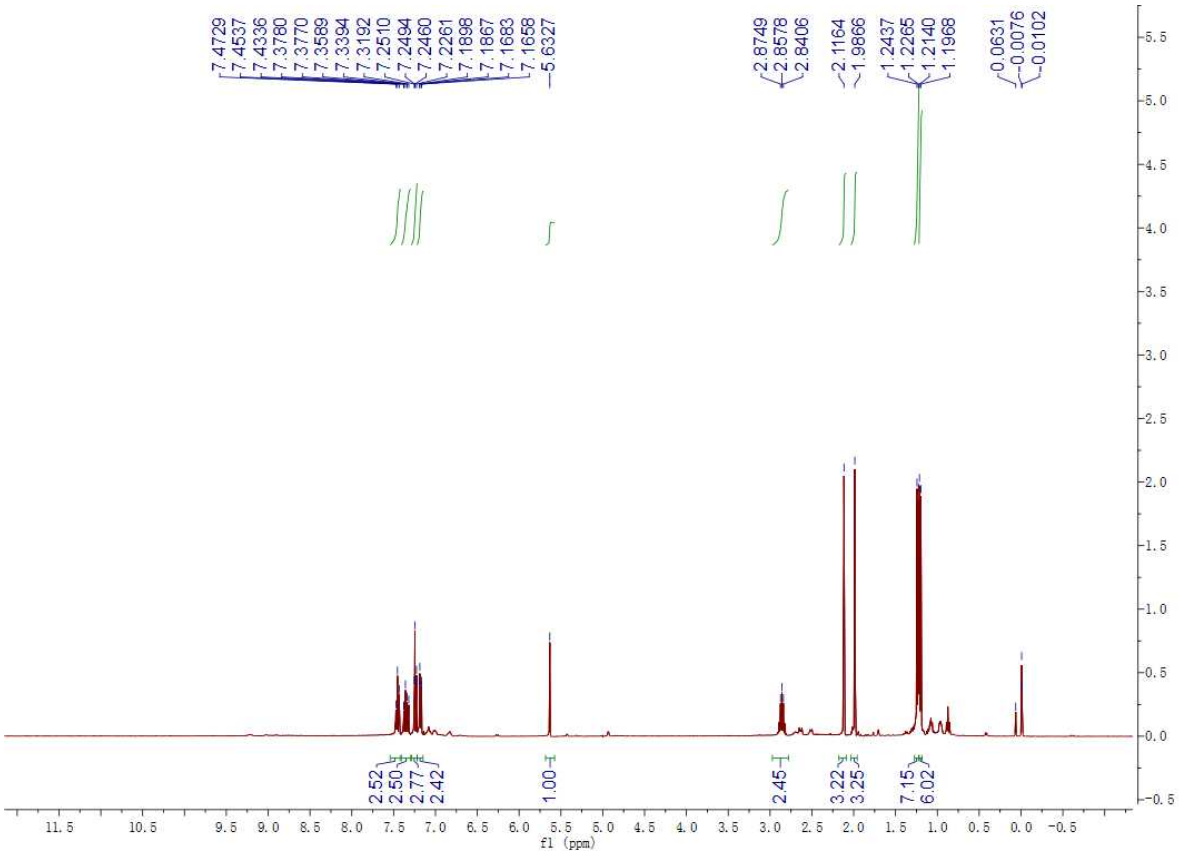

Figure S13. ^{1}H-NMR spectrum of **3e**.

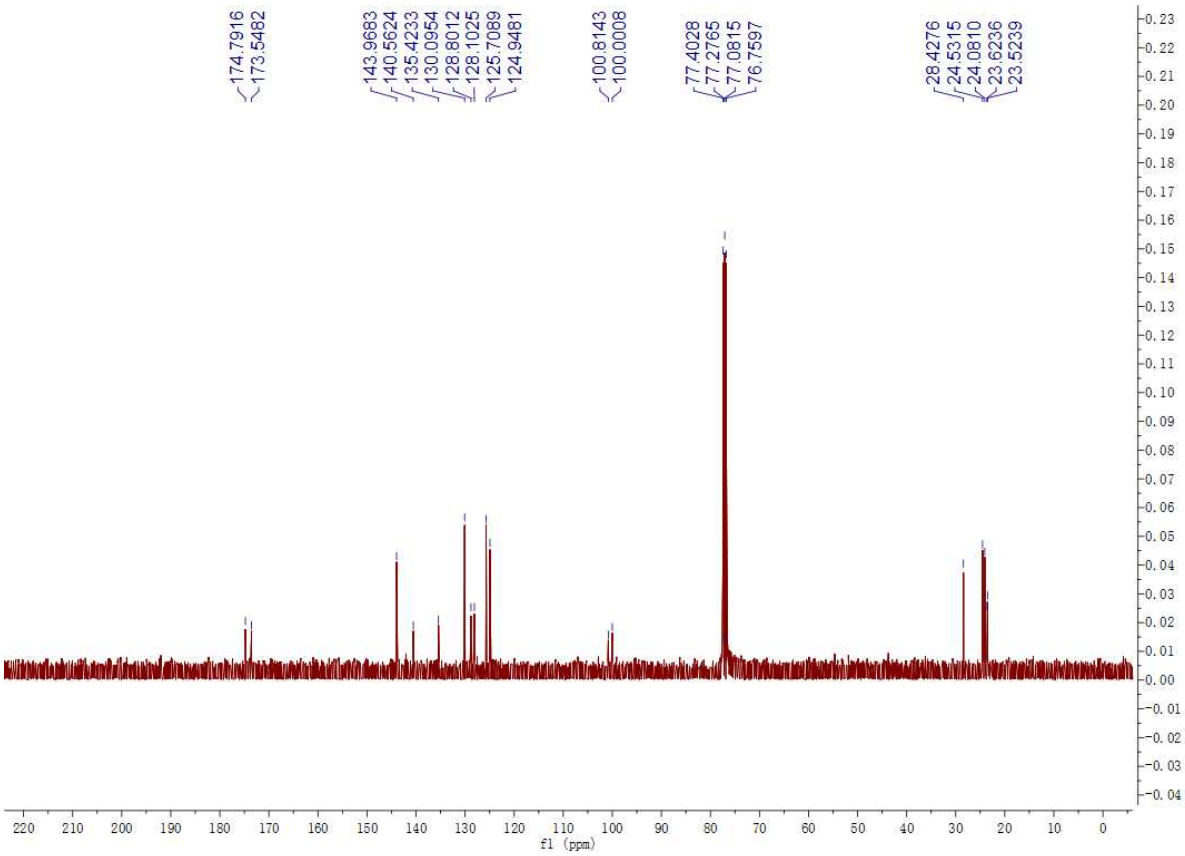

Figure S14. ^{13}C-NMR spectrum of **3e**.

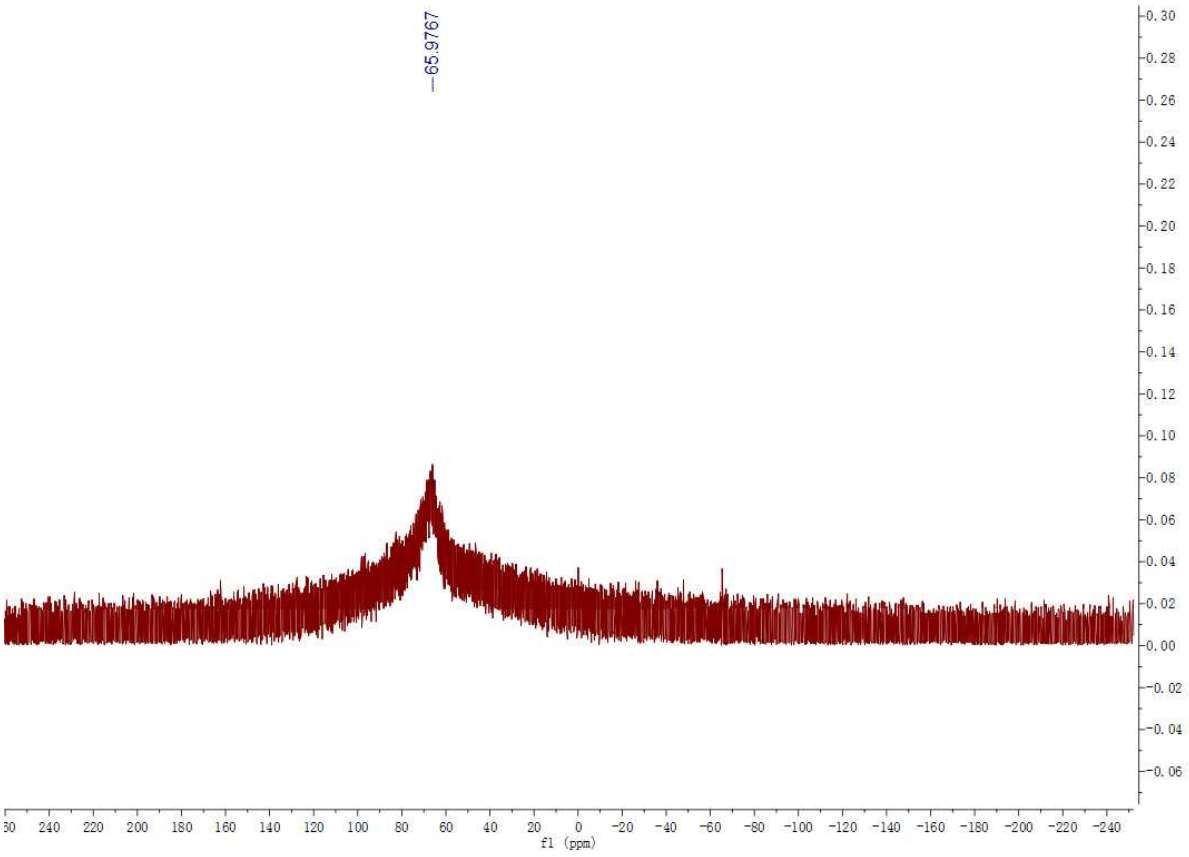

Figure S15. ^{27}Al-NMR spectrum of **3e**.

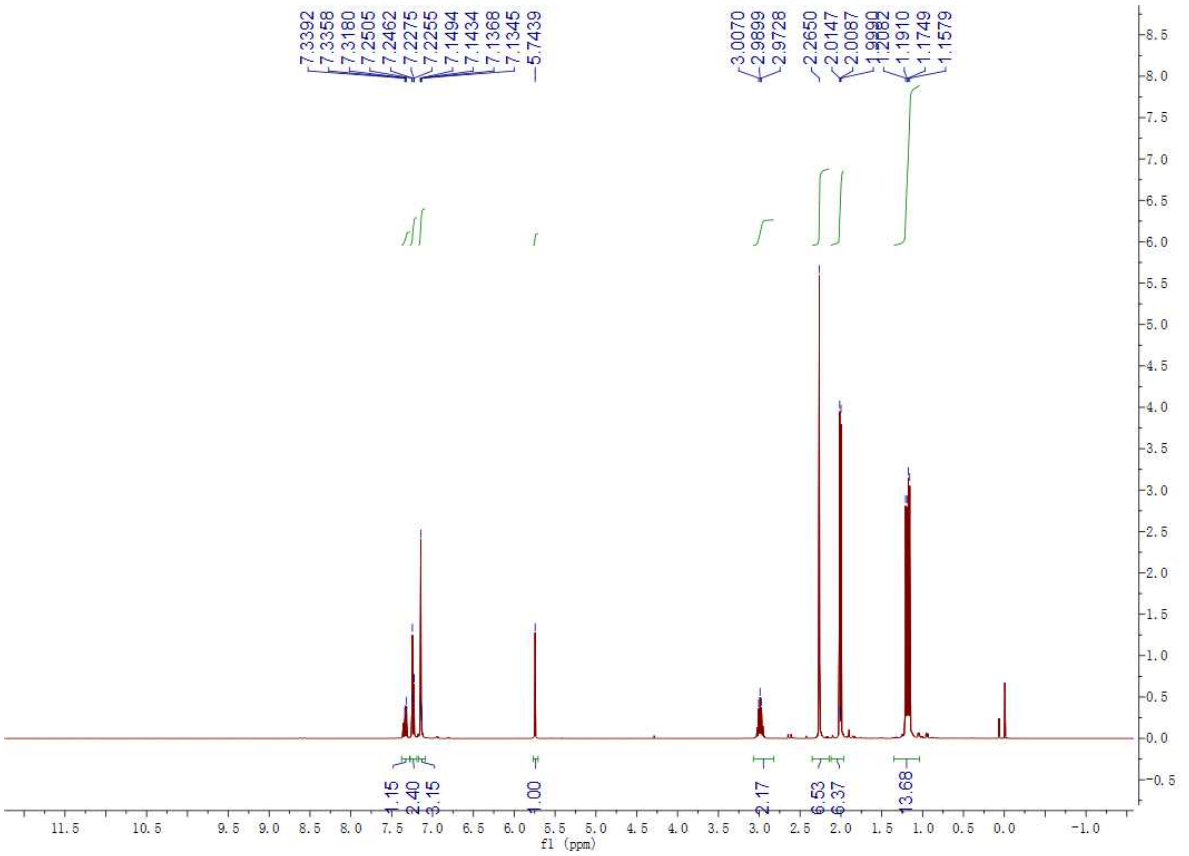

Figure S16. ^{1}H-NMR spectrum of **3f.**

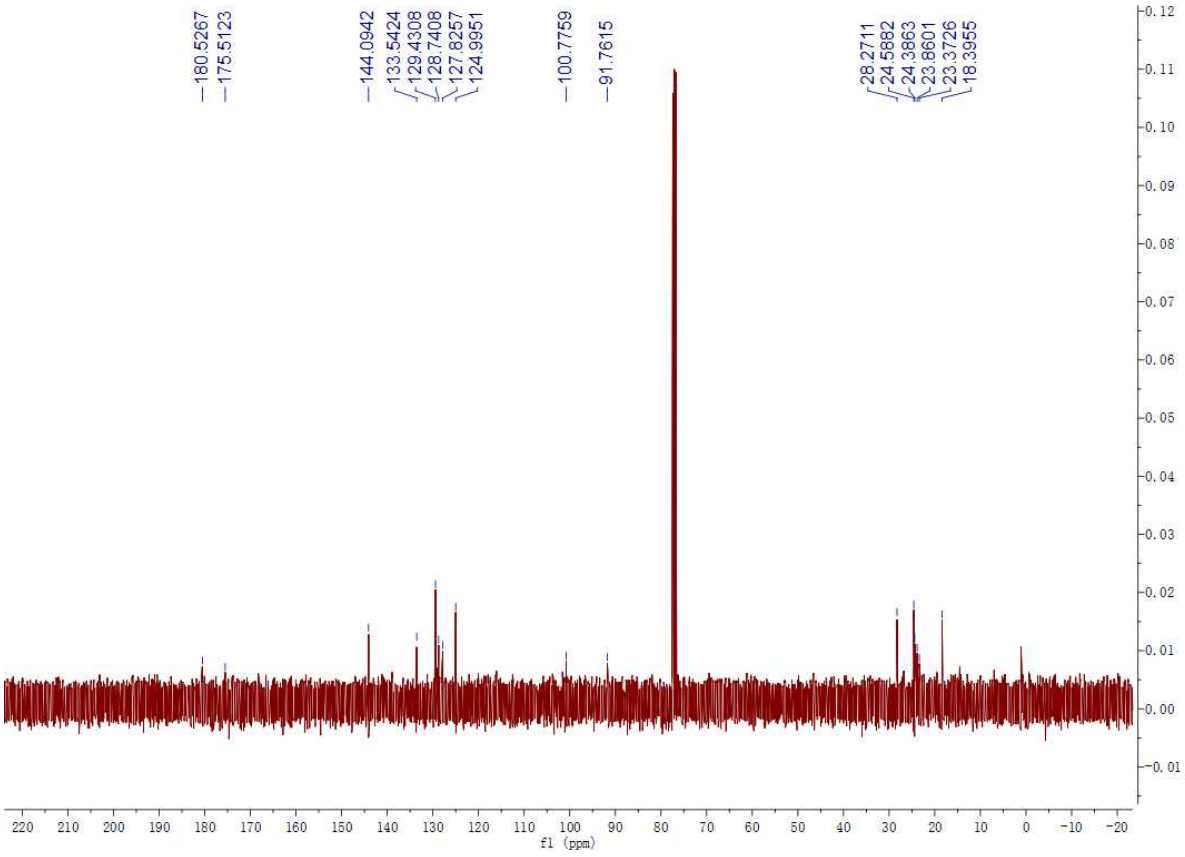

Figure S17. ^{13}C-NMR spectrum of **3f.**

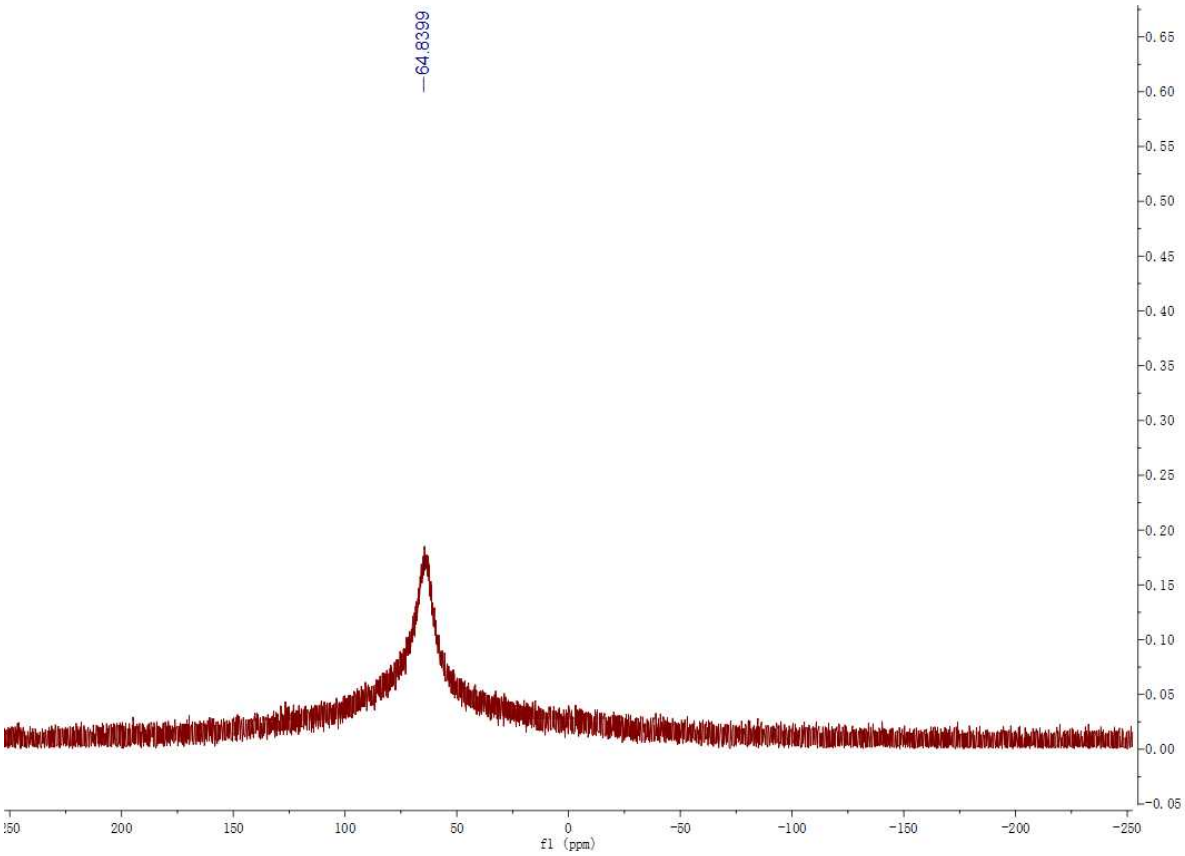

Figure S18. ^{27}Al-NMR spectrum of **3f**.

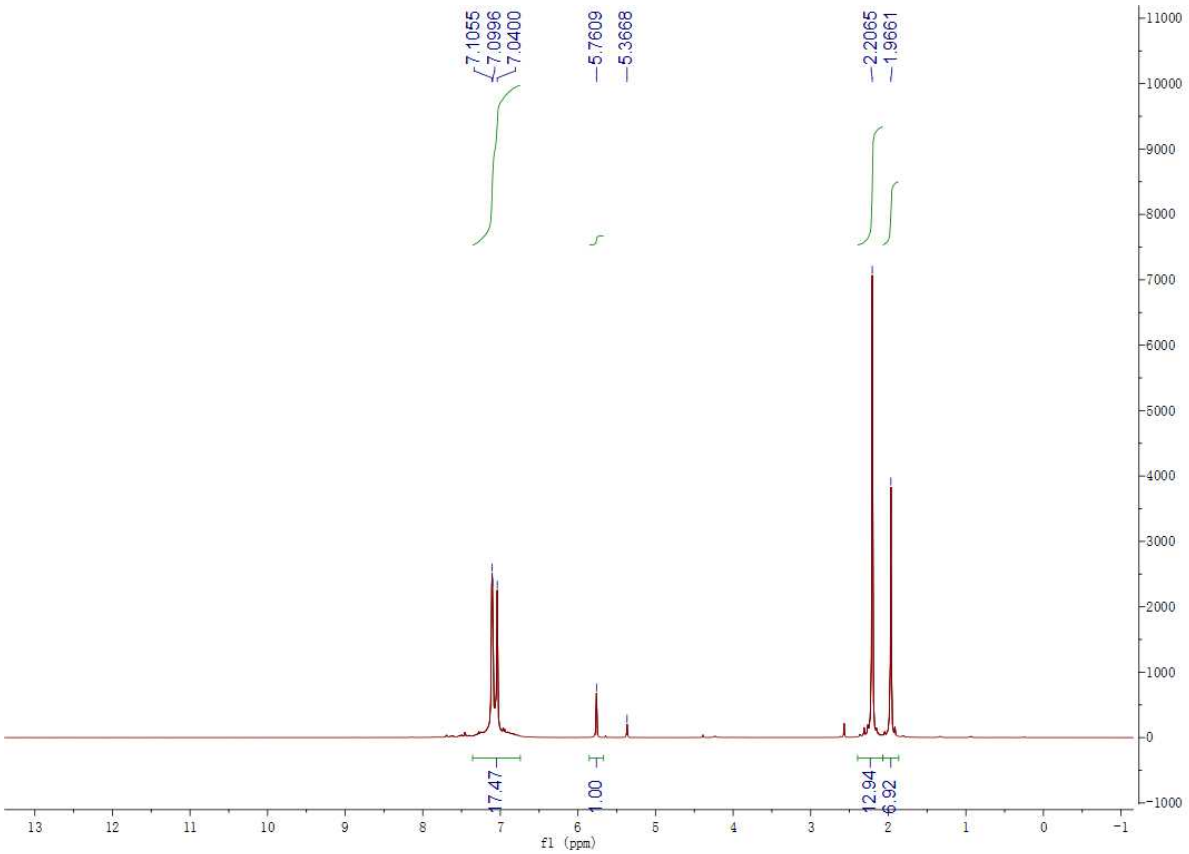

Figure S19. ^{1}H-NMR spectrum of **3b** + NaBAr$^{Cl}_{4}$.

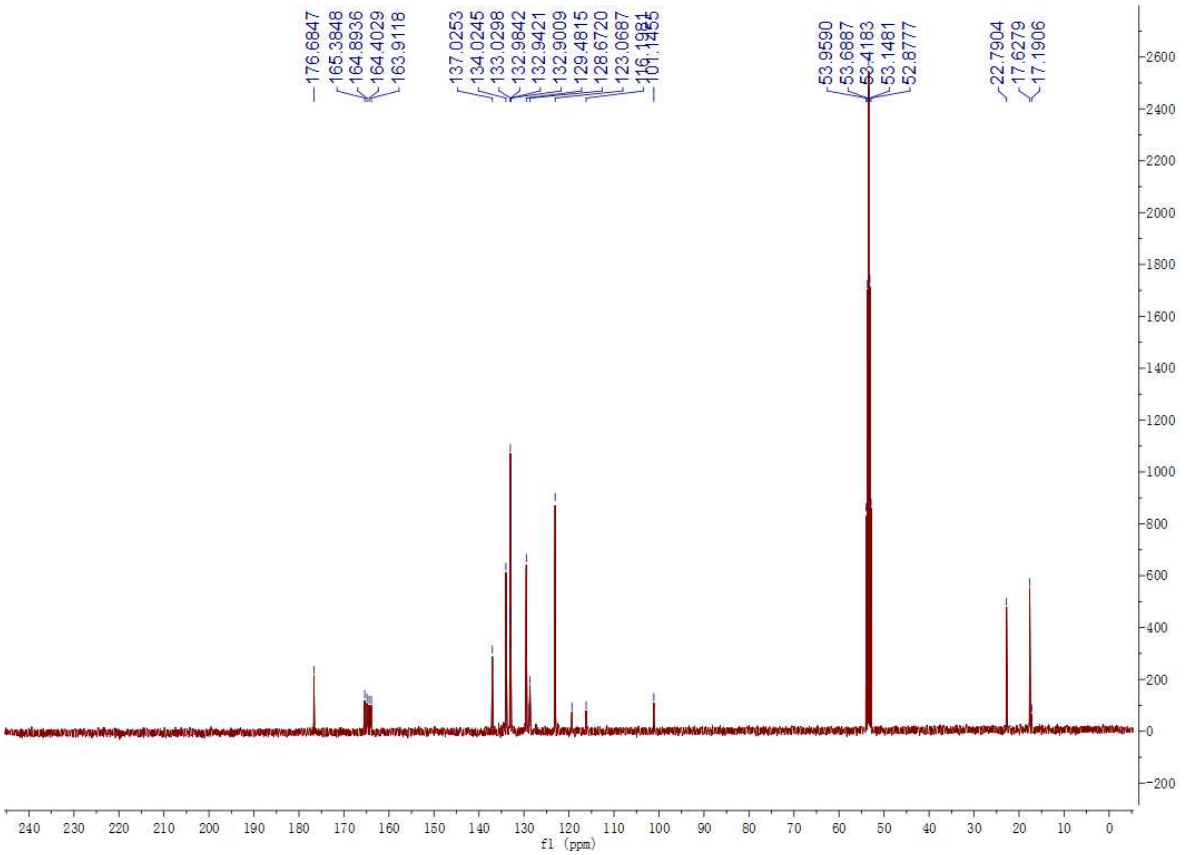

Figure S20. ^{13}C-NMR spectrum of **3b** + NaBAr$^{Cl}_{4}$.

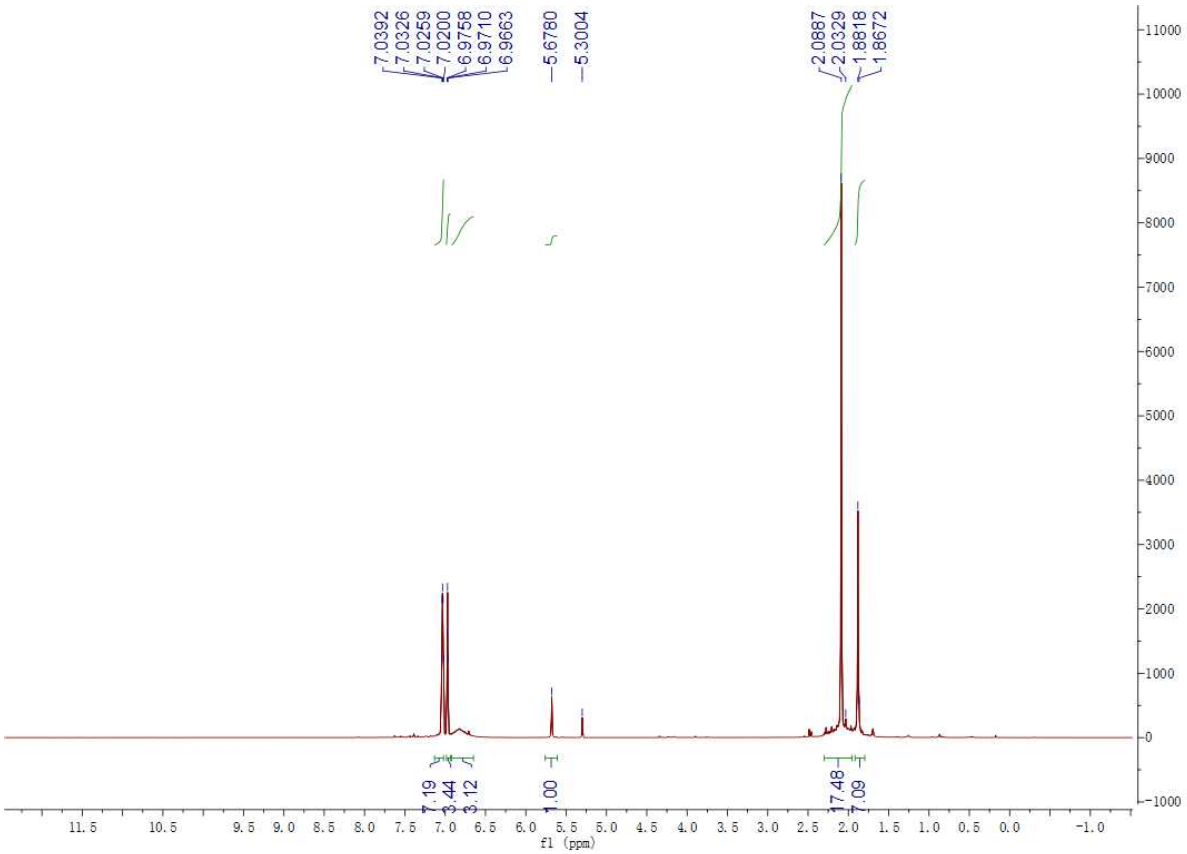

Figure S21. ^{1}H-NMR spectrum of **3c** + NaBAr$^{Cl}_{4}$.

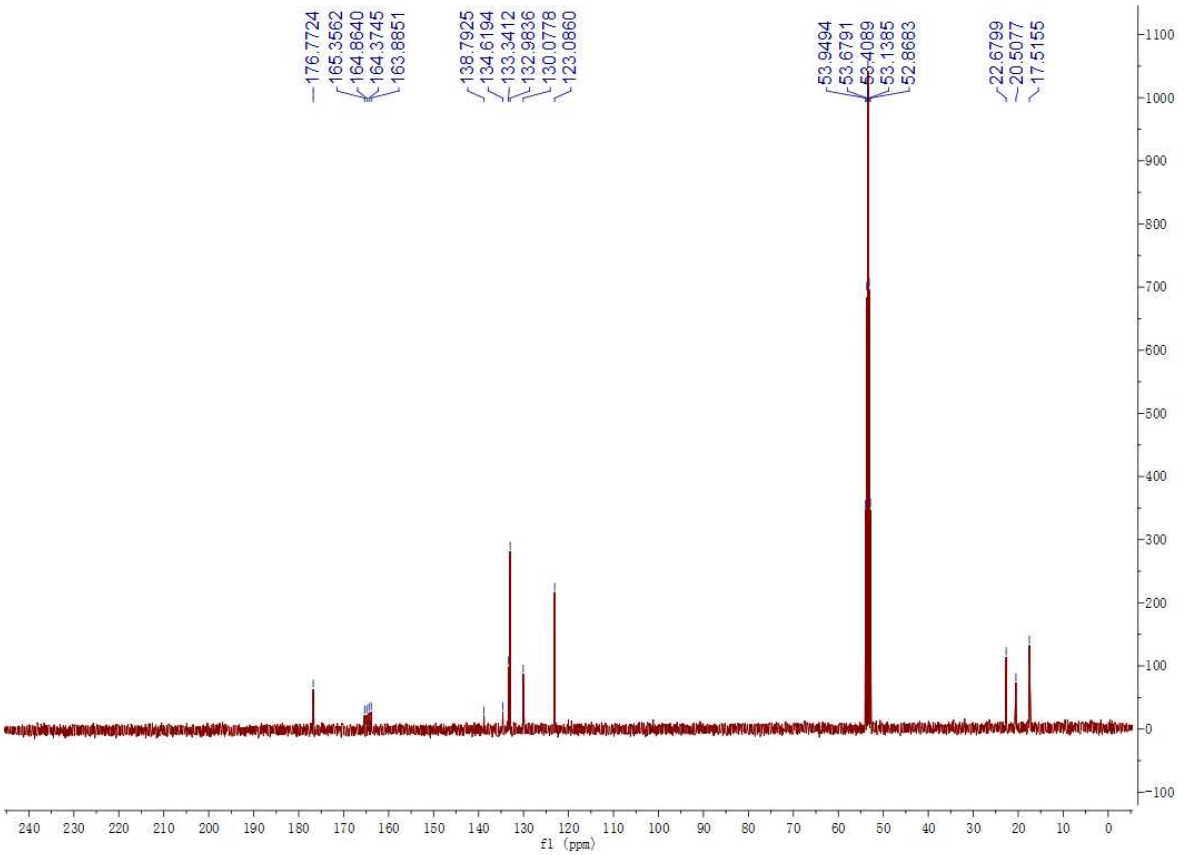

Figure S22. ^{13}C-NMR spectrum of **3c** + NaBAr$^{Cl}_{4}$.

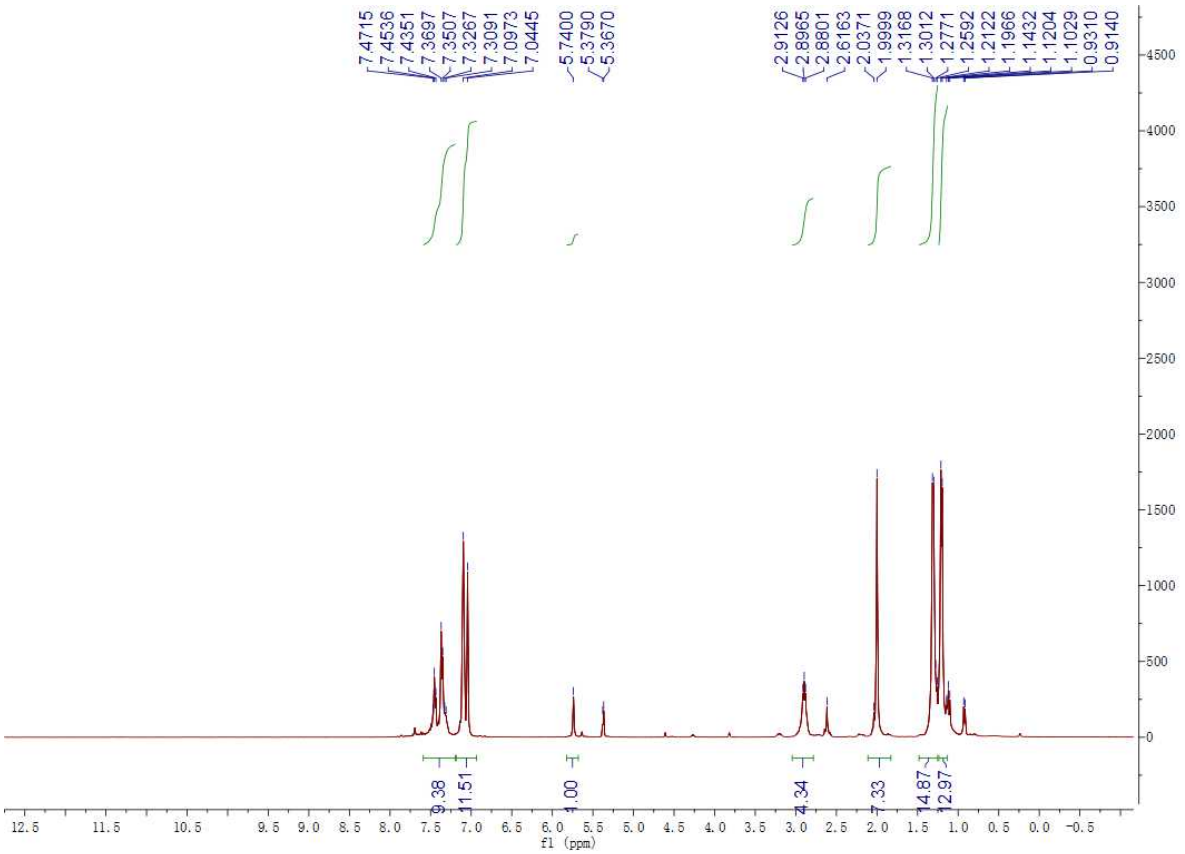

Figure S23. ^{1}H-NMR spectrum of **3d** + NaBAr$^{Cl}_{4}$.

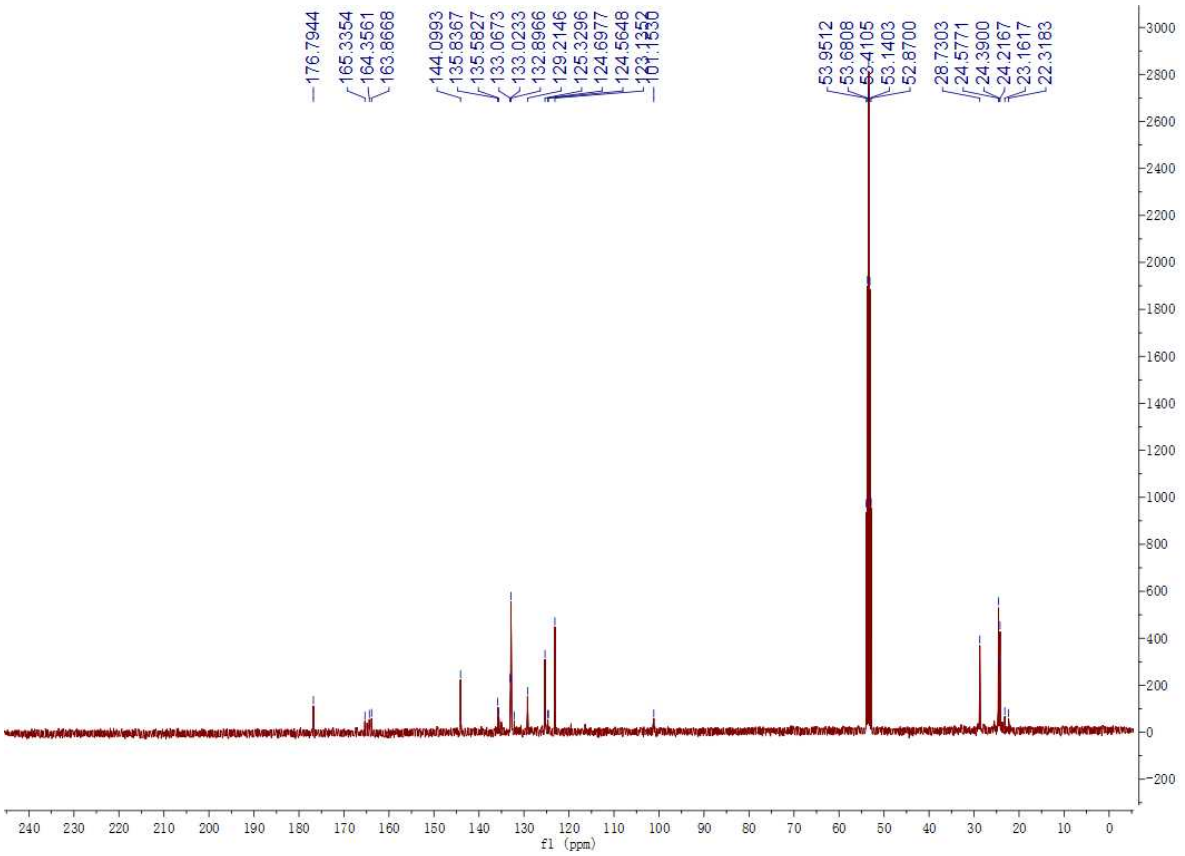

Figure S24. ^{13}C-NMR spectrum of **3d** + NaBAr$^{Cl}_{4}$.

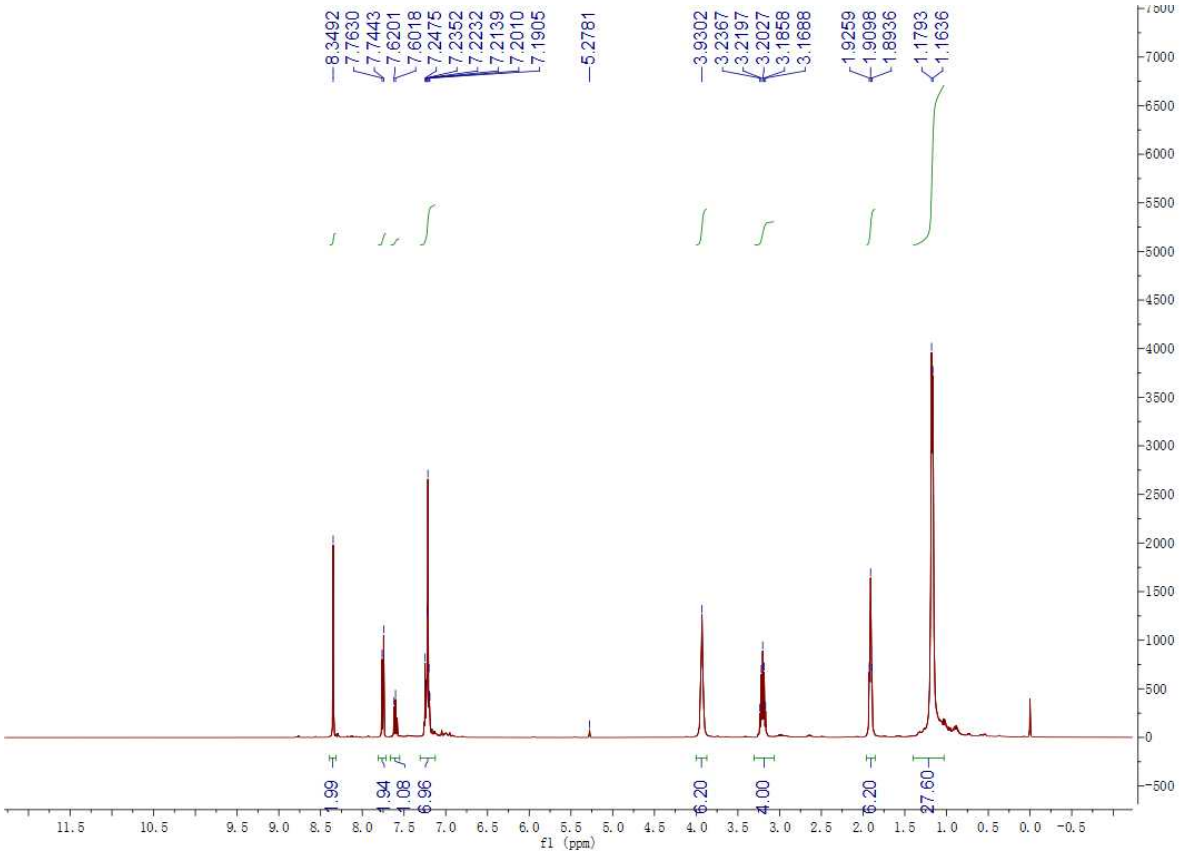

Figure S25. ^{1}H-NMR spectrum of **46**.

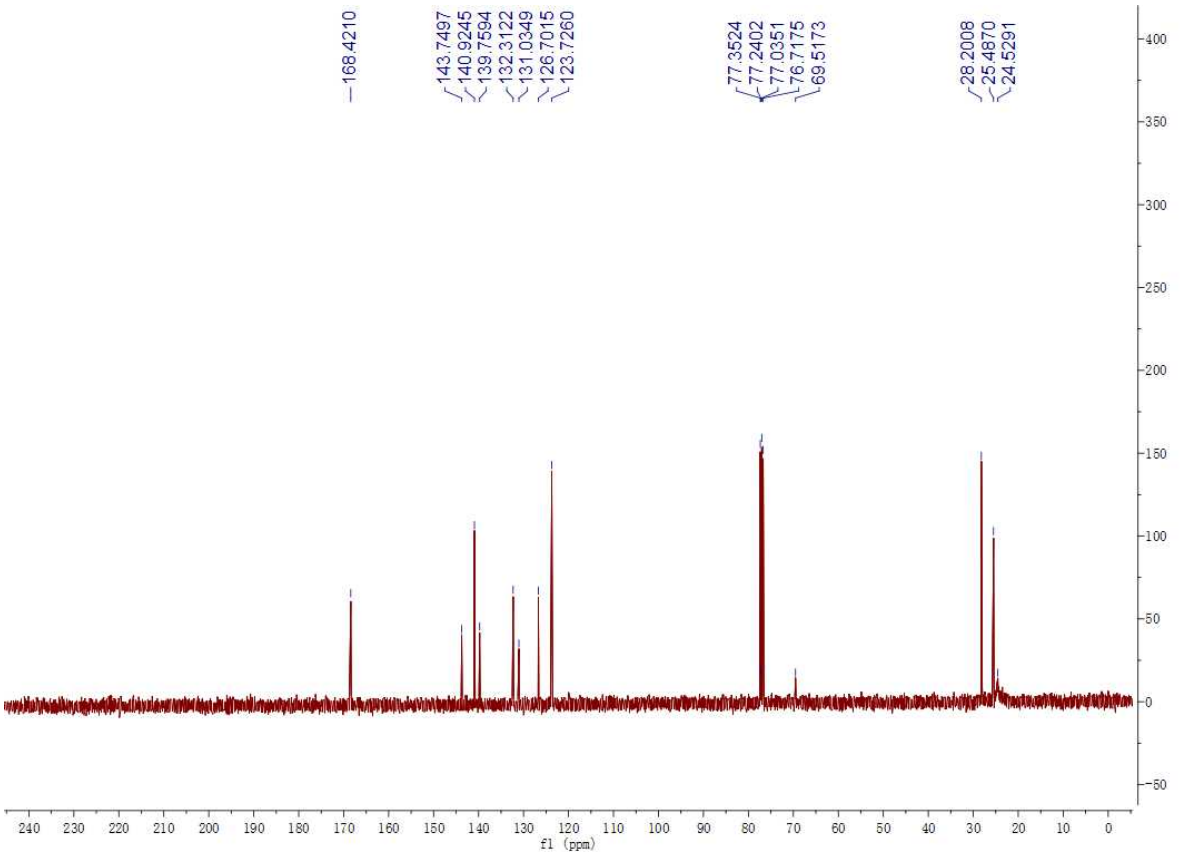

Figure S26. ^{13}C-NMR spectrum of **46.**

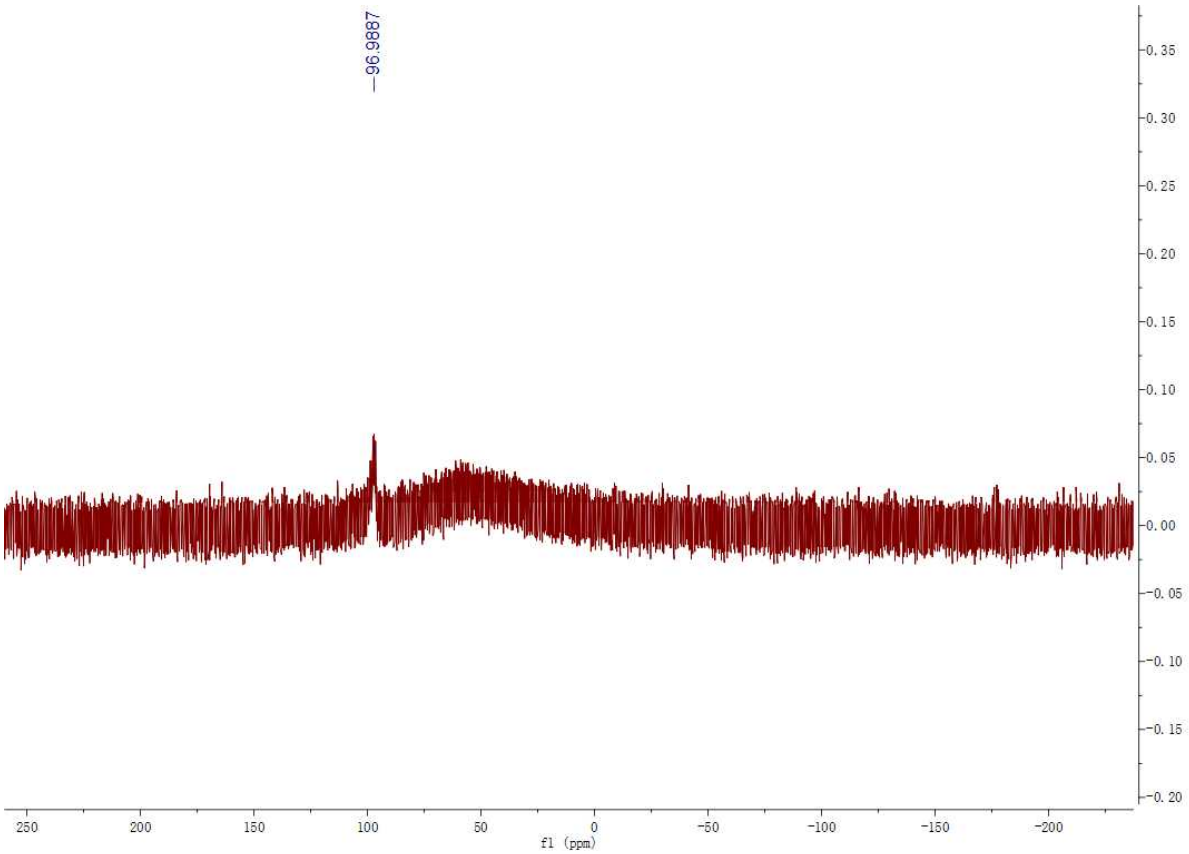

Figure S27. ^{27}Al-NMR spectrum of **46.**

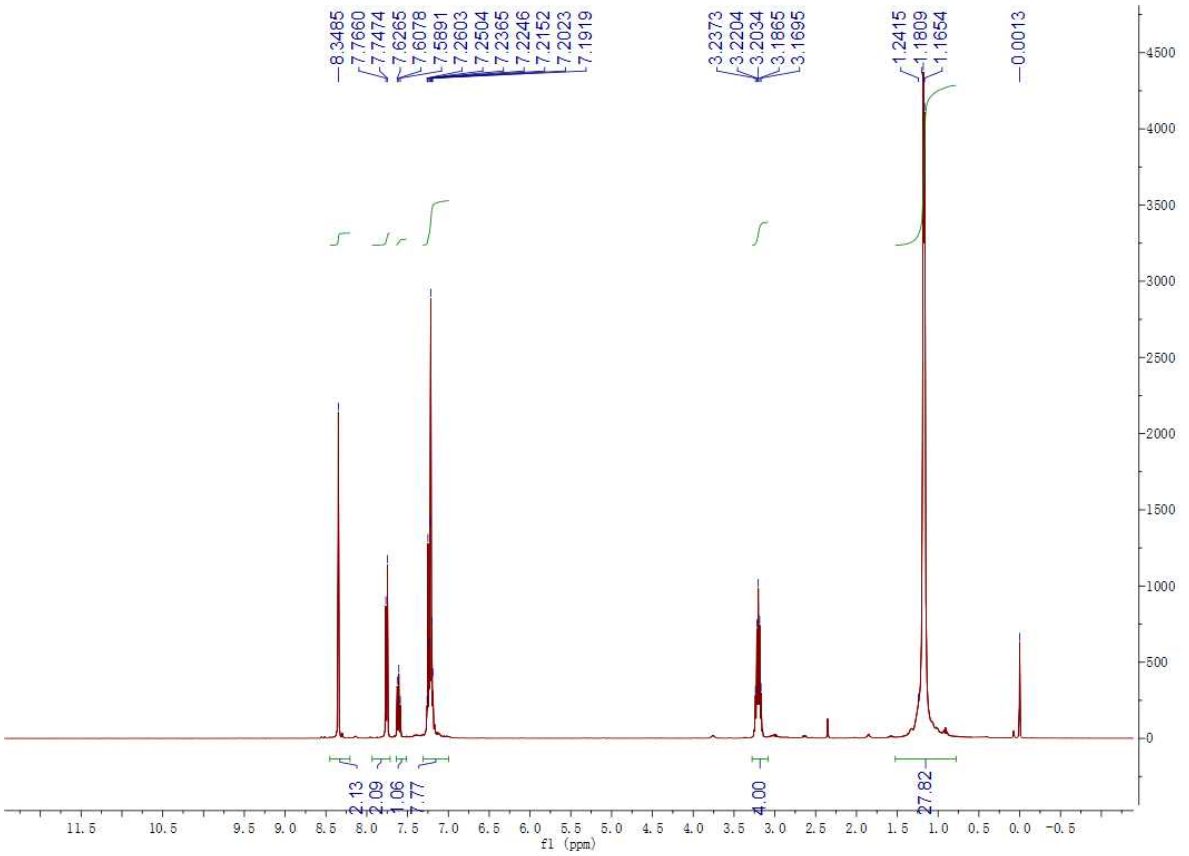

Figure S28. ^{1}H-NMR spectrum of **47**.

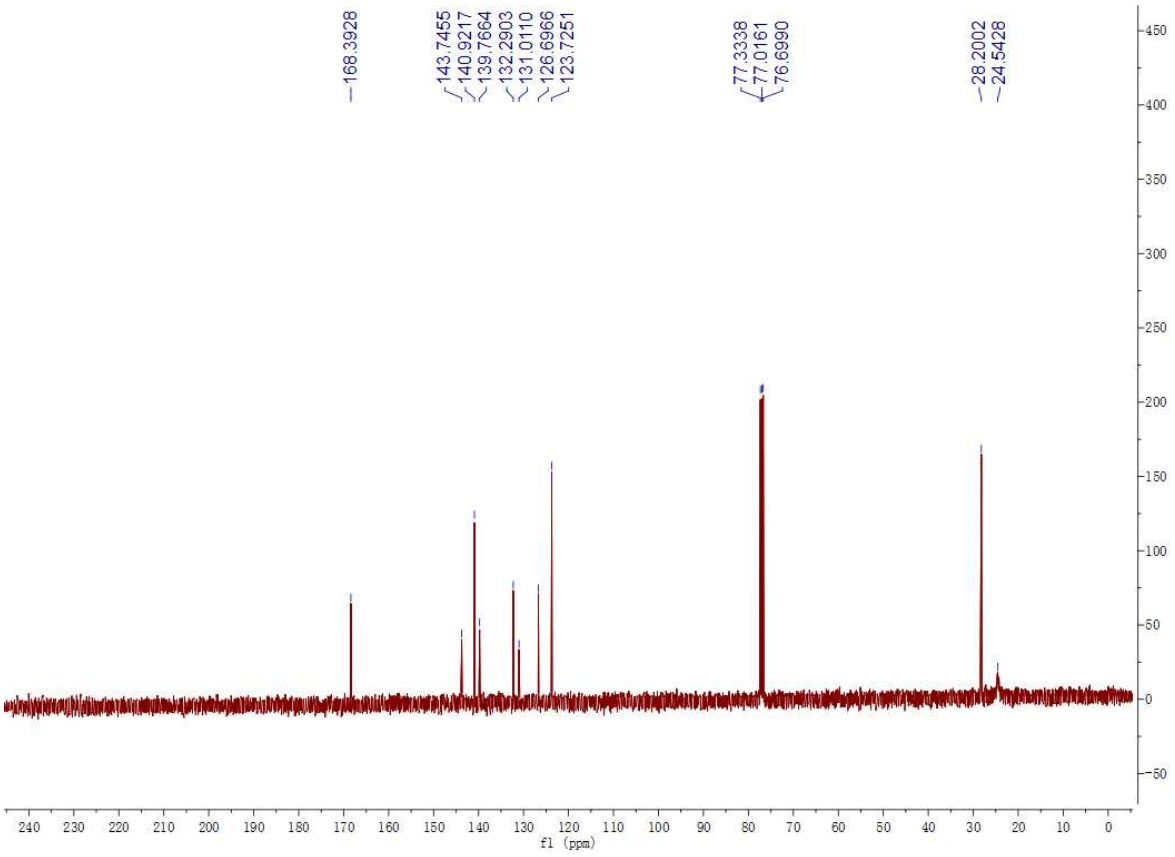

Figure S29. ^{13}C-NMR spectrum of **47**.

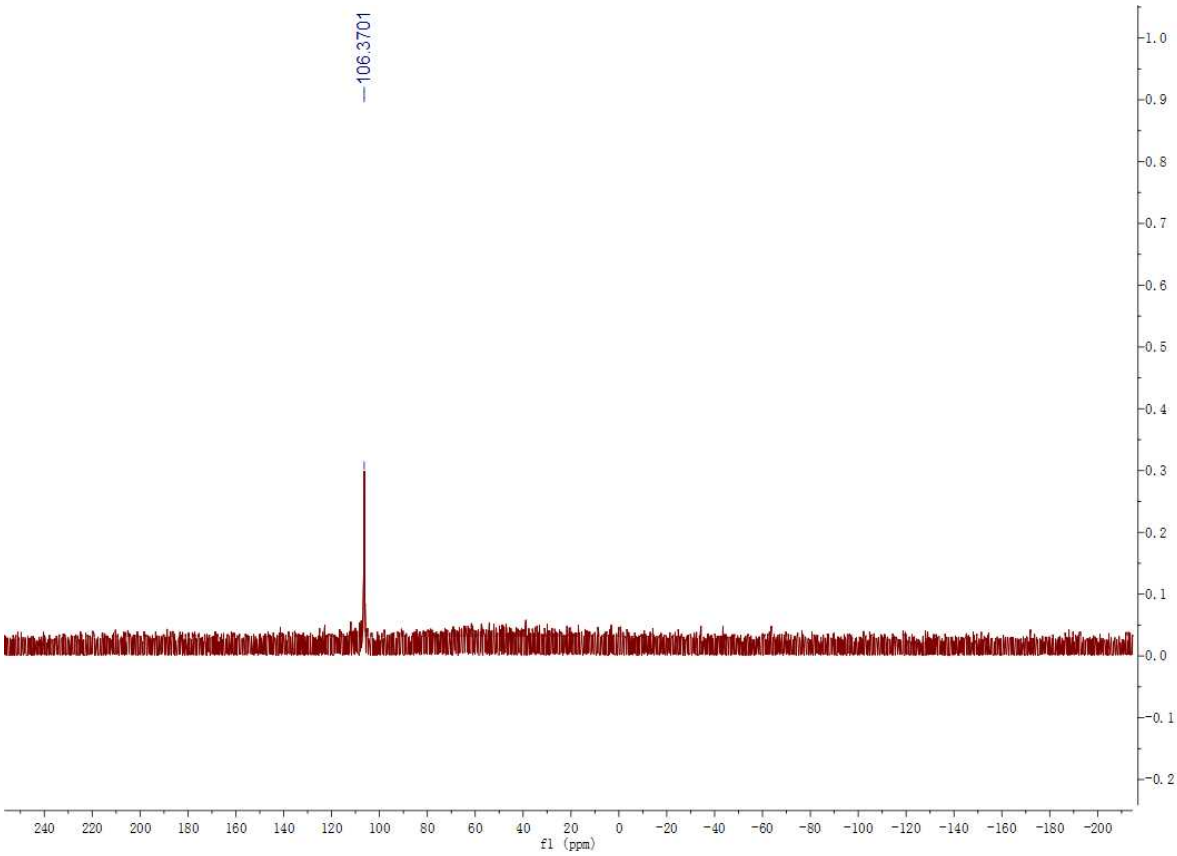

Figure S30. ^{27}Al-NMR spectrum of **47**.

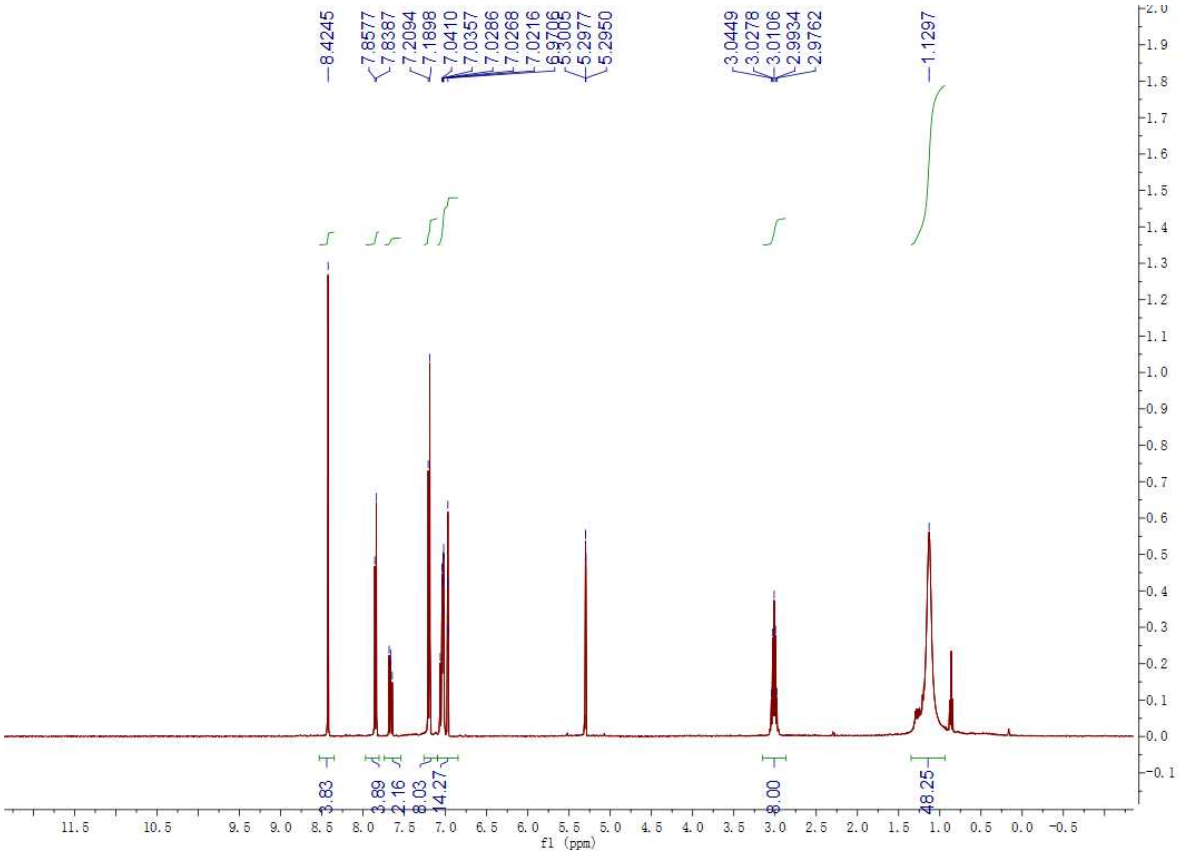

Figure S31. ^{1}H-NMR spectrum of **49**.

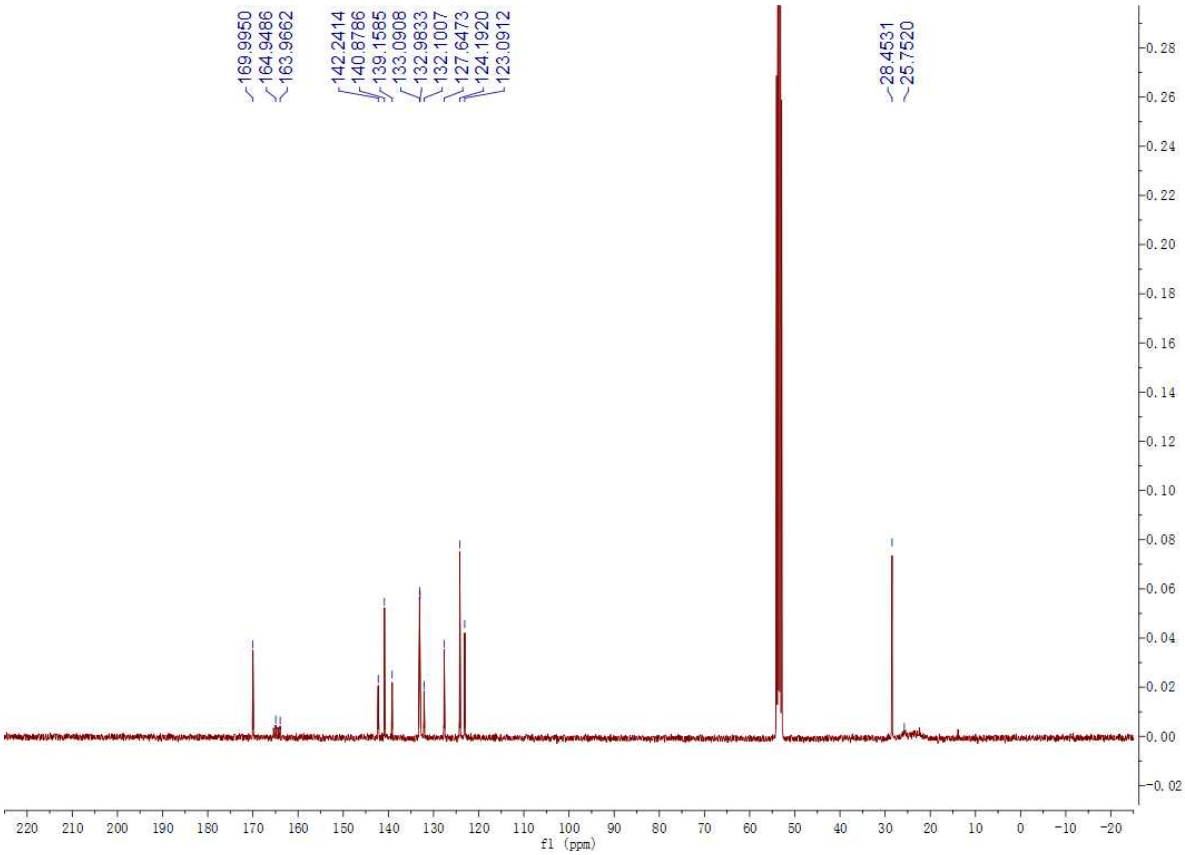

Figure S32. ^{13}C-NMR spectrum of **49**.

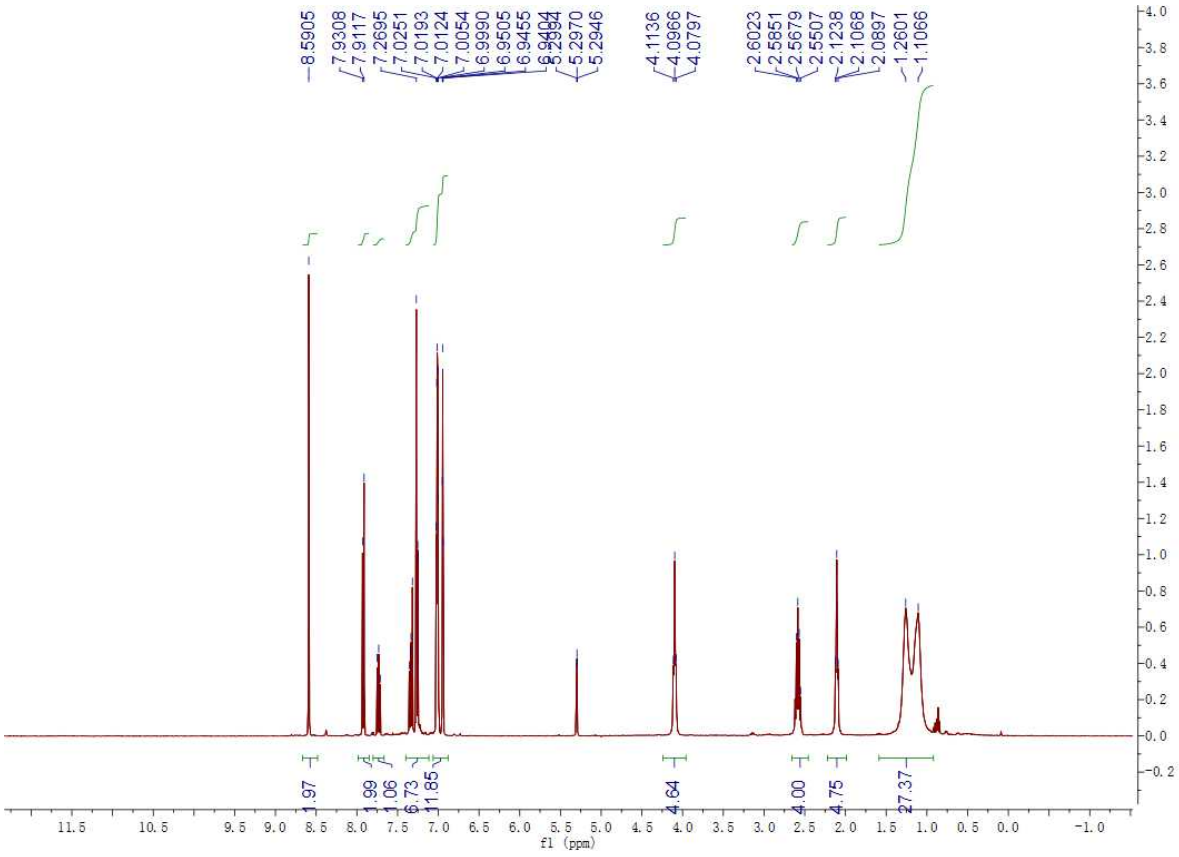

Figure S33. ^{1}H-NMR spectrum of **50.**

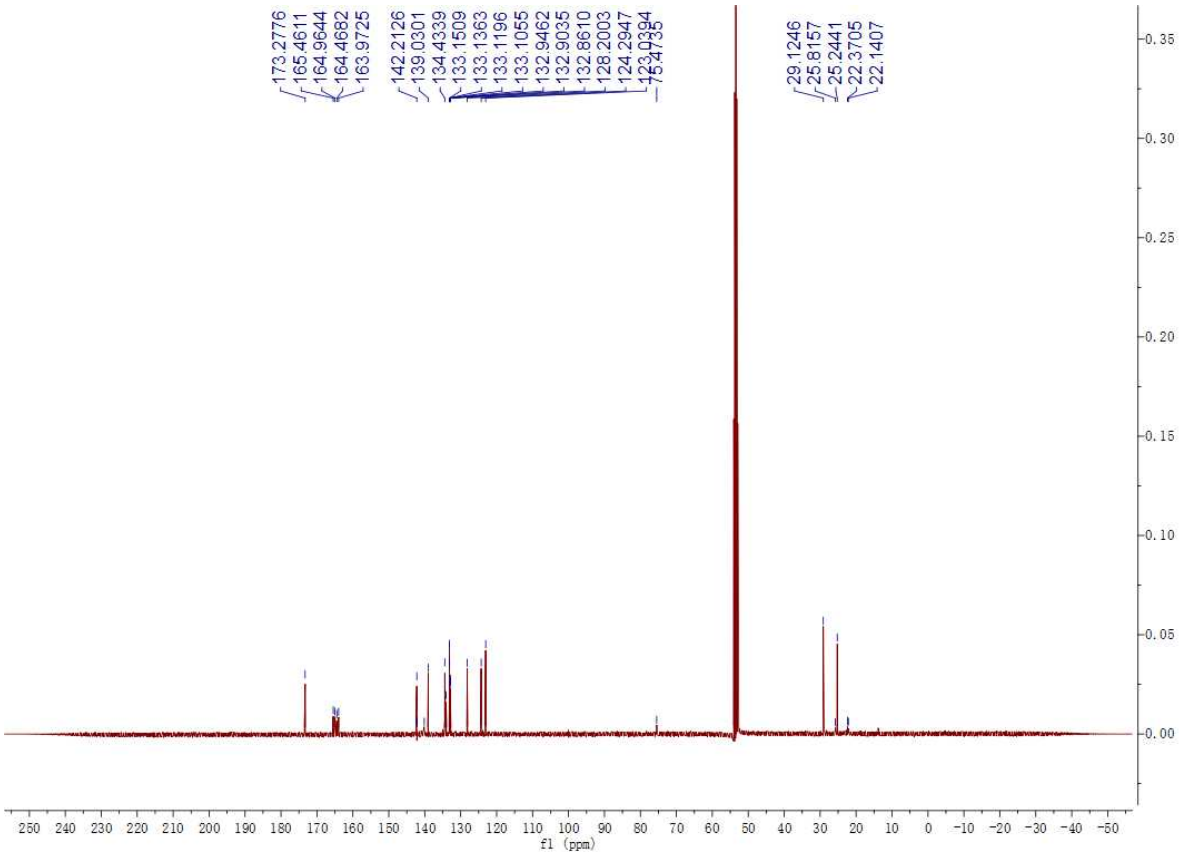

Figure S34. ^{13}C-NMR spectrum of **50**.

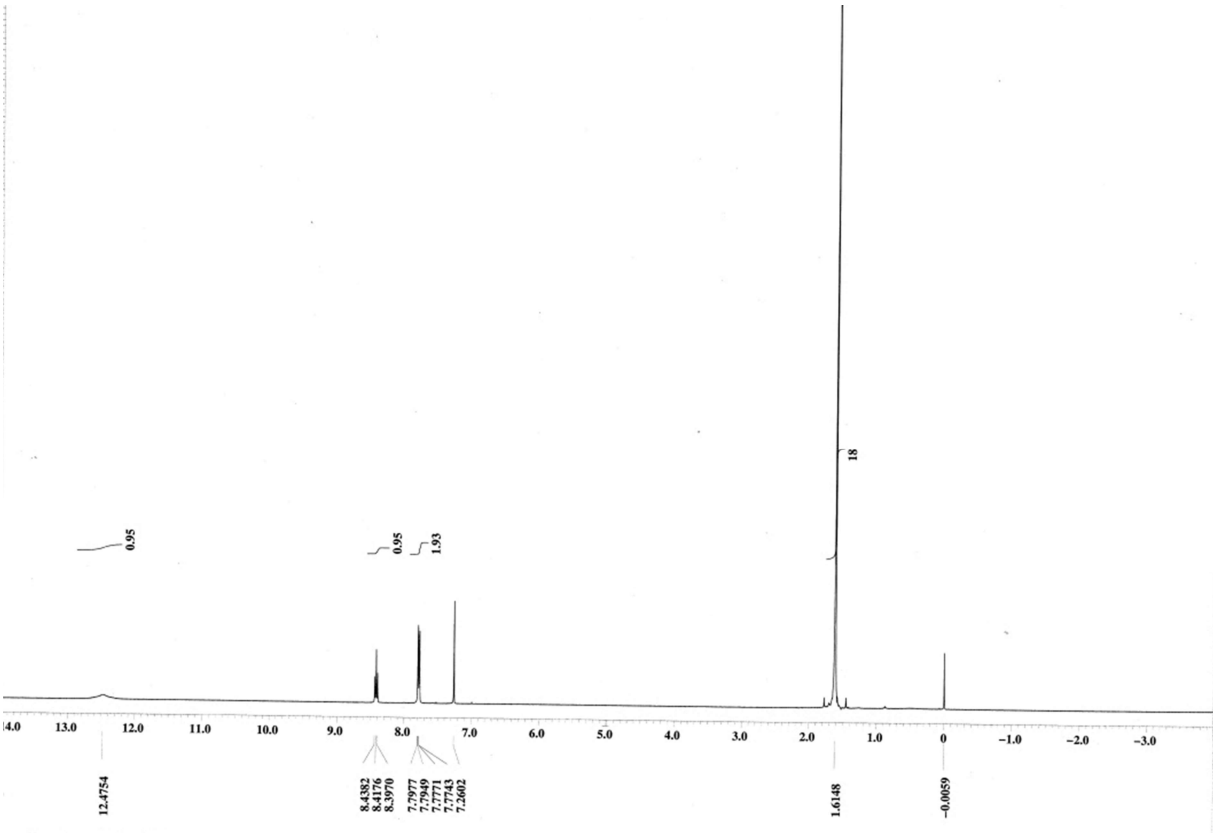

Figure S35. ^{1}H-NMR spectrum of pyridium.

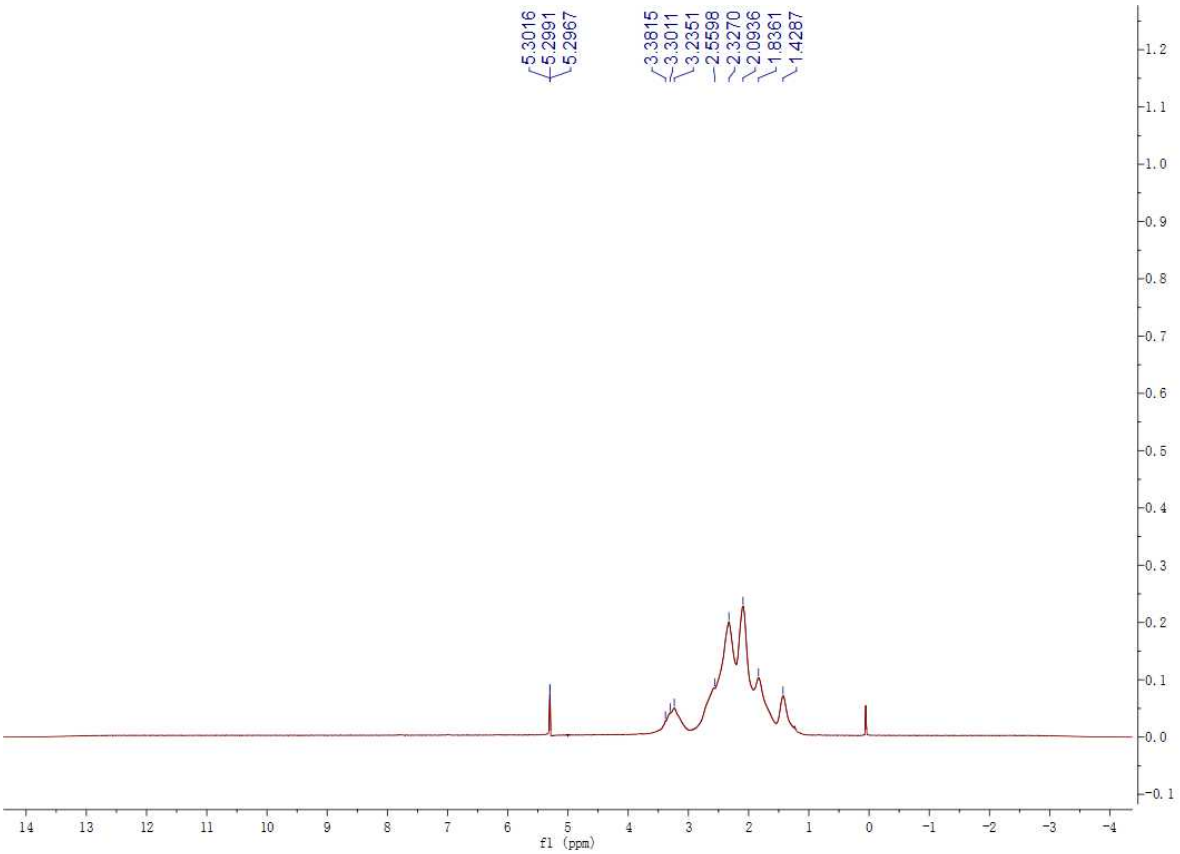

Figure S36. ^{1}H-NMR spectrum of poly-**12**.

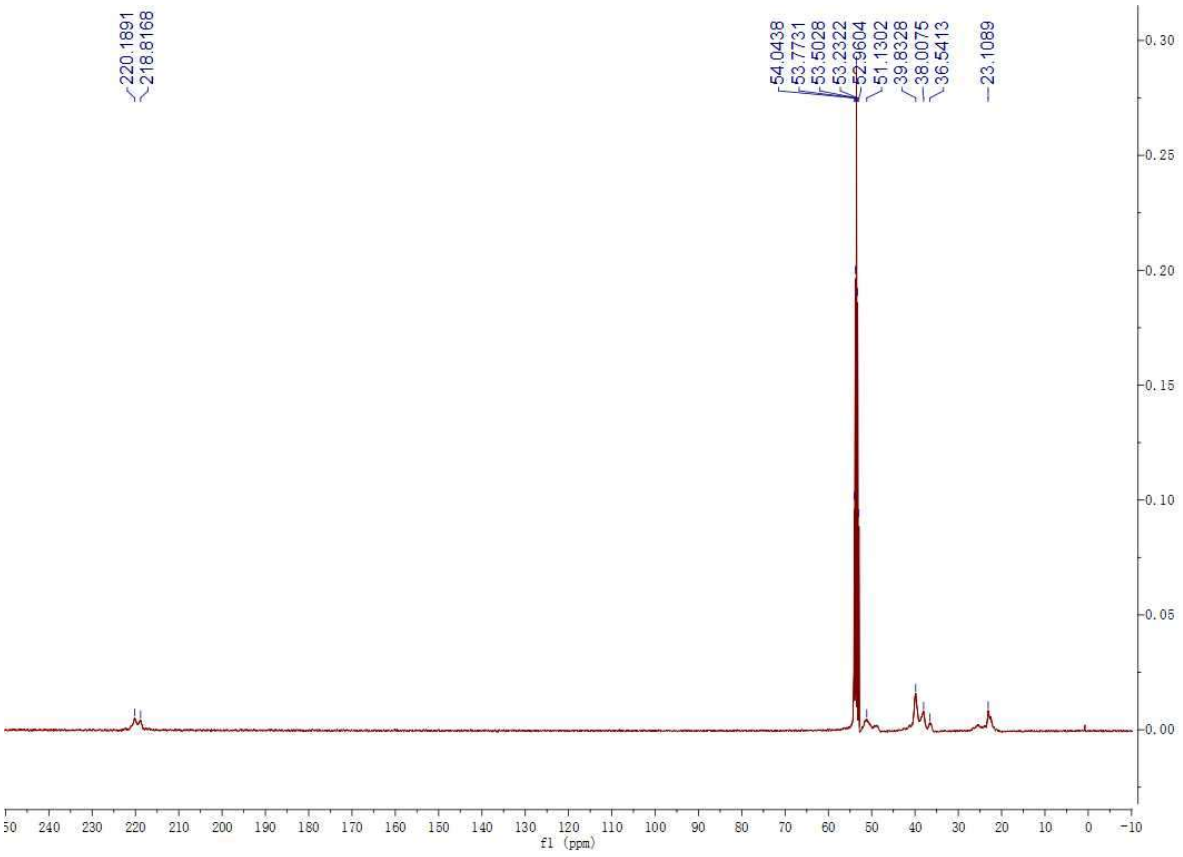

Figure S37. ^{13}C-NMR spectrum of poly-**12**

2. Spectrum for polymers.

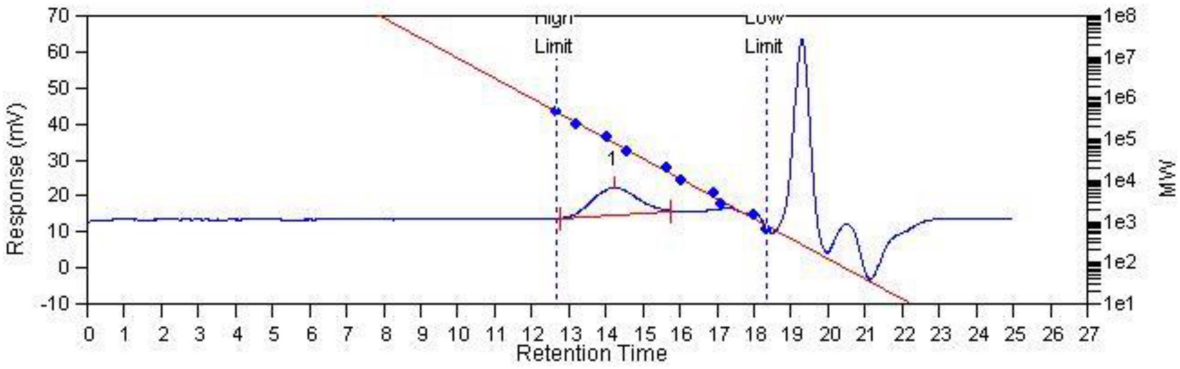

Figure S38. A typical gel permeation chromatogram for poly(cyclopentanone).

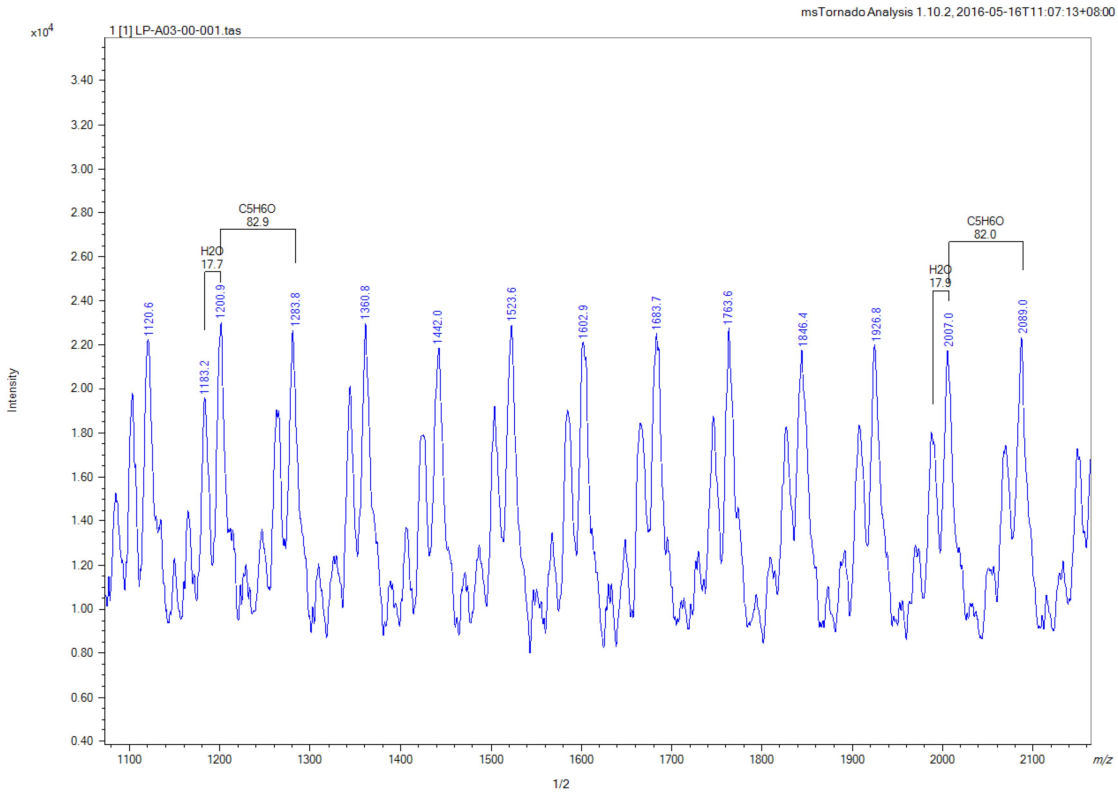

Figure S39. A typical A typical MALDI-tof mass spectrum of poly(cyclopentanone).

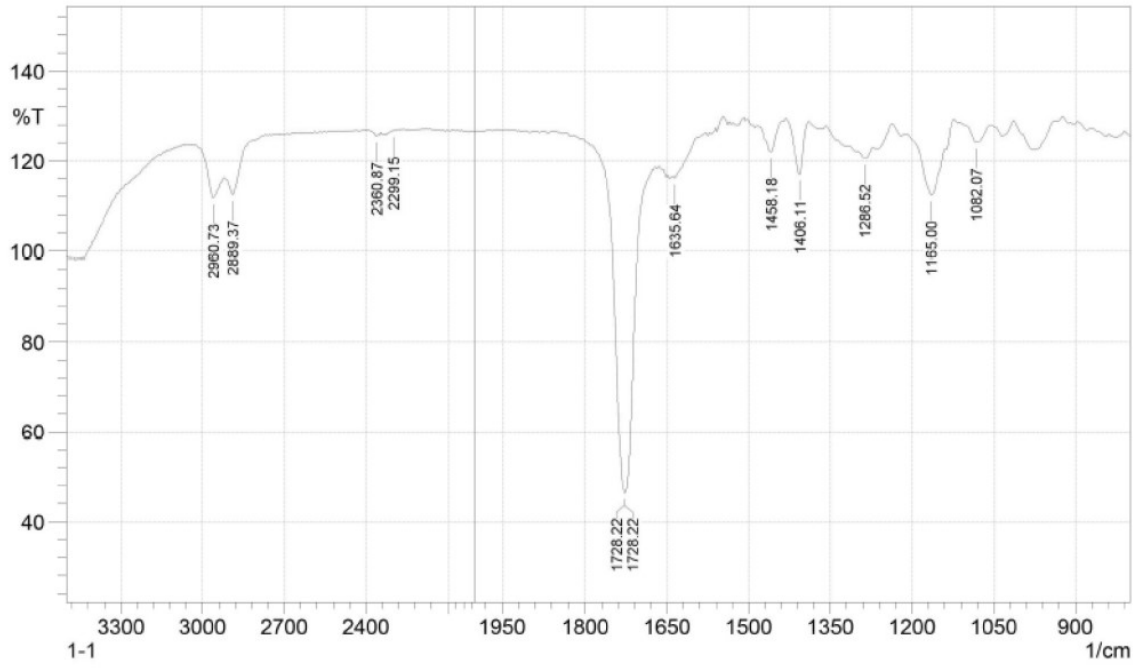

Figure S40. The FTIR spectrum for poly(cylopentanone).

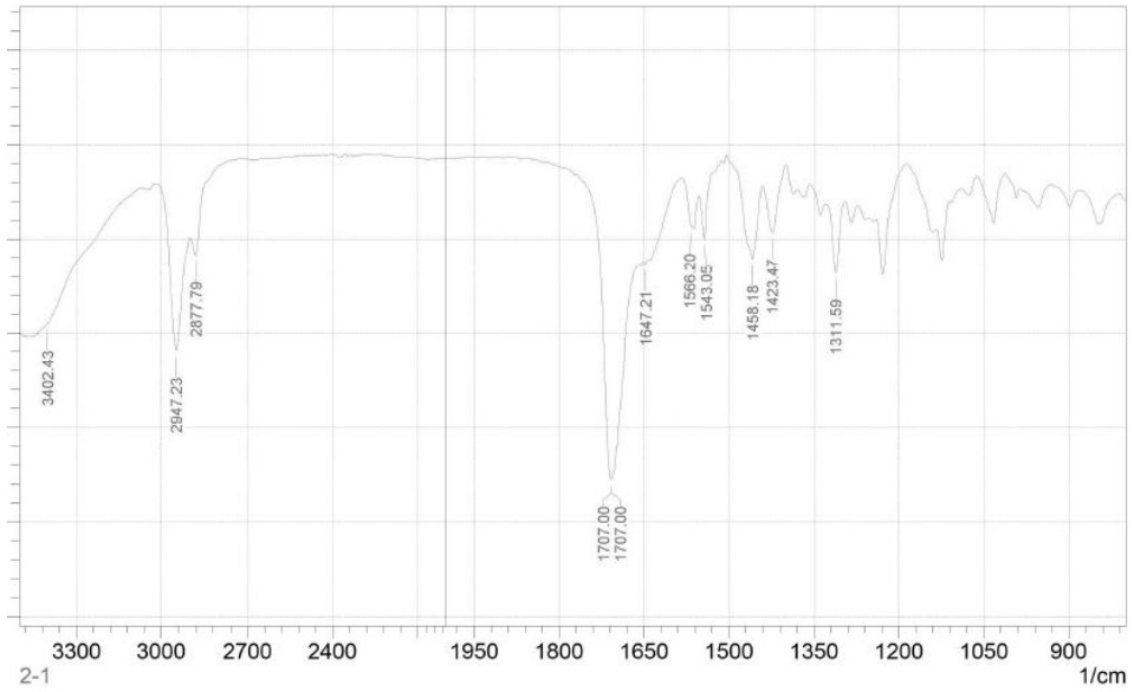

Figure S41. The FTIR spectrum for the polymerization of 2-cyclohexen-1-one.

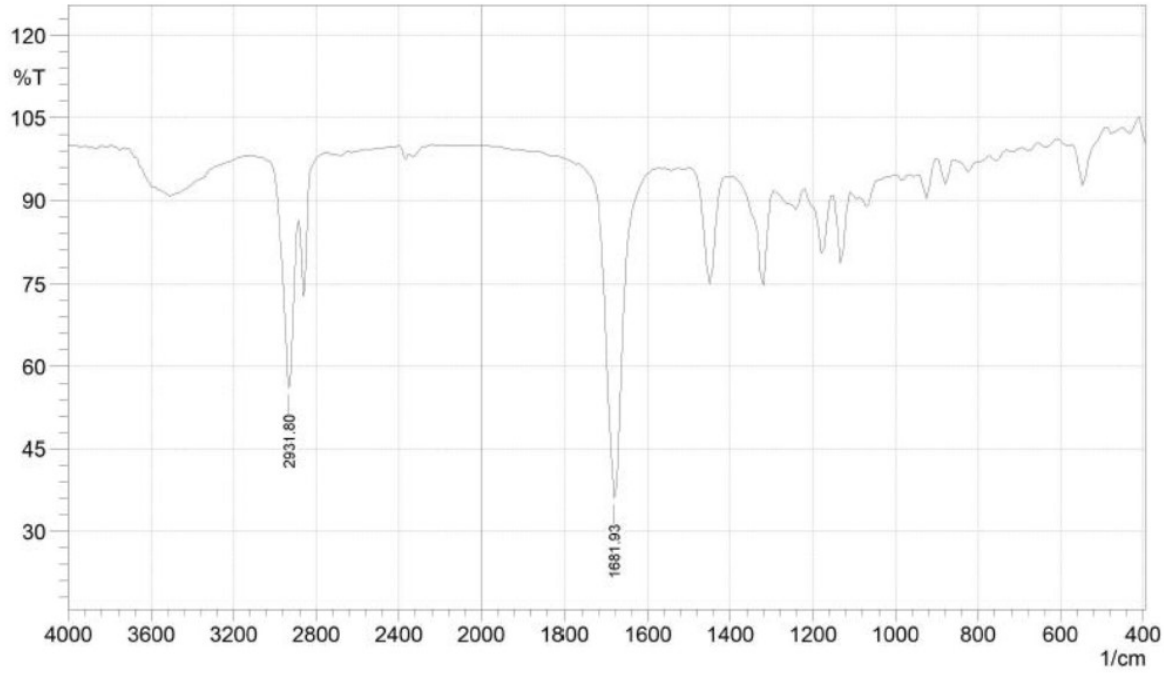

Figure S42. .The FTIR spectrum for the polymerization of 2-cyclohepten-1-one.